

UC Berkeley

Research Reports

Title

Potential Erroneous Degradation of High Occupancy Vehicle (HOV) Facilities

Permalink

<https://escholarship.org/uc/item/3z76r7tj>

Authors

Fournier, Nicholas, PhD
Farid, Yashar Zeinali, PhD
Patire, Anthony David, PhD

Publication Date

2021-07-28

PARTNERS FOR ADVANCED TRANSPORTATION TECHNOLOGY
INSTITUTE OF TRANSPORTATION STUDIES
UNIVERSITY OF CALIFORNIA, BERKELEY

Potential Erroneous Degradation of High Occupancy Vehicle (HOV) Facilities

Task ID 3710 (65A0759)

Final Report

July 28th, 2021



Partners for Advanced Transportation Technology works with researchers, practitioners, and industry to implement transportation research and innovation, including products and services that improve the efficiency, safety, and security of the transportation system.

Primary Authors

Nicholas Fournier, Ph.D.

Postdoctoral Scholar
California PATH
University of California, Berkeley

Yashar Zeinali Farid, Ph.D.

Postdoctoral Scholar
California PATH
University of California, Berkeley

Anthony David Patire, Ph.D.

Principal Investigator
California PATH
University of California, Berkeley

TABLE OF CONTENTS

List of Figures	7
List of Tables	8
1. Introduction	10
1.1. Purpose of Document.....	10
1.2. Intended Audience.....	10
1.3. Document Organization.....	10
2. Survey of Data-mining Methods	12
2.1. Anomaly Detection	12
2.2. Supervised Methods	14
Logistic Regression	15
Support Vector Machine	15
K-Nearest Neighbor	16
3-4 Decision Tree	17
2.3. Unsupervised Methods.....	18
Distance-Based Detection	19
Density-Based Detection	19
Clustering-Based Detection	20
2.4. Ensemble Methods	21
Random Forest	22
2.5. Summary.....	23
3. Performance of Methods	24
3.1. Selected Models	24
Supervised Classification Models	24
Unsupervised Anomaly Detection Models.....	25
3.2. Data.....	25
I-210 Pilot	25
3.3. Feature Extraction	26
Data Structure	26
Feature Reduction	27
3.4. Evaluation Metrics	29
3.5. Performance Evaluation	29
3.6. Summary.....	30
4. Magnitude of HOV Degradation	31

Potential Erroneous Degradation of High Occupancy Vehicle (HOV) Facilities – Final Report

- 4.1. Methodology 31
 - Selected Machine Learning Models 31
 - Study Region & Data..... 32
 - Manual Evaluation of Machine Learning Results 33
 - Process for Determining Degradation 35
- 4.2. Results..... 36
 - Detected Misconfigured Sensors 36
 - Degradation Results 38
 - Extended Analysis over Multiple Time Periods 40
- 5. Conclusions 44**
 - 5.1. Project Outputs..... 44
 - 5.1. Summary 44
 - 5.2. Recommendations 45
- References 46**
- Appendix A – Detection Results Table 47**
- Appendix B – Degradation Calculation Results Table 48**
- Appendix C – Comparative Traffic Flow Plots 49**
 - Sensor: 717822 50
 - Sensor: 718270 51
 - Sensor: 718313 52
 - Sensor: 759982 53
 - Sensor: 761384 54
 - Sensor: 762500 55
 - Sensor: 762549 56
 - Sensor: 762559 57
 - Sensor: 762600 58
 - Sensor: 764615 59
 - Sensor: 764663 60
 - Sensor: 765271 61
 - Sensor: 766171 62
 - Sensor: 766518 63
 - Sensor: 767939 64
 - Sensor: 767954 65
 - Sensor: 767985 66

Potential Erroneous Degradation of High Occupancy Vehicle (HOV) Facilities – Final Report

Sensor: 767999	67
Sensor: 768743	68
Sensor: 769238	69
Sensor: 769745	70
Sensor: 771916	71
Sensor: 772533	72
Sensor: 773543	73
Sensor: 774013	74
Sensor: 774055	75
Sensor: 774108	76
Sensor: 776658	77
Sensor: 776945	78
Appendix D – Visualization of Sensor data and misconfiguration detection.....	79

LIST OF FIGURES

Figure 2-1: Outlier examples: a) a single outlier, b) a small group of outliers (<i>source: (Aggarwal, 2017)</i>).....	13
Figure 2-2: Logistic regression model in a binary classification problem	15
Figure 2-3: Example of decision boundaries in binary classification: a) various decision boundaries, b) SVM decision boundary (<i>source: (Gandhi, 2018)</i>).....	16
Figure 2-4: K-Nearest Neighbor Example (<i>source: (Navlani, 2018)</i>)	17
Figure 2-5: Example of a decision tree classifier (<i>source: (James et al., 2013)</i>).....	18
Figure 2-6: Distance-based outlier detection	19
Figure 2-7: Density-based outlier detection	20
Figure 2-8: Clustering-based outlier detection	21
Figure 2-9: Ensemble learning (<i>source: (Borges, no date)</i>).....	22
Figure 2-10: Random forest example (<i>source: (Wikipedia, no date)</i>).....	22
Figure 3-1: Vicinity map of I-210 pilot in Caltrans District 7	26
Figure 3-2: Sensor organizational structure	27
Figure 3-3: Example HOV lane sensor versus upstream and downstream HOV sensors	27
Figure 3-4: Example K-S distribution comparison.....	28
Figure 4-1: Map of Caltrans District 7 HOV lanes and sensor locations with I-210 pilot corridor area highlighted	32
Figure 4-2: Example visual diagnosis of misconfigured HOV sensor #718313	34
Figure 4-3: Flow profiles for true HOV lane (dark green line) closely matching upstream (light blue line) and downstream (light orange line) HOV lanes.....	34
Figure 4-4: Map of Detected misconfigurations in District 7 by unsupervised learning (red dots) and supervised learning (blue dots).....	37
Figure 4-5: Conceptual Venn diagram showing the intersection of sensors detected by unsupervised and supervised methods.....	37
Figure 4-6: Map of misconfiguration detection frequency in District 7 by unsupervised learning (red dots) and supervised learning (blue dots) where larger dots indicate more detections per sensor.....	41
Figure 4-7: Sorted frequency distribution of misconfigured sensor for quarterly analyses from 2018-Q1 to 2021-Q1	42
Figure 4-8: Sorted frequency distribution of misconfigured sensor detections for quarterly analyses from 2018-Q1 to 2021-Q1, truncated to only sensors with at least two detections	42

LIST OF TABLES

Table 3-1: K-S Test variable matrix	28
Table 3-2: Confusion Matrix	29
Table 3-3: Method Accuracy.....	30
Table 4-1: Manual Diagnosis Criteria.....	33
Table 4-2: Degradation Rating System	36
Table 4-3: Percentage of diagnosis categories for detection results.....	38
Table 4-4: Comparison of existing and resolved HOV Degradation ratings.....	39
Table 4-5: Matrix of degradation status change. Horizontal and vertical axis indicates corrected and original erroneous status, respectively. Each cell below the diagonal indicates the number of sensors that improved degradation status.....	40
Table 4-6: Viability of HOV sensor data and detection rates.....	40
Table 0-1: Diagnosis of erroneous sensor detections for data on December 9 th , 2020	47
Table 0-1: AM Degradation change from reassigned misconfigured lanes.....	48
Table 0-2: PM Degradation change from reassigned misconfigured lanes	48

LIST OF ACRONYMS

HOV – High-occupancy Vehicle

PeMS – Performance Management System

VDS – Vehicle Detection Station

KNN – K-Nearest Neighbors

SVM – Support Vector Machine

LOF – Local Outlier Factor

ML – Mainline freeway lane

KS – Kolmogorov–Smirnov Test

1. INTRODUCTION

This document is the final report for Task ID 3710 (65A0759), a project titled “Potential Erroneous Degradation of High Occupancy Vehicle (HOV) Facilities”. This report contains a compilation of three previous technical memorandums titled “Survey of Data-Mining Methods”, “Performance of Methods”, and “Magnitude of HOV Degradation”.

HOV lane sensors in Caltrans’ Performance Management System (PeMS), are sometimes misconfigured as general-purpose lanes. In this situation, HOV lane data is mistakenly aggregated with general-purpose lane data and vice versa. The purpose of this project was to understand how widespread this problem might be and the extent to which it impacts performance reporting on the degradation of HOV lanes.

1.1. PURPOSE OF DOCUMENT

The purpose of this document is to report the findings and results of Task ID 3710 (65A0759), which has three objectives:

- Review existing methods in machine learning to achieve a clear understanding of algorithms that are likely to work for the task of identifying HOV misconfigurations.
- Test the effectiveness of the methods identified in the literature survey for the purpose of erroneous HOV sensor detection.
- Evaluate HOV degradation results for any misconfigured sensors detected using selected machine learning algorithms over an entire Caltrans district.

The primary overall goal is to develop automated means of detecting misconfigurations and to evaluate the impact of the misconfigurations on HOV performance measures statistics.

1.2. INTENDED AUDIENCE

The primary audience for this document includes:

- Caltrans Division of Research, Innovation and System Information (DRISI) sponsors of the project
- Caltrans Division of Traffic Operations staff at the headquarters and district level
- Project committee members

1.3. DOCUMENT ORGANIZATION

The remainder of this document is organized as follows:

- **Section 2** presents an overview of machine learning methods identified in the literature review process.

Potential Erroneous Degradation of High Occupancy Vehicle (HOV) Facilities – Final Report

- **Section 3** presents the erroneous HOV sensor detection performance of each machine learning method.
- **Section 4** presents the results of larger-scale detection over an entire Caltrans district (District 7) and an analysis of the impact of erroneous sensors on HOV degradation reporting.

2. SURVEY OF DATA-MINING METHODS

This section provides an overview of existing methods in machine learning. The primary goal is to achieve a clear understanding of algorithms that are likely to work for the task of identifying HOV misconfigurations. Key methods are listed with summary descriptions.

Subsequent discussion is organized as follows:

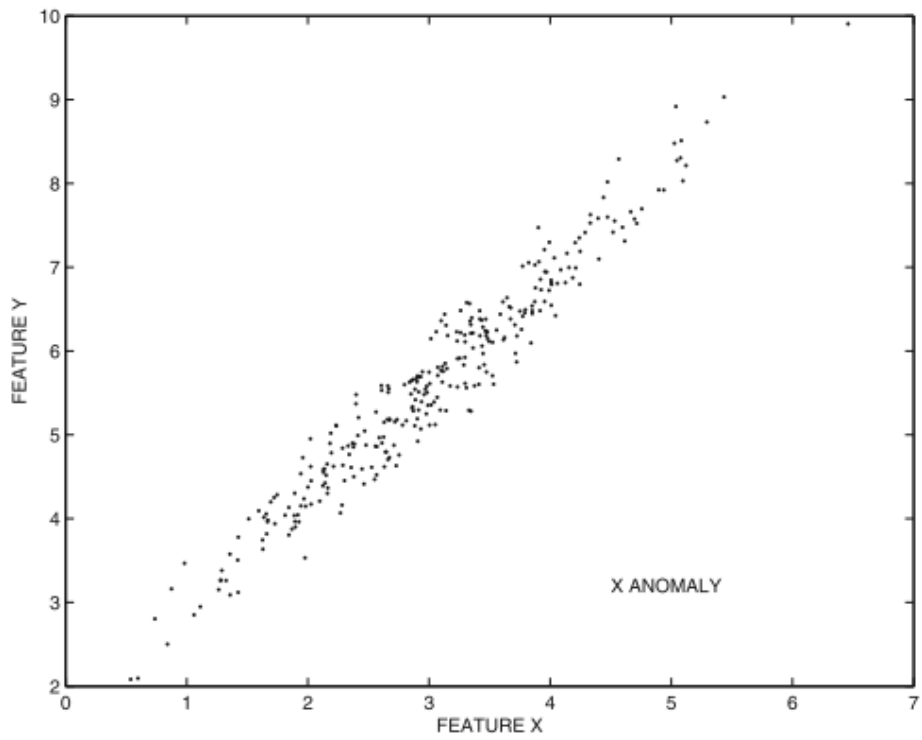
- **Section 2.2** presents a general description of anomalies, various types of anomalies, and different methods to detect anomalies
- **Section 2.3** provides a review of supervised learning techniques for classifying anomalies
- **Section 2.4** presents a review of the unsupervised learning methods such as density-based and distance-based methods to identify outliers
- **Section 2.5** provides a review of ensemble methods
- **Section 2.6** provides a summary of findings

2.1. ANOMALY DETECTION

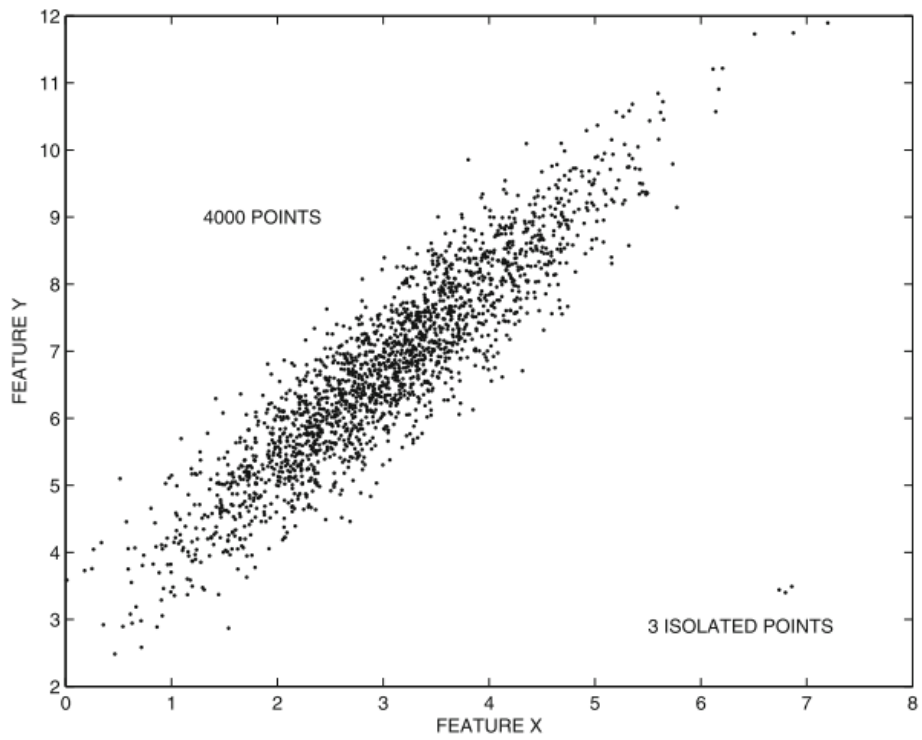
Anomaly detection is the process of identifying unusual patterns and unexpected observations (i.e., outliers) in a dataset. Outliers in data show behaviors that differ significantly from the majority. Hawkins defines an outlier as (Hawkins, 1980):

“an observation which deviates so much from other observations as to arouse suspicions that it was generated by a different mechanism”.

A dataset can include a single outlier where one observation is involved. When more than one outlier exists in a dataset, isolated or small groups of outliers might be involved. Figure 2-1 shows examples of a single outlier and a small group of outliers.



(a) Single Outlier



(b) Group of outliers

Figure 2-1: Outlier examples: a) a single outlier, b) a small group of outliers (source: (Aggarwal, 2017))

The data generating process of an outlier differs from the normal observations; hence, an outlier contains valuable information about unusual characteristics of a system and its data generation processes (Aggarwal, 2017). Analyzing such abnormal characteristics can provide valuable insights and guide the actions that should be performed. Examples of outlier generation processes include (Kotu and Deshpande, 2018):

- **Errors:** Various errors, such as measurement errors, human errors, or data collection errors can generate outliers
- **Normal variance:** When data is drawn from a certain distribution, the data points at the tails of the distribution do not occur frequently; however, these data points are legitimate
- **Data from other distribution classes:** Drawing data points from distributions that differ from the distribution of the *normal* points, can generate outliers
- **Distributional assumptions:** Outliers can be generated when incorrect assumptions on the data and distributions are made

To identify anomalies, various supervised and unsupervised models exist in the literature. In supervised models, ground truth labels indicating whether an observation is an outlier or not are available while in unsupervised techniques, labels are not required. Selecting a model for anomaly detection depends on various factors such as objectives of the analysis, data size, and data type.

The output of anomaly detection algorithms can be (Aggarwal, 2017):

- **Binary labels:** indicating whether an observation is an outlier or not
- **Scores:** quantifying the level of “outlierness” of each observation

2.2. SUPERVISED METHODS

In supervised learning, a model is developed to predict or estimate an output based on one or more inputs. When the output is a continuous or quantitative variable the model is a regression problem; while classification problems consist of outputs that are categorical or quantitative variables.

In a dataset of example pairs $D = \{(x_i, y_i), i = 1: N\}$ where $y_i \in Y$ is a class label and $x_i \in R^D$ is a feature vector, a classification problem learns a function $f: R^D \rightarrow Y$ which predicts the class label y for any feature vector x . Accuracy of the classification model can be determined via:

$$Accuracy(f, D) = \frac{1}{N} \sum_{i=1}^N \mathbb{I}(y_i = f(x_i)) \quad \text{Equation 1}$$

where \mathbb{I} is the indicator function.

The HOV misconfiguration problem deals with the type of detectors (e.g., mainline, HOV, off ramp, on ramp) which is a categorical variable. The objective of the model might be to identify the labels that are misconfigured; therefore, the HOV misconfiguration problem can be formulated as a classification problem. Identifying anomalies using classification models requires ground truth labels (e.g., whether an HOV detector is misconfigured or not). This section explores some of the most widely used classification models that can be used to detect HOV anomalies.

LOGISTIC REGRESSION

Logistic regression is a probabilistic model that directly estimates the probability that Y belongs to a category given feature vector X ($Pr(Y|X)$). For the HOV misconfiguration problem, logistic regression models the probability of having a misconfigured HOV detector given the feature data (X). The model output ($Pr(misconfigured = Yes | X)$ or simply $p(X)$) ranges between 0 and 1. In a binary class situation, the dependent variable has two possible values, such as correct and incorrect, which can be represented by 0 and 1 values. Figure 2-2 shows an example logistic regression estimation of a binary classification problem.

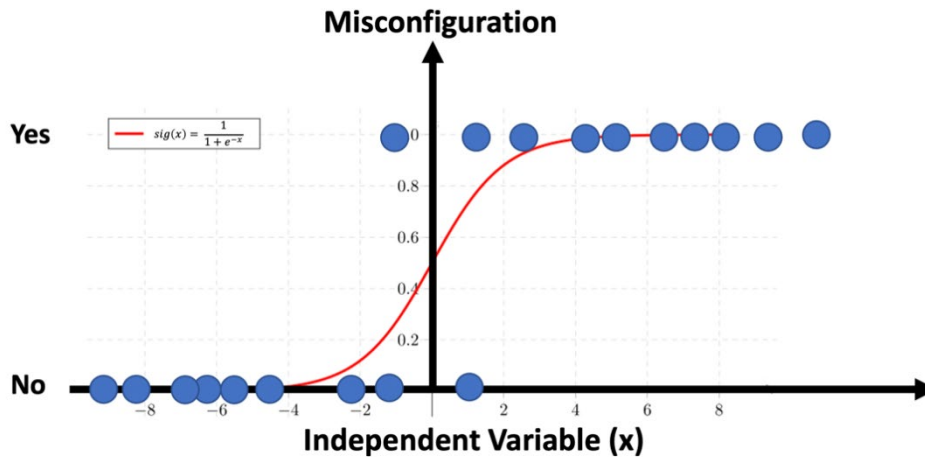


Figure 2-2: Logistic regression model in a binary classification problem

The logistic regression model uses the logistic function:

$$p(X) = \frac{e^{w^T X}}{1 + e^{w^T X}} \tag{Equation 2}$$

where W is the vector of model parameters.

SUPPORT VECTOR MACHINE

The support vector machine (SVM) is a classifier that was built on the maximal margin classifier model (James *et al.*, 2013). Unlike logistic regression, SVM does produce probabilistic outputs. The main objective of SVM is to find a decision boundary in M-dimensional space (where M is the number of independent variables) with a maximum margin. Figure 2-3 shows an example of an SVM decision boundary. To distinguish two classes, several possible decision boundaries can be selected (Figure 2-3a). As shown in Figure 2-3b, SVM finds a decision boundary that has maximum margin.

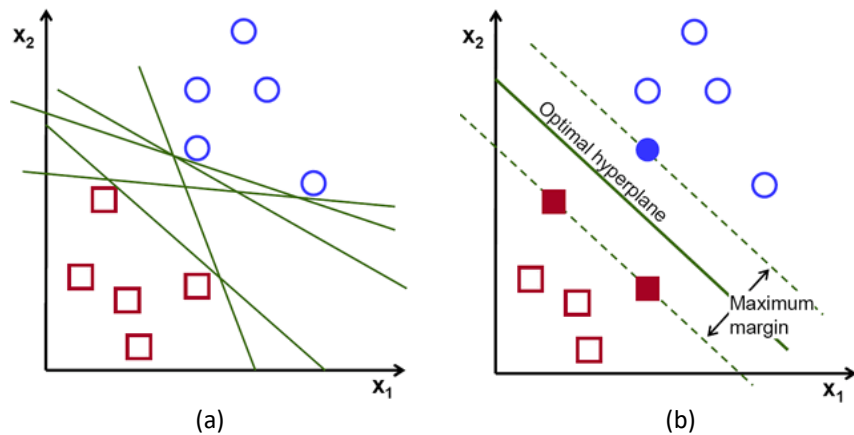


Figure 2-3: Example of decision boundaries in binary classification: a) various decision boundaries, b) SVM decision boundary (source: (Gandhi, 2018))

A binary SVM takes labels in the set $\{-1, 1\}$. The decision function is shown in Equation 4. SVM uses a hinge loss function to estimate the parameters. A hinge loss function is shown in Equation 5. Finally, an SVM loss function using Hinge loss with norm 2 (l_2) regularization, is shown in Equation 6.

$$g(\mathbf{X}) = \mathbf{W}^T \mathbf{X} + b \quad \text{Equation 3}$$

$$f_{SVM}(\mathbf{X}) = \text{sign}(g(\mathbf{X})) \quad \text{Equation 4}$$

$$L_h(y_i, g(\mathbf{X})) = \max(0, 1 - y_i \cdot g(\mathbf{X})) \quad \text{Equation 5}$$

$$L_{SVM}(y_i, \mathbf{X}) = C \sum_{i=1}^N \max(0, 1 - y_i \cdot g(\mathbf{X})) + \|\mathbf{W}\|_2^2 \quad \text{Equation 6}$$

where \mathbf{W} is the vector of model parameters, b is the bias term, $y_i \in Y$ is class label for $i \in 1: N$, N is the number of data points, and C is cost parameter of the model.

K-NEAREST NEIGHBOR

K-Nearest Neighbor (KNN) is a non-parametric model that stores training data and outputs a class for an instance \mathbf{X} based on a majority vote over its K nearest neighbors ($N_K(\mathbf{X})$). In KNN the nearest neighbors can be identified using different distance functions such Manhattan (norm 1) and Euclidean (norm 2).

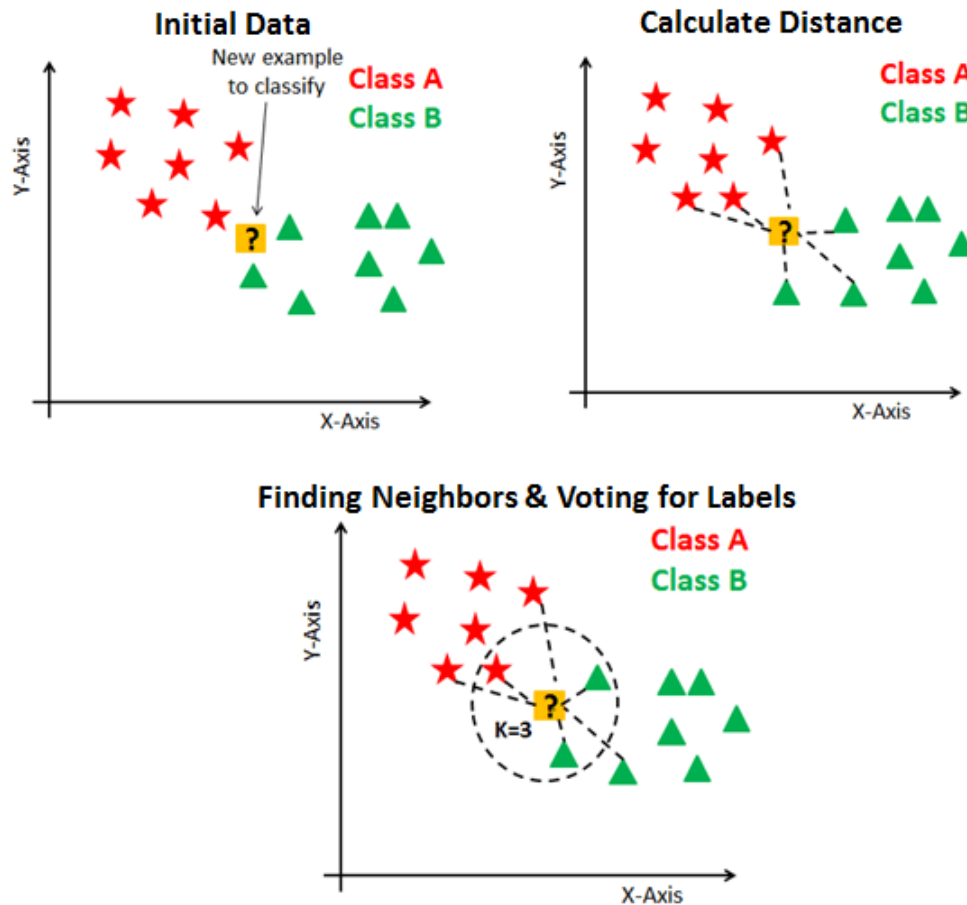


Figure 2-4: K-Nearest Neighbor Example (source: (Navlani, 2018))

A KNN classifier requires the number of neighbors K and the distance function. These two parameters are the hyperparameters of KNN. For a given number of neighbors and a distance function, KNN outputs the predictions using:

$$f(X) = \operatorname{argmax}_{y \in Y} \sum_{i \in N_k(x)} \mathbb{I}(y_i = y) \quad \text{Equation 7}$$

where \mathbb{I} is an indicator function, $y_i \in Y$ is class label, $N_K(X)$ is the set of K nearest neighbors.

3-4 DECISION TREE

A decision tree model uses a conjunction of rules to classify data. The rules in the decision tree model are organized into a binary tree structure. Each leaf node is associated with a class and all internal nodes include a rule with a threshold value. The internal nodes evaluate the rule and assign data points to the left or right of the tree.

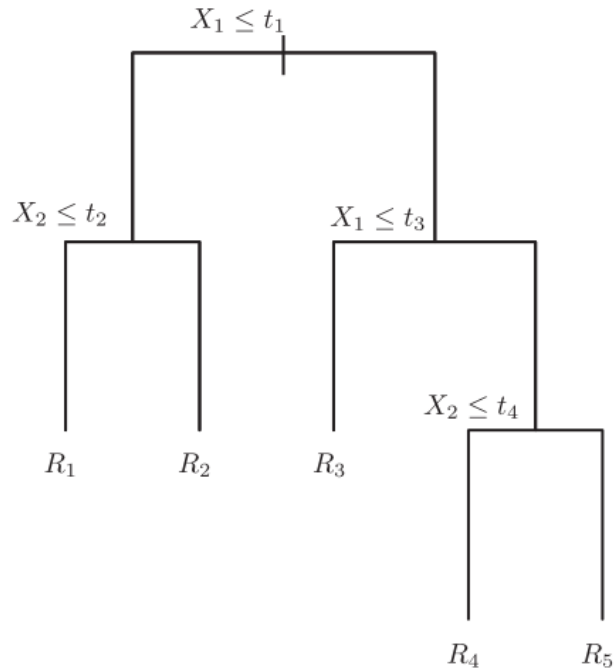


Figure 2-5: Example of a decision tree classifier (source: (James *et al.*, 2013))

In decision trees, variables and thresholds at each internal node need to be selected. Gini impurity (Equation 8) and information gain (Equation 9) are the two main criteria used for assessing the variables and thresholds.

$$C_{GI} = \sum_{c=1}^c p_i (1 - p_i) \quad \text{Equation 8}$$

$$C_{IG} = - \sum_{c=1}^c p_i \log(p_i) \quad \text{Equation 9}$$

Decision tree classifiers require the depth of the tree and a given criteria to estimate the model parameters.

2.3. UNSUPERVISED METHODS

In unsupervised learning, only features (independent variables) are observed and there are no measurements of the outcome (Hastie, Tibshirani and Friedman, 2009). In contrast to supervised learning, unsupervised learning does not use labeled data and identifies patterns in a dataset. Therefore, identifying anomalies using unsupervised models does not require ground truth labels. This section describes some of the most well-known unsupervised anomaly detection models including distance-based, density-based, and clustering-based techniques.

DISTANCE-BASED DETECTION

In a multidimensional space, outliers are distant from other points. The idea in distance-based outlier detection models is to use distance functions and identify data points that are isolated from the rest of the dataset.

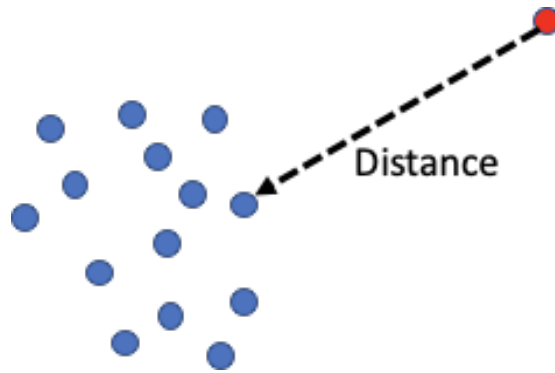


Figure 2-6: Distance-based outlier detection

Distance-based anomaly detection approaches include (Mehrotra, Mohan and Huang, 2017):

- **Distance to all points:** This is the simplest approach in which the anomalousness metric is the sum of distances from all data points

$$\alpha(p) = \sum_{q \in \mathcal{D}} d(p, q) \quad \text{Equation 10}$$

where p is the point of interest, q is another point in dataset \mathcal{D} , and $d(p, q)$ is the distance of point p from point q

- **Distance to nearest neighbor:** The anomalousness metric is the distance to the nearest data point in the dataset

$$\alpha(p) = \min_{q \in \mathcal{D}, q \neq p} d(p, q) \quad \text{Equation 11}$$

where p is the point of interest, q is another point in dataset \mathcal{D} , and $d(p, q)$ is the distance of point p from point q

- **Average distance to k nearest neighbors:** This approach requires a set of k nearest data points where k is less than the total number of data points in the dataset ($k < N = |\mathcal{D}|$). The anomalousness metric is computed as the average distance to k nearest points.

$$\alpha(p) = \sum_{j=1}^K d(p, \text{Near}(p, j)) / K \quad \text{Equation 12}$$

where p is the point of interest, $\text{Near}(p, j)$ returns the j^{th} nearest neighbor of p , K is the number of nearest neighbors, and $d(p, \text{Near}(p, j))$ is the distance of point p from the j^{th} nearest neighbor

- **Median distance to k nearest neighbors:** The anomalousness metric is the median distance to k nearest points. The arithmetic average value can be sensitive to changes in the data points, while median values are more robust.

DENSITY-BASED DETECTION

The idea in density-based outlier detection models is that outliers appear in regions with relatively low densities while normal points are located in high density regions (Wang, Bah and Hammad, 2019). Density-based models utilize more complicated algorithms in comparison to distance-based methods.

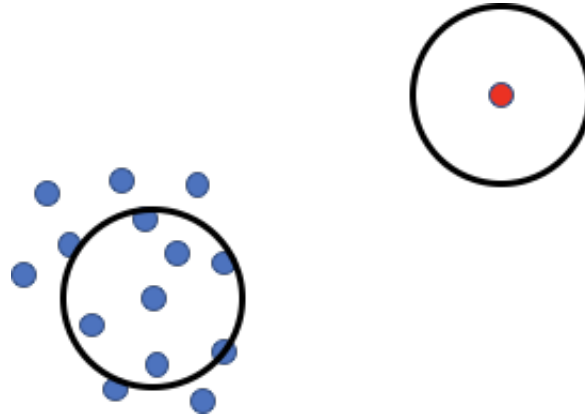


Figure 2-7: Density-based outlier detection

Local Outlier Factor (LOF) is a density-based algorithm which makes use of KNN (Wang, Bah and Hammad, 2019)(Markus M. Breunig, Hans-Peter Kriegel, Raymond T. Ng, 2009). LOF computes local reachability density (lrd) for each point as the inverse of the average reachability distance based on their K nearest neighbors. The local outlier

$$lrd(p) = 1 / \frac{\sum_{o \in N_k(p)} \max \{k - \text{distance}(o), d(p, o)\}}{|N_k(p)|} \quad \text{Equation 13}$$

$$LOF_K(p) = \frac{1}{|N_k(p)|} \sum_{o \in N_k(p)} \frac{lrd_k(o)}{lrd_k(p)} \quad \text{Equation 14}$$

where $lrd_k(o)$ and $lrd_k(p)$ are local reachability density of points o and p , respectively, $N_K(p)$ is the set of K nearest neighbors of point p , $d(p, o)$ is the distance between points o and p , $k - \text{distance}(o)$ is the distance to the k^{th} ordered neighbor of point o .

CLUSTERING-BASED DETECTION

Anomalies in a dataset can be detected using explicit identification of clusters in the data. Outliers by definition are not similar to the majority of data points; therefore, they often cannot form a tight cluster. Outliers can be identified as the points that do not belong to a cluster. Even when the outliers form a cluster, they are distant from other clusters (Kotu and Deshpande, 2018).

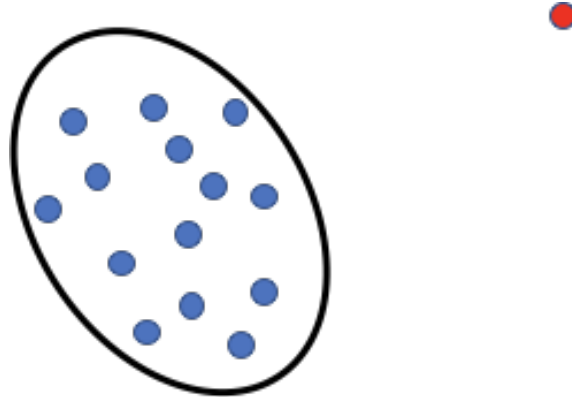


Figure 2-8: Clustering-based outlier detection

The first step in clustering-based models is to use an algorithm to identify the clusters. Then, the anomalousness metric can be determined based on the identified clusters. Clustering algorithms used in outlier detection include (Mehrotra, Mohan and Huang, 2017):

Nearest neighbor: This method takes into account the local properties of data spaces. Nearest neighbor is based on the idea that each data point is similar to its neighbors rather than to a centroid.

k-means clustering: Identifies k clusters by computing centroids for each cluster and assigning each data point to a cluster. The number of clusters is a hyperparameter and can be learned directly from the training dataset.

2.4. ENSEMBLE METHODS

Ensembles combine results of different models to produce more powerful models to identify outliers. In an ensemble, a weighted combination of base models is learned (Murphy, 2012). An ensemble can include different types of models or different versions of the same model. The model form is:

$$f(y|X, \pi) = \sum_{m \in M} w_m f_m(y|X) \quad \text{Equation 15}$$

where f_m is the m^{th} model and w_m are weights (tunable parameters).

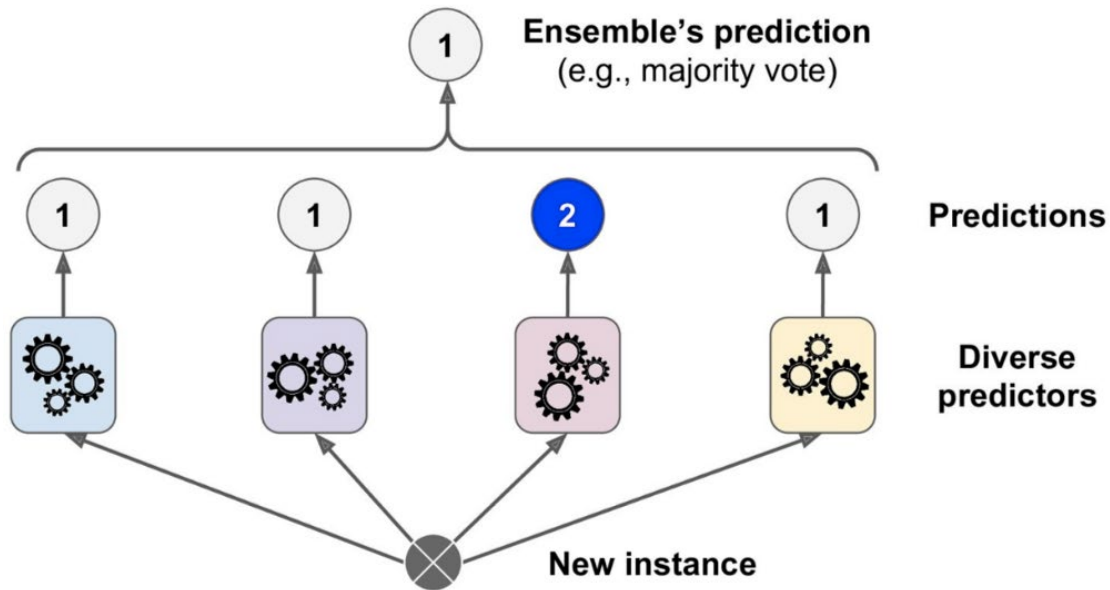


Figure 2-9: Ensemble learning (source: (Borges, no date))

RANDOM FOREST

Random forest is an ensemble of decision trees that use bootstrap aggregation (bagging). In bagging, the variance of an estimate is reduced by averaging together many estimates (Murphy, 2012). In random forest classifiers, a single training set is randomly divided into M samples and each sample is used to train a classifier to perform the same task.

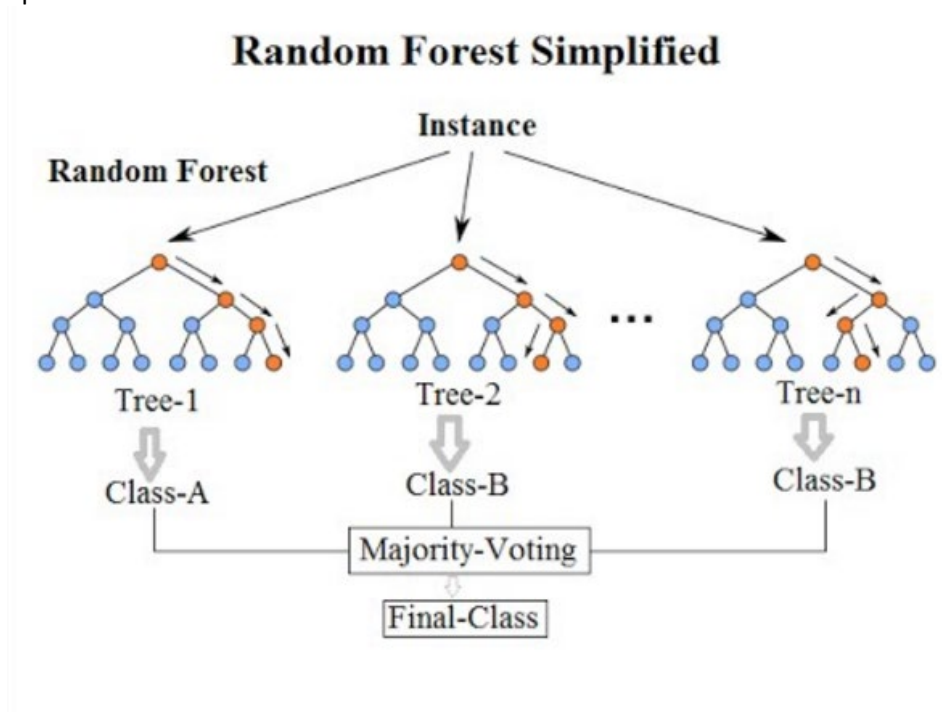


Figure 2-10: Random forest example (source: (Wikipedia, no date))

The model output is determined using a majority vote over the M trained classifiers (Murphy, 2012).

$$f(\mathbf{X}) = \sum_{m=1}^M \frac{1}{M} f_m(\mathbf{X}) \quad \text{Equation 16}$$

where f_m is the m^{th} tree

To further decorrelate the M trained classifiers, random forest considers a random subset of the available features for each classifier.

2.5. SUMMARY

This section described anomaly detection methods which identify unusual patterns and unexpected observations in a given dataset. The review indicated that HOV misconfigurations can be identified using supervised learning, unsupervised learning, and ensemble learning techniques.

In supervised learning, ground truth labels (e.g., whether an HOV detector is misconfigured or not) is required. The research team has ground truth labels for a segment of I-210 highway near Pasadena, California. Several widely used classification models were explained, including SVM, decision tree, logistic regression, and KNN, which can be used to train classifiers. Once the classifiers are learned, the generalization power of the models is analyzed.

In unsupervised learning, ground truth labels are not required. The models are trained to detect patterns using feature data and outcomes are not considered. Consequently, accuracy of the model cannot be studied in unsupervised learning. For detecting HOV misconfigurations, various unsupervised techniques, such as distance-based, density-based, and clustering-based methods can be explored.

Furthermore, ensemble learning techniques can be utilized in which different models are combined to produce more powerful models. Random forest is a well-known ensemble model which has been widely used in the literature.

3. PERFORMANCE OF METHODS

This section reports the tested effectiveness of the methods identified in the literature survey. The test is conducted using Vehicle Detection Station (VDS) data along the I-210 corridor where data integrity has been confirmed (i.e., no erroneous sensors), but then a random selection of HOV sensors is intentionally misconfigured to test method accuracy. The primary goal is to compare the accuracy of methods, choosing the most effective method based on its accuracy of erroneous HOV detection for the next stage of this project. A summary of methodology and results are explained.

The remainder of this document is organized as follows:

- **Section 3.2** provides a general description of the models selected for comparison.
- **Section 3.3** presents the I-210 test location and VDS data used for the machine learning tests.
- **Section 3.4** describes feature extraction, or the key features identified in the data that can be targeted and reduced for more effective machine learning.
- **Section 3.5** describes the evaluation metrics used to assess the different methods' effectiveness.
- **Section 3.6** presents the accuracy results from each method based on the evaluation metrics prescribed.
- **Section 3.7** provides a summary of findings and recommendations.

3.1. SELECTED MODELS

This report utilizes a variety of differing machine learning approaches identified in the previous section. The specific methods utilized in this report are modified to suit the objective at hand (i.e., anomaly detection and binary classification) and may differ slightly from the basic approaches identified, which may be suited for other purposes (e.g., regression or multivariate classification). The following methods are tested and compared for detecting erroneous or misconfigured HOV sensors. These methods can be categorized into two types: *supervised classification models* and *unsupervised anomaly detection models*.

SUPERVISED CLASSIFICATION MODELS

Classification models function by attempting to assign the data into known classifications. These methods rely on known classification labels as a dependent variable used to train the model, and thus are deemed "supervised" learning methods due to this *a priori* data available for training.

- **K-Nearest Neighbors (KNN)** – A non-parametric model which uses stored training data to classify the target variable based on nearest neighboring data points in the training set.
- **Logistics Regression** – A probabilistic model which estimates the probability of the target variable belonging to one category or another using a sigmoid function to represent the distribution.
- **Decision Tree** – Uses a conjunction of rules to organize the data into a tree structure where each branch is a binary decision with a threshold for each variable (i.e., belongs to one group or another). Following the branches along each decision point will determine final classification.

- **Random Forest** – Is an ensemble of decision trees where a single training data set is randomly divided into M samples and each used to train the classifiers before being aggregated (i.e., bootstrapped) in a final combined result.

UNSUPERVISED ANOMALY DETECTION MODELS

Anomaly detection functions by attempting to identify statistical outliers in the data. Rather than training the data using a label as a predicted variable (i.e., HOV or mainline), the label is part of the data itself and not the dependent variable, thus making the approach unsupervised. As a result, unsupervised methods do not need to be trained and are run directly on the data.

- **Isolation Forest** – An unsupervised method utilizing decision trees, but instead of profiling normal values into classifications it attempts to isolate anomalies.
- **Local Outlier Factor (LOF) (Density-based detection)** – Uses KNN to compute local reachability for each point to its nearest neighbors, enabling statistical outliers to be detected.
- **One-class Support Vector Machine (SVM)** – SVMs find a decision boundary between points that maximizes the margins, dividing the data into discrete classifications. A one-class SVM is a special case of SVM where no labels are provided, making it an unsupervised method.
- **Robust Covariance (Distance-based detection)** – Another variation of KNN which relies on the median distance to the nearest neighbors. The median value, rather than the mean, provides a more “robust” calculation of distance less sensitive to anomalous data.

3.2. DATA

To evaluate the different machine learning methods, a sample from the Caltrans Performance Measurement System (PeMS) database is used for testing. Known misconfigurations are introduced randomly into the data set and used to validate detection accuracy of each method. Since all misconfigurations are known, accuracy can be calculated as a percent detected of the total. For this reason, it is critical that no unknown misconfigurations exist in the sample data, otherwise accuracy cannot be calculated.

The location selected to extract PeMS data are real traffic data from VDS locations along the I-210 corridor in Pasadena, California, located within Caltrans District 7. The I-210 corridor was selected because the area has already been extensively verified for the simulation model as part of the Connected Corridors I-210 Pilot Project (Connected Corridors, 2020).

I-210 PILOT

Figure 3-1 shows the vicinity of the I-210 Connected Corridors pilot study area in Caltrans District 7. The corridor is a 16-mile freeway (located inside the red box) with 33 HOV VDS locations near Pasadena, California. The machine learning methods are then tested using traffic data for these 33 VDS locations where data integrity is ensured. The traffic data are downloaded from the PeMS database for 5-minute

increments collected over a 24-hour time span for the week of October 25th to 31st, 2020. Machine learning is performed independently for each day, aggregating the results.

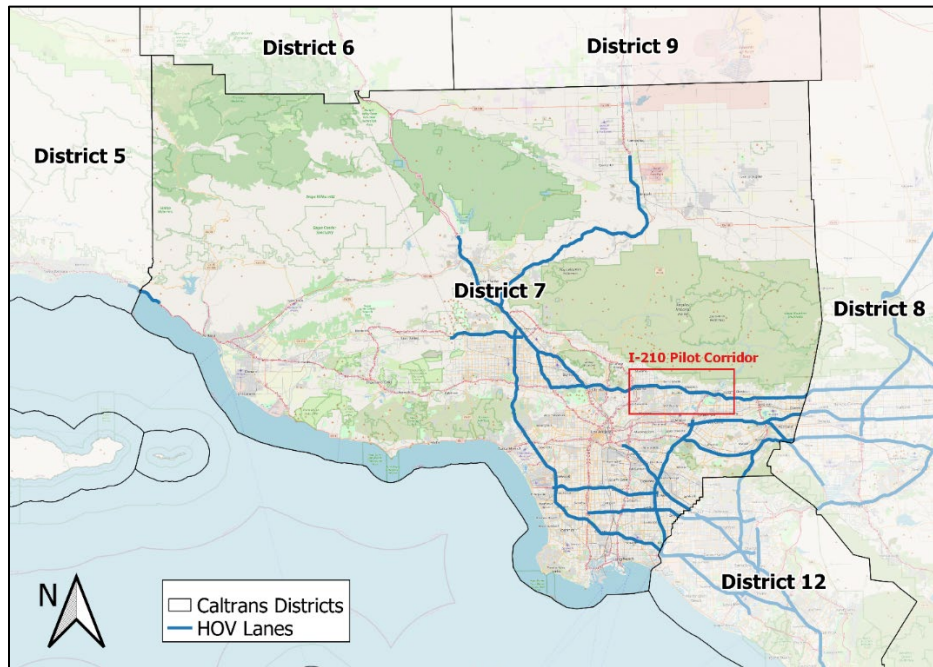


Figure 3-1: Vicinity map of I-210 pilot in Caltrans District 7

3.3. FEATURE EXTRACTION

To conduct machine learning on the traffic data, it is necessary to reduce the data and extract critical features that the machine learning methods can analyze and use to identify the erroneous labels.

DATA STRUCTURE

The data are first organized into a structure that relates the sensor positions to each other in a group, and to nearby groups, in a way that the algorithm can analyze each HOV sensor systematically, shown in Figure 3-2. A sensor group is composed of sensors that share the same *longitudinal* position (postmile) along the roadway but have different *lateral* lane positions (e.g., mainline or HOV lanes). These sensor groups are then further organized into a structure of groups linearly relative to each other as being either upstream or downstream. Upstream sensors precede the current sensor group relative to traffic flow (i.e., vehicles cross upstream sensors before the current sensor), and downstream sensors succeed the current sensor group. In this organizational structure, data from sensors can either be compared laterally between sensors in the current group (at the same postmile), or longitudinally across upstream and downstream sensors within the same lane.

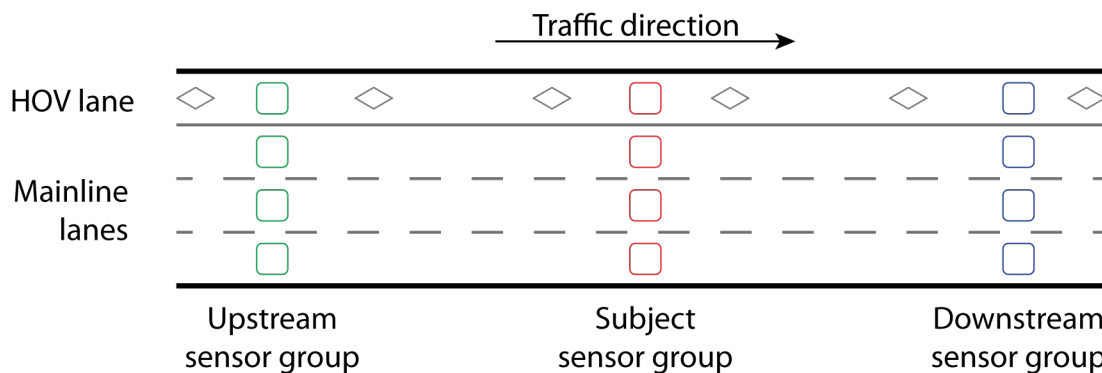


Figure 3-2: Sensor organizational structure

The machine learning algorithm will then analyze each HOV sensor as the subject, comparing its features to the other sensors within the group and to the nearest upstream and downstream sensors. After each HOV analysis, the algorithm will move onto the next sensor and repeat the analysis for all HOV sensors in the dataset.

FEATURE REDUCTION

Traffic sensors collect two fundamental measurements: Flow and Occupancy. Flow is a count per unit time, such as vehicles per hour. Occupancy is the proportion of time that the sensor is active, in other words, the amount of time that a vehicle is on the sensor. While occupancy can serve as a useful feature to further discriminate for erroneous sensors, a key feature identified by the researchers for indicating whether a HOV lane is misconfigured is the average nighttime traffic flow. It was observed that nighttime traffic flow in HOV lanes tends to be at or near zero. This can be intuitively explained by there being little or no reason to utilize an HOV lane at night since traffic congestion is at its lowest.

Figure 3-3 shows a misconfigured HOV lane in blue where the upstream and downstream HOV lane flows in orange are near zero at night and clearly do not match the current subject sensor. In this case, is it likely that this HOV sensor is a mainline lane mislabeled as an HOV lane.

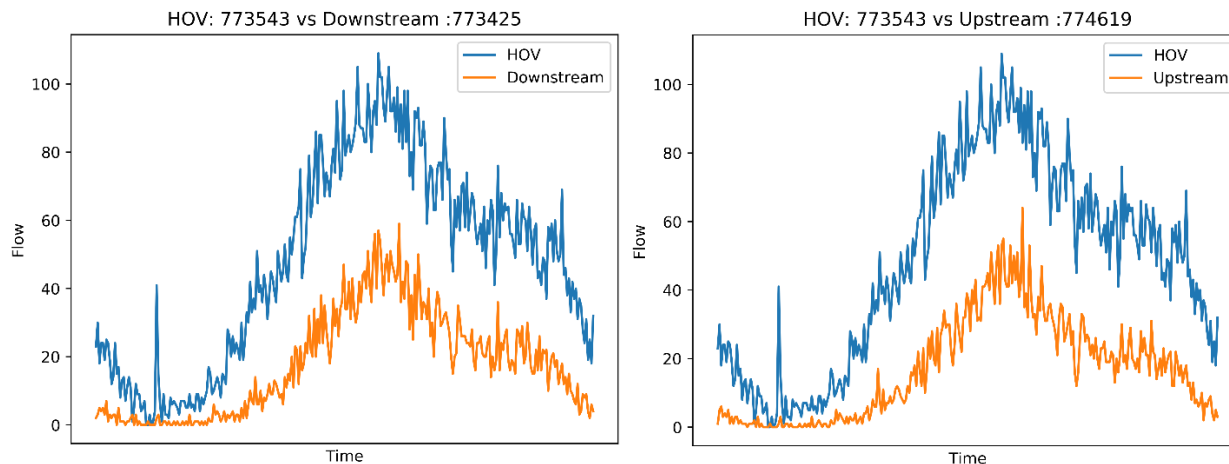


Figure 3-3: Example HOV lane sensor versus upstream and downstream HOV sensors

This obvious mismatch in nighttime flows makes it a useful feature for identifying erroneous HOV sensor labels. Although this erroneous HOV sensor label is easily identifiable by human eye, computers require a much more analytical and structured statistical comparison to make these determinations. This is achieved by preprocessing the data to extract the following features:

- Average nighttime traffic flow between the hours of 1:00-3:00AM, and
- a Kolmogorov–Smirnov test (K-S test) to indicate probability that the flow and occupancy profiles between sensors are statistically equal.

A K-S test is a useful hypothesis testing tool to compare two distributions and determine whether they are statistically different, as shown in the example in Figure 3-4.

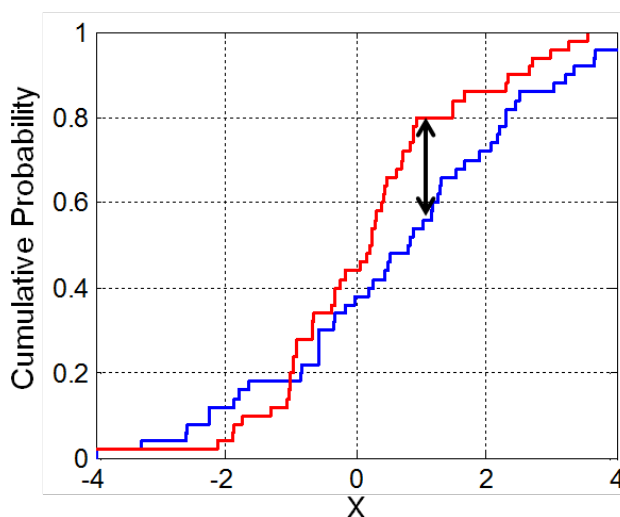


Figure 3-4: Example K-S distribution comparison

The K-S test is conducted between HOV and mainline lane sensors within a group, and the upstream and downstream sensors in the same lane. It can be conceptually organized into a variable matrix as shown in Table 3-1. The result of each test combination is a p-value reflecting the statistical probability that the two distributions (i.e., flow or occupancy profiles) are significantly different.

Table 3-1: K-S Test variable matrix

	<i>HOV vs Mainline</i>	<i>Upstream</i>	<i>Downstream</i>
HOV	K-S flow K-S occupancy	K-S flow upstream HOV K-S occupancy upstream HOV	K-S flow downstream HOV K-S occupancy downstream HOV
Mainline		K-S flow upstream mainline K-S occupancy upstream mainline	K-S flow downstream mainline K-S occupancy downstream mainline

The extracted feature data set is a substantially reduced table where each row is a unique HOV sensor with ten associated values and the average nighttime flow in columns. These extracted features are then used in the various machine learning methods to predict the binary outcome of whether each HOV sensor is correctly labeled or not.

3.4. EVALUATION METRICS

Each machine learning method ultimately provides some prediction of whether the HOV sensor is misconfigured or not. When evaluating predictive results, there are four potential outcomes:

1. **True Positive (TP)** – A correctly predicted misconfiguration,
2. **True Negative (TN)** – A correctly predicted non-misconfiguration,
3. **False Positive (FP)** – An incorrectly predicted misconfiguration, and
4. **False Negative (FN)** – An incorrectly predicted non-misconfiguration.

These four possible outcomes can be conceptually organized into a table, called a confusion matrix, as shown in Table 3-2.

Table 3-2: Confusion Matrix

		Actual	
		Misconfigured	Not misconfigured
Predicted	Misconfigured	True positive (TP)	False positive (FP)
	Not misconfigured	False negative (FN)	True negative (TN)

The overall accuracy is then calculated as the proportion of correct predictions, including true positives and true negatives, over the total number of predictions. It is for this reason that there is no unknown, misconfigured, HOV sensors in this testing data set. Otherwise, evaluation of the different methods would not be possible.

3.5. PERFORMANCE EVALUATION

To evaluate the machine learning methods performance, they are each run on the same I-210 test data set with known misconfigurations. To further assess the impact of increased data quantity and relative stability of results, seven days of traffic data from October 25th to 31st, 2020 are tested in two ways:

- **Separate daily traffic data tests** – The machine learning algorithms are run for a single day of traffic data, repeating the run for each of the seven days independently.
- **Contiguous daily traffic data tests** – The machine learning algorithms are run using all seven consecutive days of traffic data as one input data set.

The separate daily tests are intended to reveal the stability of results, that is, the extent to which results can vary when a different day of data is used. The contiguous daily test is intended to determine whether providing more data to the algorithm affects the results.

The overall accuracy of each machine learning method is presented in Table 3-3. The values in this table present results from both testing paradigms. The separate daily tests represent the overall aggregated

accuracy calculated as the mean and standard deviation of the seven test days. Note that the unsupervised models do not require a training data set and thus do not have an accuracy result in this case.

Table 3-3: Method Accuracy

Model	<u>Separate Daily Data Test</u>				<u>Contiguous Daily Data Test</u>	
	<u>Training Accuracy</u>		<u>Testing</u>		<u>Training Accuracy</u>	<u>Testing</u>
Supervised Classification	Mean	Std Dev.	Mean	Std Dev.		
<i>K-Nearest Neighbors</i>	97.5%	0.021	96.9%	0.029	100%	100%
<i>Logistics Regression</i>	95.8%	0.028	96.9%	0.029	100%	94.4%
<i>Decision Tree</i>	98.4%	0.015	91.3%	0.160	100%	100%
<i>Random Forest</i>	98.4%	0.015	90.5%	0.100	100%	100%
Unsupervised Anomaly Detection						
<i>Isolation Forest</i>	–	–	83.2%	0.023		70.4%
<i>Local Outlier Factor</i>	–	–	82.6%	0.019		81.5%
<i>One-class SVM</i>	–	–	80.4%	0.046		68.5%
<i>Robust Covariance</i>	–	–	72.7%	0.047		70.0%

In general, all methods performed well and were able to identify most of the misconfigured sensors. Approximately 70-80% accuracy or higher was achieved for most methods. However, the supervised methods tended to perform better than the unsupervised methods, achieving approximately 90-100% accuracy. When comparing the separated data test to the contiguous data test, it appears that the supervised methods accuracy is near perfect while the unsupervised methods decreased in performance. While it appears that classification methods are superior in this application, some caution should be taken when reviewing these results. The suspiciously perfect accuracy is somewhat confounding and may be an indicator that overfitting is occurring in the supervised methods.

These results are not entirely unexpected because the availability of pre-identified training data enables the model to be calibrated to a specific target, rather than more general anomaly detection. In contrast, unsupervised anomaly detection methods merely scan for statistical outliers. Since traffic data is inconsistent and prone to irregularities on its own, it may be difficult for these unsupervised methods to properly identify misconfigurations. However, training data tends to be locally biased (i.e., overfitted) and may offer diminished accuracy when applied to regions with substantially different traffic data. Moreover, training data itself may not be available in all Caltrans districts, making the flexibility of unsupervised methods an attractive feature.

3.6. SUMMARY

Overall, the machine learning methods performed well, achieving accuracy of over 80% detection. The supervised methods tended to perform better than unsupervised methods by a 10% accuracy margin. However, caution should be taken in assuming supervised models are superior in this case. It is possible that the relatively small scope of the 16-mile I-210 corridor test is prone to localized overfitting or bias, meaning that the models are well trained for the I-210 corridor but may perform poorly elsewhere. This is particularly crucial when considering largescale deployment to entire districts. Moreover, the flexibility of unsupervised models in not requiring training data may be a useful feature if widespread implementation is intended. These factors should be considered when deciding which methodology to employ.

4. MAGNITUDE OF HOV DEGRADATION

This section uses the methods described above to evaluate HOV misconfigurations and to report the potential magnitude of erroneous degradation of HOV facilities. The district used for analysis is Caltrans District 7 in Los Angeles. The study was conducted using the most effective machine learning methods identified in the previous two sections. A summary of the methodology and results are explained.

This section is organized as follows:

- **Section 4.2** presents the methodology for large-scale machine learning implementation and HOV degradation evaluation. This section presents the selected machine learning methods, the study region, data used, degradation calculation procedure, and manual evaluation procedure.
- **Section 4.3** presents a summary of results. This includes the overall detection results, a preliminary manual diagnosis of individual sensors, and the impact on HOV degradation results.

4.1. METHODOLOGY

In the previous sections, a variety of different machine learning techniques were identified in the literature and tested. This section builds on the previous two sections to achieve two fundamental goals:

- To implement the selected machine learning methods on real-world HOV sensor data for a larger region; and
- To evaluate the impact of these misconfigurations on reportedly “degraded” HOV lanes.

The following subsections describe the two machine learning models selected for further implementation, the study region under test, and a description of the calculation process required for determining whether an HOV facility is considered degraded by legal definition.

SELECTED MACHINE LEARNING MODELS

Of the eight different machine learning methods, the best performing methods from each of the two machine learning approaches of *Supervised Classification* and *Unsupervised Anomaly Detection* were selected for implementation. The following two methods are as follows:

- **Random Forest – Supervised Classification Method:** Is an ensemble of decision trees where a single training data set is randomly dived into M samples and each used to train the classifiers before being aggregated (i.e., bootstrapped) in a final combined result.
- **Local Outlier Factor (LOF) – Unsupervised Anomaly Detection Method:** Is a density-based detection method that uses KNN to compute local reachability for each point to its nearest neighbors, enabling statistical outliers to be detected.

The reason that the two methods were utilized, and not simply the best overall, is to further compare the effectiveness of each fundamentally dissimilar approach. To recall, unsupervised learning methods have no *a priori* knowledge of misconfigured sensors and rely on statistical groupings and outliers to identify misconfigurations in the data. In contrast, supervised learning methods utilize an initial training data set with known misconfigurations. This enables supervised methods to better account for otherwise

unexplained correlations in the data and achieve a higher degree of precision once extrapolated to larger datasets. However, this reliance on training data may potentially be a hindrance if the model is overfitted to the local training dataset, diminishing its broader predictive strength.

STUDY REGION & DATA

The machine learning methods were implemented for the entirety of Caltrans District 7, as shown in Figure 4-1. The rectangular region noted in the figure is part of the I-210 pilot corridor. As described in the previous section, the data in this region has been extensively verified as part of the pilot and was used to test the different machine learning methodologies in a controlled setting (i.e., few if any unknown misconfigurations exist in this region). For this same reason, these data are again utilized to train the supervised learning models.

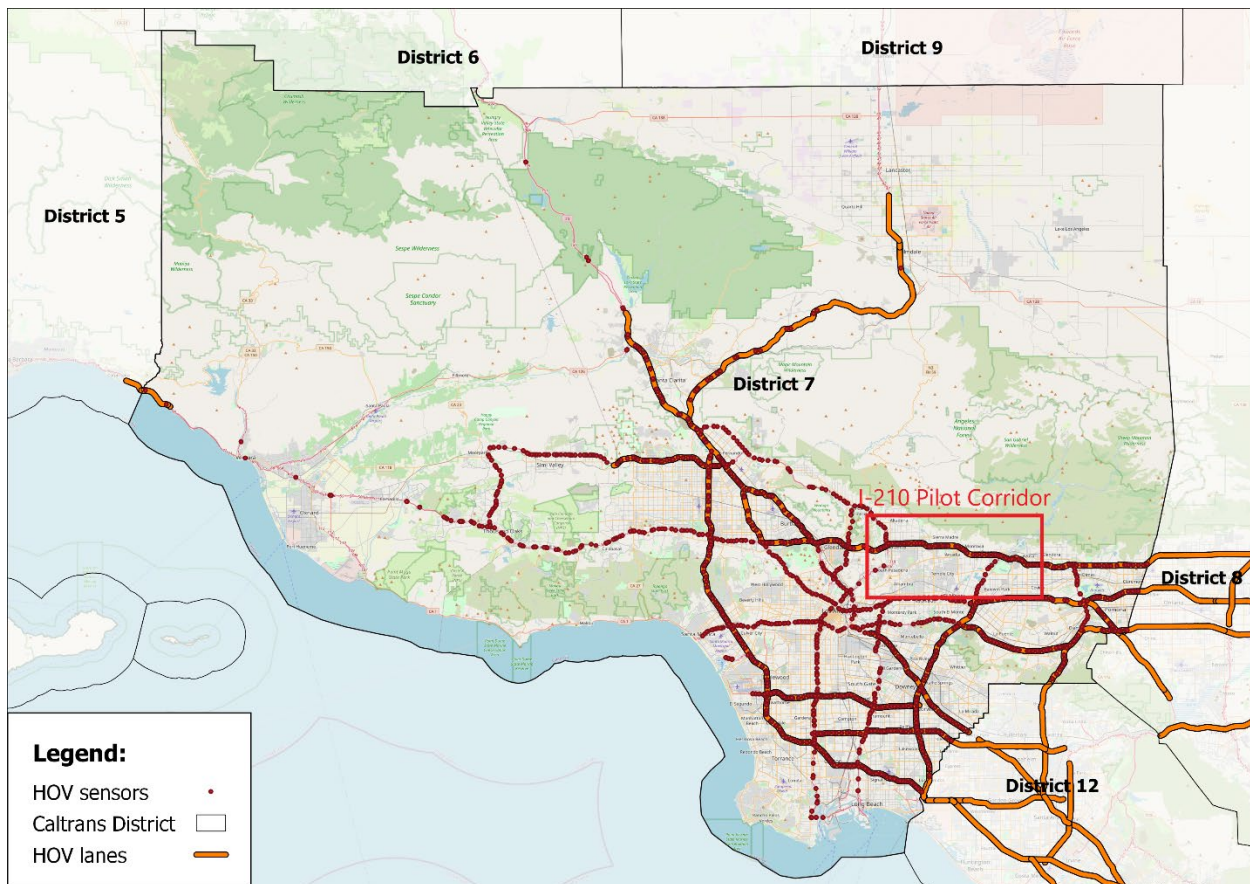


Figure 4-1: Map of Caltrans District 7 HOV lanes and sensor locations with I-210 pilot corridor area highlighted

Potential Erroneous Degradation of High Occupancy Vehicle (HOV) Facilities – Final Report

Within District 7, there were a total of 866 HOV sensors listed in the meta data at the time of analysis. However, not all sensors were currently operational or reliably reporting traffic data. Sensors were excluded based on the following criteria:

- < 5 total samples per lane
- < 50% “Observable” data
- < 50% of the timestamps reporting flow

This reduced number of sensors to only 314 sensors. From these sensors, two types of data are used:

- **5-minute traffic counts** – Used in the machine learning models to identify potentially misconfigured sensors. Since these data are higher fidelity, only one week worth of data are used from December 6th to December 12th, 2020.
- **Hourly traffic counts** – Used to calculate the degradation status of HOV facilities. 180-days’ worth of aggregated hourly counts are used in this calculation.

MANUAL EVALUATION OF MACHINE LEARNING RESULTS

The results from the machine learning models are a list of HOV sensors that may or may not be misconfigured. Moreover, the models do not determine what the misconfiguration issue is, only that it may be misconfigured. To validate, the results are manually evaluated to confirm machine learning results and diagnose the problem. Each sensor detected by the machine learning algorithm, is given one of the following categories in Table 4-1 based on evaluation.

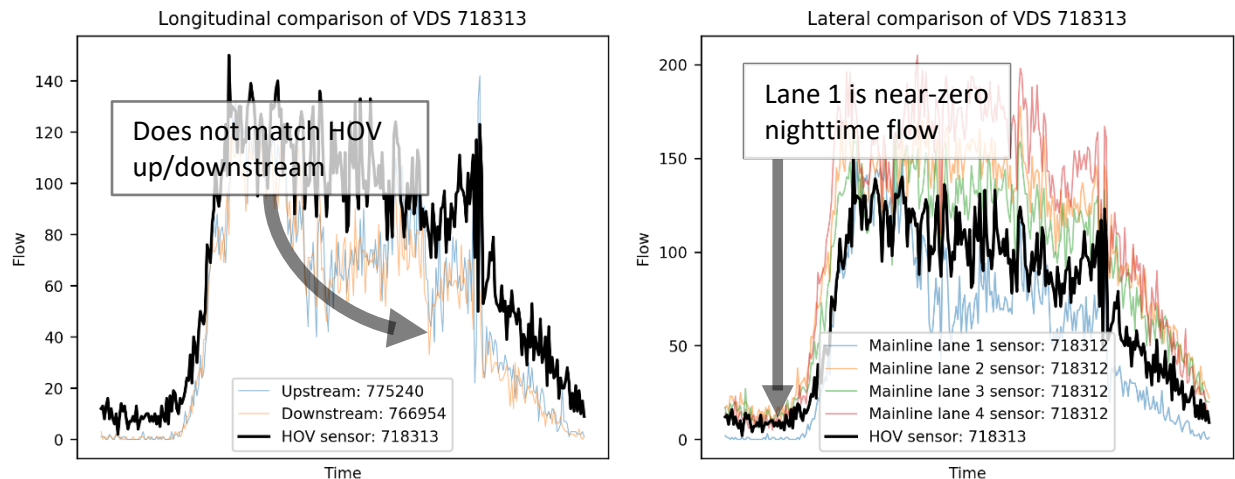
Table 4-1: Manual Diagnosis Criteria

Criteria	Description
Misconfigured	Lane label swapped, but data appears OK
Corrupted	Data has errors, label may be OK
Indeterminate	Lane label is likely erroneous, but requires further analysis
OK	Data and label appear fine

It should be emphasized that all sensors diagnosed as “indeterminate” are likely to be misconfigured. However, for this set of indeterminate sensors, it was not possible to select the correct HOV lane just by looking at the available data. Further analysis or physical inspection of the device in the field would be necessary to be 100% conclusive.

However, for the sensors diagnosed as “misconfigured” it was possible to select the correct HOV lane just by looking at the data in the adjacent lanes. This is a common situation, when the labels for HOV and mainline sensor data are obviously swapped. Figure 4-3 shows one such case where the HOV sensor appeared swapped with what should have been the Lane 1 sensor.

Potential Erroneous Degradation of High Occupancy Vehicle (HOV) Facilities – Final Report



(a) Longitudinal comparison showing mislabeled HOV sensor (bold black line) not matching upstream (blue line) and downstream (orange line) sensors

(b) Lateral comparison showing mislabeled HOV sensor (dark black line) has non-zero nighttime flow, but mainline lane 1 sensor (light blue) does

Figure 4-2: Example visual diagnosis of misconfigured HOV sensor #718313

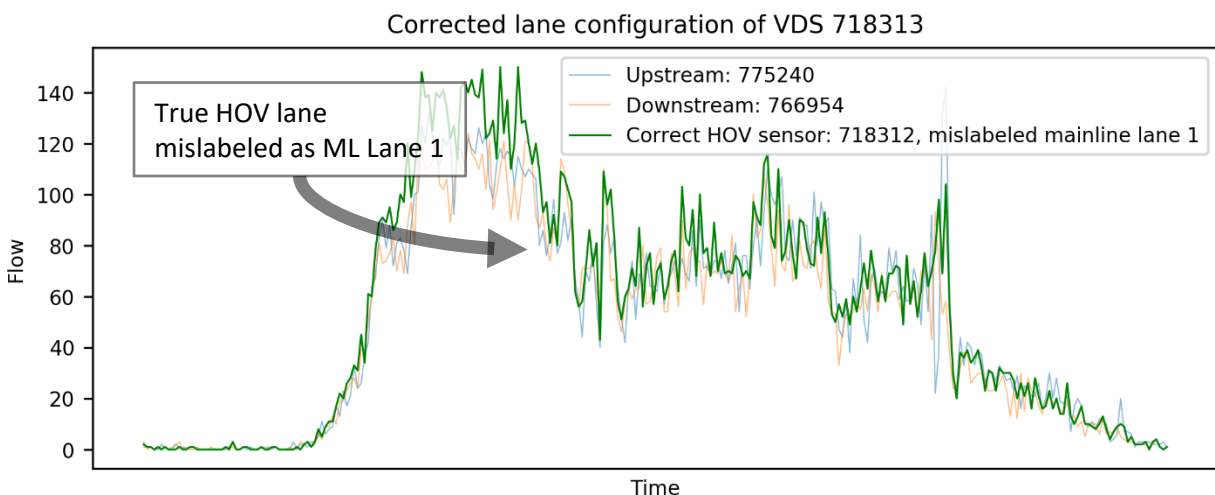


Figure 4-3: Flow profiles for true HOV lane (dark green line) closely matching upstream (light blue line) and downstream (light orange line) HOV lanes

The first indication of a problem is in the longitudinal comparison shown in Figure 4-2 (a) where the HOV sensor matches the flow from neither the upstream nor downstream sensors. The problem can be diagnosed in Figure 4-2 (b) where the HOV lane flow is not near-zero at night, but lane 1 is near zero, which is highly irregular. Swapping the labels from the HOV and Lane 1 sensors in Figure 4-3 show that the newly re-labeled HOV lane matches the upstream and downstream sensors. Not all detected misconfigurations were easily diagnosable as in the above example, but where possible a suggested diagnosis is given.

PROCESS FOR DETERMINING DEGRADATION

To determine whether an HOV facility is degraded, it must follow a very strict legal definition of the term. This definition in Subsection (d) of 23 U.S.C. § 166 is as follows:

(2) DEGRADED FACILITY. —

(A) Definition of minimum average operating speed.—*In this paragraph, the term “minimum average operating speed” means—*

- (i) 45 miles per hour, in the case of a HOV facility with a speed limit of 50 miles per hour or greater; and*
- (ii) not more than 10 miles per hour below the speed limit, in the case of a HOV facility with a speed limit of less than 50 miles per hour.*

(B) Standard for determining degraded facility. —

For purposes of paragraph (1), the operation of a HOV facility shall be considered to be degraded if vehicles operating on the facility are failing to maintain a minimum average operating speed 90 percent of the time over a consecutive 180-day period during morning or evening weekday peak hour periods (or both).

(C) Management of low emission and energy-efficient vehicles. —

In managing the use of HOV lanes by low emission and energy-efficient vehicles that do not meet applicable occupancy requirements, a public authority may increase the percentages described in subsection (f)(3)(B)(i).

This essentially states that an HOV facility is degraded if the average speed during weekday peak hours is less than 45 miles per hour for more than 10% of the time over a 180-day period. 180-days of hourly traffic counts were obtained from the PeMS data clearinghouse for all sensors in Caltrans District 7. From these data, degradation was determined through the following steps:

1. Data filtering and Cleaning:
 - a. Remove all non-HOV sensors from data.
 - b. Remove data for any days where data is less than 100% observable.
 - c. Remove all non-weekday and non-peak hour data (Monday-Friday, 6-9AM and 3-6PM).
2. Calculate Vehicle Miles Traveled (VMT) for each hour as $VMT_i = L \cdot q_i$ where q_i is the number of vehicles that passed over the VDS and L is the length of its associated freeway segment for hour increment i .
3. Calculate Vehicle Hours Traveled (VHT) for each hour as $VHT_i = \frac{L \cdot q_i}{v_i}$ where v is the spot speed from the VDS in data.
4. Calculate Average Speed as $\bar{v}_j = \sum \frac{VMT_i}{VHT_i}$ where is the average speed for day j .
5. Determine number of degraded days:

$$n_{degraded} = \begin{cases} |\bar{v}_j < 45|, v_{limit} \geq 50 \\ |v_{limit} - \bar{v}_j \geq 10|, v_{limit} < 50 \end{cases}$$

Where v_{limit} is the speed limit. In words, the above inequality states that for roads with a speed limit of 50 mph or higher, it is degraded if average speed goes below 45 mph; and for roads with a speed limit below 50 mph, it is degraded if average speed is more than 10 mph less than the speed limit. $n_{degraded}$ is then a count of the number of days where the degradation threshold is exceeded.

6. Calculate the percentage of days degraded from available days as

$$\%degraded = \frac{n_{degraded}}{N_{total}} \times 100$$

Where N_{total} is the total number of days with available data,

The resulting percent of ‘degraded’ days then determines whether the road is, by legal definition, degraded if it exceeds more than 10% of the days over a 180-day period. Although this is a binary threshold, additional levels of degradation are also defined by Caltrans as *Not degraded (<10%)*, *Slightly degraded*, *Very degraded*, and *Extremely degraded*, as shown in Table 4-2.

Table 4-2: Degradation Rating System

<i>Degradation Status</i>	<i>Percent degraded criteria</i>
Extremely degraded	≥75%
Very degraded	50 – 74%
Not degraded	≤10%

4.2. RESULTS

This section presents a summary of findings for Caltrans District 7, describing the misconfigurations that were detected and the effect of these misconfigurations on HOV degradation results. A map illustrates the locations of the sensors detected by both supervised and unsupervised learning methods. A summary table of manual evaluation results categorize the diagnosis of sensors as prescribed in Table 4-1 (i.e., misconfigured, corrupted, indeterminate, or OK). Where possible, the sensor categorization is corrected, and the traffic degradation results are recalculated. In almost all cases this results in reduced degradation. Based on these findings, sensor misconfiguration causes in an overestimation of the true level of HOV degradation.

DETECTED MISCONFIGURED SENSORS

Figure 4-4 shows the approximate location of each sensor detected by each of the machine learning methods. A total of 29 sensors were detected by the unsupervised method, and 17 by the supervised

method, as shown in Table 4-3. Interestingly, all 17 of the supervised method’s detections were also detected by the unsupervised method.

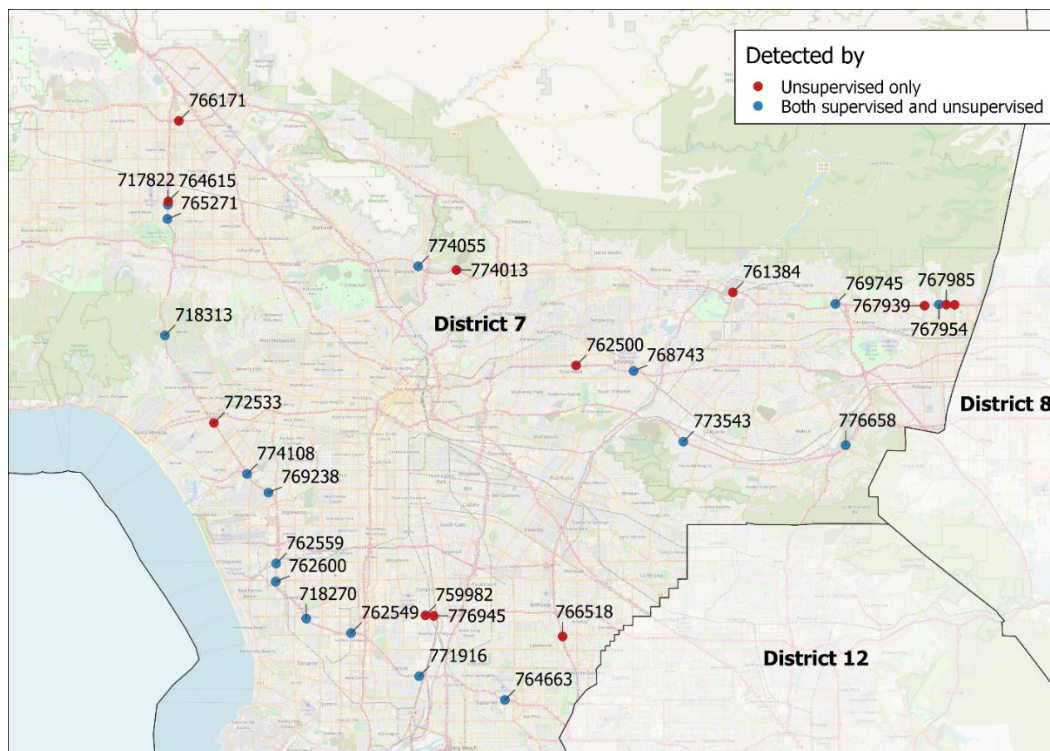


Figure 4-4: Map of Detected misconfigurations in District 7 by unsupervised learning (red dots) and supervised learning (blue dots)

Table 4-3 provides a breakdown of the manual evaluation results, showing how many sensors fell into each of the manual diagnosis criteria from Table 4-1 (i.e., misconfigured, corrupted, indeterminate, or OK). A more detailed table of detection results is presented in Appendix A – Detection Results Table. Table 4-3 also breaks down detection by machine learning method depending on whether it was detected by supervised, unsupervised, or by both methods. It is possible for each sensor to be detected by either, both, or neither of the supervised or unsupervised machine learning methods, the right-most four columns of Table 4-3 are visually conceptualized in Figure 4-5, showing the number of sensors flagged by each of the two algorithms.

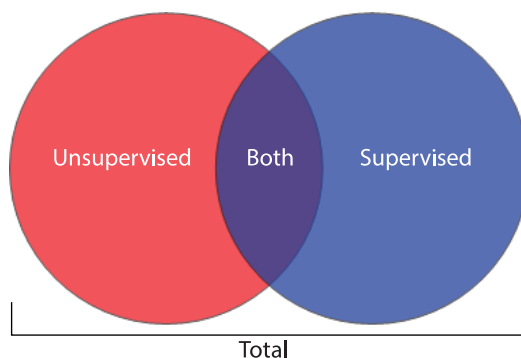


Figure 4-5: Conceptual Venn diagram showing the intersection of sensors detected by unsupervised and supervised methods

Potential Erroneous Degradation of High Occupancy Vehicle (HOV) Facilities – Final Report

The first of these columns “Both Supervised and Unsupervised” shows the number of sensors flagged by both algorithms (the intersection of both sets). The second of these columns “Supervised Only” shows the number of sensors flagged by the supervised algorithm, but not flagged by the unsupervised algorithm. To obtain all sensors flagged by the supervised algorithm, one would take the sum of the “Both Supervised and Unsupervised” and “Supervised Only” columns. The third of these columns “Unsupervised Only” shows the number of sensors flagged by the unsupervised algorithm, but not flagged by the supervised algorithm. To obtain all sensors flagged by the unsupervised algorithm, one would take the sum of the “Both Supervised and Unsupervised” and “Unsupervised Only” columns. The fourth of these columns “Total Detections” shows the number of sensors flagged by both algorithms (the union of both sets). This is also equal to the sum of the prior three columns.

Table 4-3: Percentage of diagnosis categories for detection results

	Both supervised and unsupervised		Supervised only		Unsupervised only		Total	
	Count	%	Count	%	Count	%	Count	%
Misconfigured	8	2.5%	0	0%	1	0.3%	9	2.9%
Corrupted	3	1.0%	0	0%	4	1.3%	7	2.2%
Indeterminate	6	1.9%	0	0%	2	0.6%	8	2.5%
OK (false positive)	0	0.0%	0	0%	5	1.6%	5	1.6%
Total detections	17	5.4%	0	0%	12	3.8%	29	9.2%
Total analyzed	314							

One clear result in Table 4-3 is that no sensors were detected by *only* supervised learning, meaning that all potential misconfigured sensors detected supervised learning were also detected by unsupervised learning. For detections by unsupervised learning, the opposite is true where 12 additional sensors were detected by unsupervised learning only. Of the 12 additional sensors detected by the unsupervised learning method, 5 were false positives where the data appeared “OK”. This shows that the supervised method provides a more conservative result with fewer false positives. Unsupervised learning also detected an additional four sensors with a “corrupted” diagnosis and an additional two with “indeterminate” diagnosis. While there does appear to be some amount of trade-off between a more restrictive supervised method and a more inclusive unsupervised method, both machine learning methods performed well.

Overall, 9% of the sensors in the total 314 were flagged as potentially misconfigured, with 4% of those being detected by only the unsupervised method. This means that the machine learning algorithms reviewed the bulk (91% to 95%) of the sensors, reducing the total burden to a handful where more in-depth manual evaluation is required. Of the 9% potential misconfigurations, between 30% and 60% were diagnosed as true misconfigurations, depending on if the probable misconfigurations (i.e., indeterminate) are included. This makes the overall rate of misconfiguration in Caltrans District 7 to be approximately between 3% and 5%, based on these results.

DEGRADATION RESULTS

Through manual evaluation, nine sensors are diagnosed as “misconfigured”, meaning that the traffic data itself appears to be correct, but the data labels are swapped. For each of these nine sensors, a proposed

Potential Erroneous Degradation of High Occupancy Vehicle (HOV) Facilities – Final Report

correction can be deduced through manual evaluation (e.g., the Lane 1 label appears swapped with the HOV label). In these cases, the proposed correction is made, and the degradation results are re-calculated using the data associated with the corrected label. A summary of degradation results is presented in Table 4-4. These results are presented for the morning (AM) and evening (PM) peaks separately because degradation tended to differ by peak hour (i.e., some only were degraded in one peak hour or another).

Table 4-4: Comparison of existing and resolved HOV Degradation ratings

Erroneous HOV ID	Correct ID from ML	Correct ML lane #	% Degradation			% Degradation		
			AM (Erroneous)	AM (Corrected)	Difference	PM (Erroneous)	PM (Corrected)	Difference
718313	718312	Lane 1	90%	61%	-29%	4%	2%	-2%
762549	717742	Lane 1	88%	81%	-7%	87%	0%	-87%
717822	717821	Lane 1	76%	58%	-18%	2%	1%	-2%
762500	717121	Lane 2	61%	22%	-39%	0%	0%	0%
774055	774053	Lane 1	51%	57%	6%	4%	29%	24%
769745	769744	Lane 3	40%	24%	-16%	8%	8%	0%
718270	764604	Lane 2	26%	0%	-26%	88%	88%	0%
769238	718287	Lane 1	4%	0%	-4%	63%	6%	-57%
768743	717152	Lane 4	1%	0%	-1%	92%	41%	-52%
Legend:	Not Degraded (≤10%)		Very Degraded (50 – 74%)	Extremely Degraded (≥75%)				

Overall, there was an improvement in percent degradation across nearly all sensors. This change in degradation percent frequently translated into a change in the discrete degradation status. Only one sensor, sensor #774055, did not improve, changing from “not degraded” to “slightly degraded” in the PM peak. However, upon closer inspection of Table 0-1 and Table 0-2 in Appendix B – Degradation Calculation Results Table reveals that there were only 7 days where data were available. Such a small sample is not likely to provide a reliable result and will exaggerate error. A summary of overall degradation status improvement is presented in Table 4-5 which compares the frequency of degradation status using the erroneous label (in the rows) and the corrected label (in the columns). Cells below the diagonal indicate there was an improvement in degradation status. For example, sensor 762549 was erroneously evaluated as extremely degraded in the PM peak. However, the corrected result shows that it is not degraded at all. This sensor appears in Table 4-5 as a “1” in the bottom left-most cell corresponding to extremely degraded in the bottom row and not degraded in the first column. Several sensors, #768743 and #718270, improved percent degradation to no longer be degraded in one peak hour, and one sensor, #769238, is no longer degraded at all.

Table 4-5: Matrix of degradation status change.

Horizontal and vertical axis indicates corrected and original erroneous status, respectively. Each cell below the diagonal indicates the number of sensors that improved degradation status.

		Corrected sensor status			
		(≤10%) Not Degraded	(10 – 49%) Slightly Degraded	(50 – 74%) Very Degraded	(≥75%) Extremely Degraded
Erroneous sensor status	(≤10%) Not Degraded	6	1	0	0
	(10 – 49%) Slightly Degraded	1	1	0	0
	(50 – 74%) Very Degraded	1	1	1	0
	(≥75%) Extremely Degraded	1	1	2	2

EXTENDED ANALYSIS OVER MULTIPLE TIME PERIODS

One key goal of this project was to identify misconfigured HOV sensors in the field. However only 314 sensors out of 866 had available data during the initial analysis time-period. To address this limitation, additional testing was performed quarterly from 2018 to 2021; results are shown in Table 4-6.

The analysis dates were chosen systematically as the first full week of weekdays of the last month of each quarter. The analysis itself was run using the machine learning model trained from December 6-12th, 2020. This date was used because data from this date along I-210 had no unknown misconfigurations and could be relied on for robust training of the model.

The right-most four columns shown shaded in Table 4-6 show the number of sensors flagged by each of the two algorithms. This is a similar representation as conceptualized in Figure 4-5.

Table 4-6: Viability of HOV sensor data and detection rates

Analysis Date	Total sensors in meta data	Total viable sensors (rate)	Detected by:			Total detections (rate)
			Both Supervised and Unsupervised (rate)	Supervised only (rate)	Unsupervised only (rate)	
Mar. 5-9, 2018 (Q1)	868	329.0 (37.9%)	12.0 (3.6%)	18.0 (5.5%)	18.0 (5.5%)	48.0 (14.6%)
Jun. 4-8, 2018 (Q2)	868	392.0 (45.2%)	10.0 (2.6%)	43.0 (11.0%)	26.0 (6.6%)	79.0 (20.2%)
Sep. 3-7, 2018 (Q3)	870	381.0 (43.8%)	10.0 (2.6%)	37.0 (9.7%)	25.0 (6.6%)	72.0 (18.9%)
Dec. 3-7, 2018 (Q4)	870	440.0 (50.6%)	10.0 (2.3%)	26.0 (5.9%)	30.0 (6.8%)	66.0 (15.0%)
Mar. 4-8, 2019 (Q1)	870	409.0 (47.0%)	16.0 (3.9%)	15.0 (3.7%)	21.0 (5.1%)	52.0 (12.7%)
Jun. 3-7, 2019 (Q2)	870	386.0 (44.4%)	7.0 (1.8%)	27.0 (7.0%)	28.0 (7.3%)	62.0 (16.1%)
Sep. 16-20, 2019 (Q3)	870	390.0 (44.8%)	11.0 (2.8%)	34.0 (8.7%)	25.0 (6.4%)	70.0 (17.9%)
Dec. 2-6, 2019 (Q4)	870	403.0 (46.3%)	14.0 (3.5%)	25.0 (6.2%)	23.0 (5.7%)	62.0 (15.4%)
Mar. 2-6, 2020 (Q1)	870	396.0 (45.5%)	14.0 (3.5%)	24.0 (6.1%)	22.0 (5.6%)	60.0 (15.2%)
Jun. 1-5, 2020 (Q2)	870	324.0 (37.2%)	15.0 (4.6%)	0.0 (0.0%)	15.0 (4.6%)	30.0 (9.3%)
Sep. 7-11, 2020 (Q3)	870	321.0 (36.9%)	18.0 (5.6%)	12.0 (3.7%)	11.0 (3.4%)	41.0 (12.8%)
Dec. 6-12, 2020 (Q4)	870	314.0 (36.1%)	17.0 (5.4%)	0.0 (0.0%)	12.0 (3.8%)	29.0 (9.2%)
Mar. 1-7, 2021 (Q1)	870	338.0 (38.9%)	13.0 (3.8%)	17.0 (5.0%)	18.0 (5.3%)	48.0 (14.2%)
Mean		371.0 (42.7%)	12.8 (3.5%)	21.4 (5.6%)	21.1 (5.6%)	55.3 (14.7%)
Median		386.0 (44.4%)	13.0 (3.5%)	24.0 (5.9%)	22.0 (5.6%)	60.0 (15.0%)
Standard Deviation		40.6 (4.7%)	3.2 (1.2%)	13.0 (3.3%)	6.0 (1.2%)	15.6 (3.3%)

The rate of data availability among the total HOV sensors was consistently below 50%, with an average of 42.66%. The total detection rate is somewhat variable with an average total detection rate from both machine learning methods of 14.7%. It is likely that over time different subsets of sensors are operational or non-operational. As a result, the variability in the detection of potential misconfigurations can be

partially explained by variability in the available pool of sensors providing data during each analysis date range.

Another import pattern is the frequency of sensor detection over time. Some of the detections occur due to corrupted data specific to the date when the sensor data are analyzed. Since sensor operation is constantly changing, many sensors were detected as misconfigured only once or twice. It is likely these rare detections are false positives flagged due to one-off circumstances whereas sensors repeatedly detected as misconfigured are more likely to be truly misconfigured. Figure 4-6 shows the location of all sensors in District 7 and their detection results. Red and blue dots denote detection by supervised or unsupervised learning; respectively, with the dot size indicating detection frequency. Black dots denote no anomaly detection and black Xs denote sensors with no data available for any of the analysis dates.

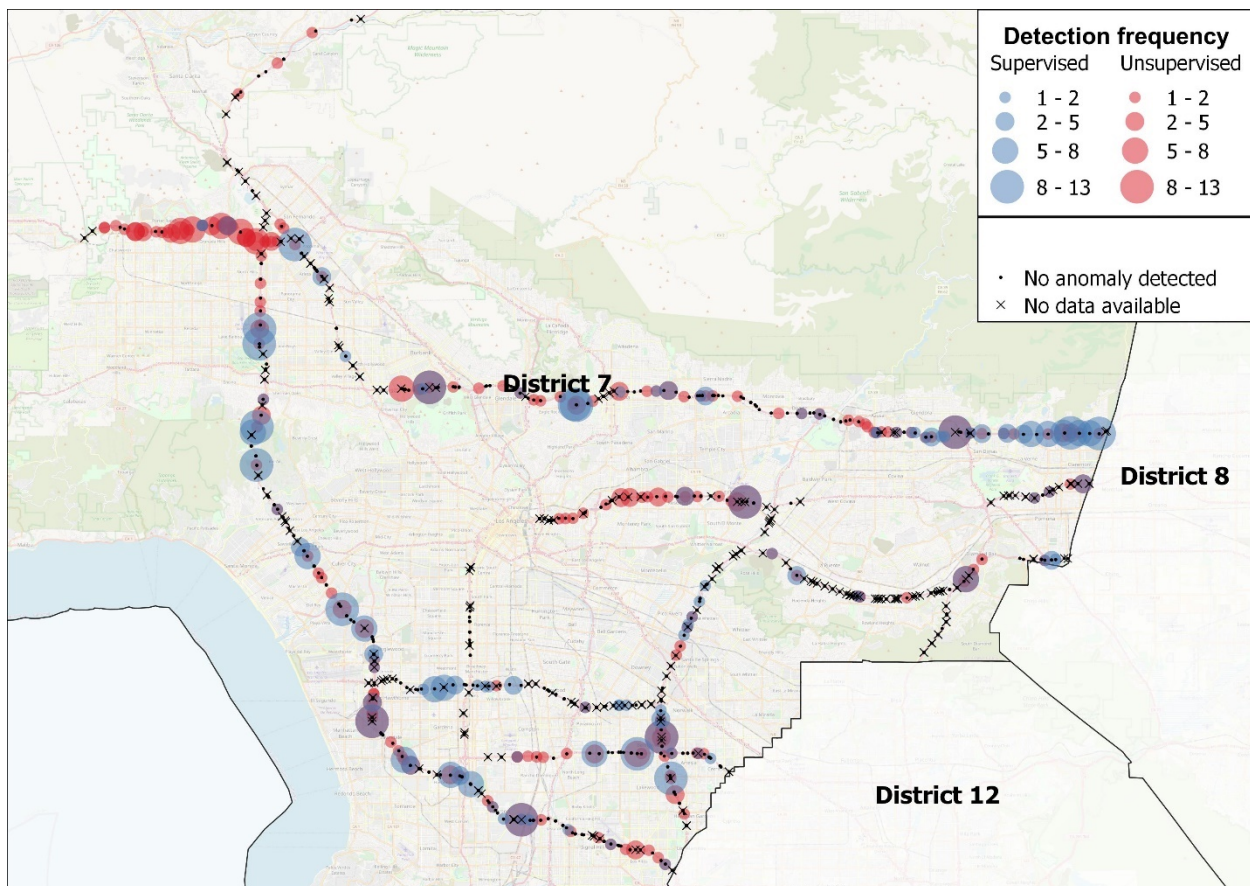


Figure 4-6: Map of misconfiguration detection frequency in District 7 by unsupervised learning (red dots) and supervised learning (blue dots) where larger dots indicate more detections per sensor

These results can be visualized statistically in the distribution shown in Figure 4-6 where the frequency of sensor detection is plotted along the vertical axis and the sensor ID is along the horizontal axis. For clarity, the sensor IDs are removed and plotted in order of detection frequency.

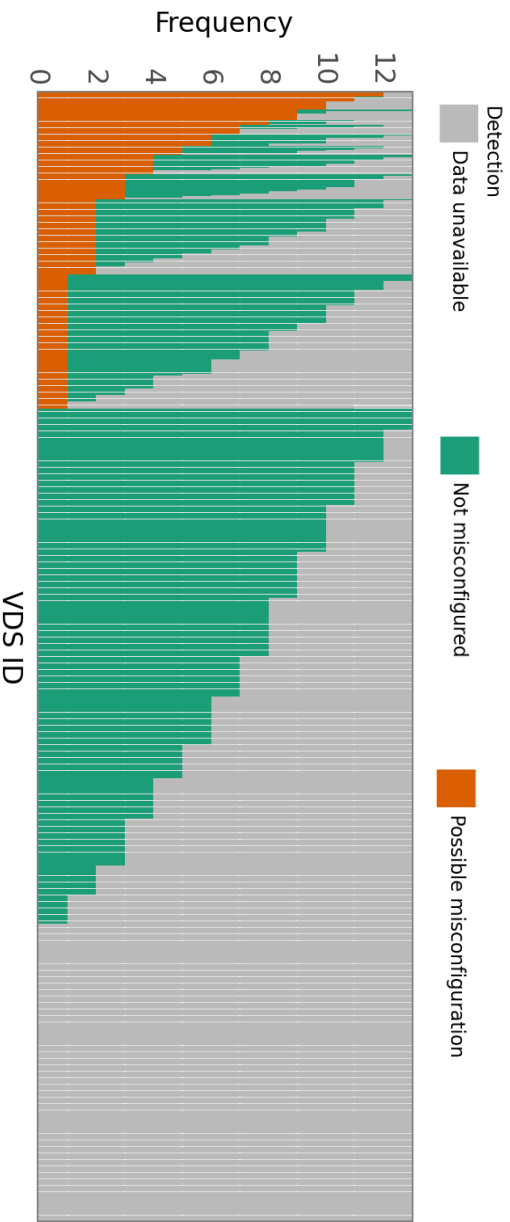


Figure 4-7: Sorted frequency distribution of misconfigured sensor for quarterly analyses from 2018-Q1 to 2021-Q1

A closer view of this distribution with sensor ID labels is presented in Figure 4-7, truncating the sensor IDs to only those detected at least 3 times. A fully labeled visualization is included in the Appendix D – Visualization of Sensor data and misconfiguration detection, this visualization is sorted in order of sensor ID.

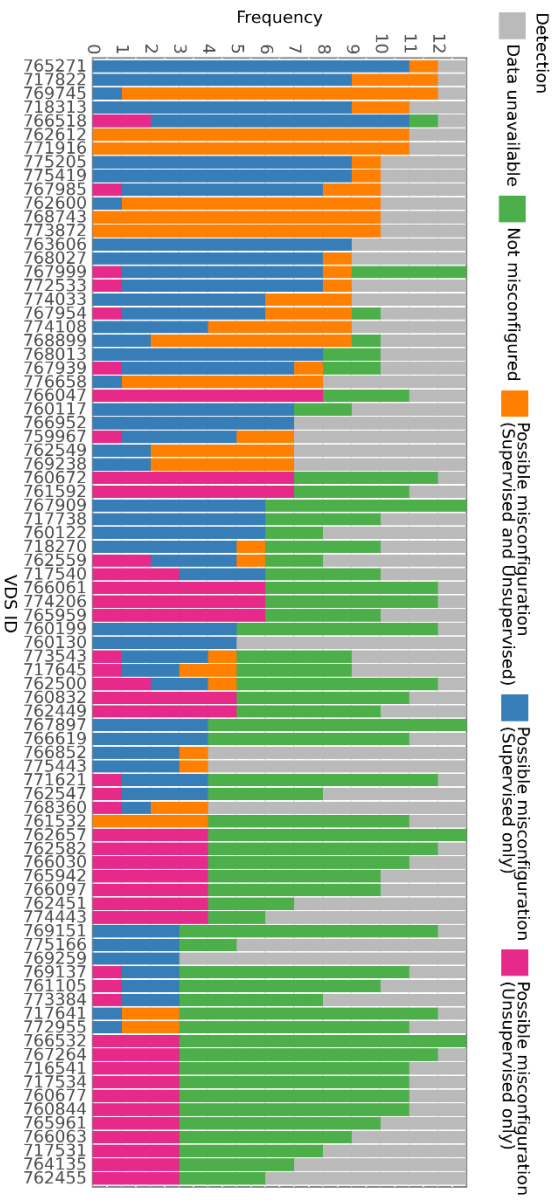


Figure 4-8: Sorted frequency distribution of misconfigured sensor detections for quarterly analyses from 2018-Q1 to 2021-Q1, truncated to only sensors with at least two detections

Most sensors fall into the category of either not having data available or are not misconfigured; but nearly a third of sensors are detected as possibly misconfigured (or at least having some suspicious data characteristics) at some point between 2018-Q1 and 2021-Q1. Of these detections, most of these sensors are detected only once or twice, with a much smaller portion detected more frequently. These more frequent detections are much more likely to be misconfigured and should be prioritized for manual review.

Approximating average misconfiguration rate

The detailed study in this report used data from December 6-12th, 2020 to manually evaluate and diagnose the sensor results for true misconfigurations and false positives. This corresponded to a week of good data on I-210 for training the models, but relatively low data availability in other parts of district 7. During 2018 and 2019, more data is available for the district as a whole. For these other years, the detection of misconfigurations is much greater, reaching as high as 20%. The exact number of true misconfigurations in these other years was not determined as it would require manual review of hundreds of sensors. However, it is possible to approximate the average number of misconfigured sensors based on the overall results.

The detailed analysis results with manual evaluation for December 2020 showed that 17 out of the 29 sensors (59%) flagged by the algorithms were either definitively misconfigured, or likely to be misconfigured. If similar results hold across other years, then about 5% to 8% of HOV sensors in district 7 are likely misconfigured based on this analysis. The range depends on if the 8 indeterminate, but probable misconfigurations, are included with the 9 confirmed misconfigured, for a total of 17. However, this assumed that the proportion of misconfiguration holds.

Alternatively, the frequency of detection can be used to approximate an average rate. Assuming sensors repeatedly detected as misconfigured are less likely to be a random false positive, then higher frequency detections are more likely to be a true misconfiguration. Based on the frequency distribution in Figure 4-7, assuming sensors with at least three detections are considered misconfigured, there are 81 sensors out of a total of about 870 that lie in this category. This yields a misconfiguration rate of approximately 9.3%, which is not far off from the 5-8% when extrapolating the detailed manual analysis.

Approximating average degradation impact

Further extrapolating the average misconfiguration rate (5-9%) by the average length of roadway covered by a sensor (0.64 miles), then there are approximately 12 to 21 miles of erroneously measured HOV lanes at any given time. Based on the proportion of misconfigured sensors that improved degradation rating (38%) in Table 4-5 for either the AM or PM, this means that approximately 5 to 8 miles of HOV lanes are erroneously degraded and are less degraded than currently reporting.

5. CONCLUSIONS

This project titled “Potential Erroneous Degradation of High Occupancy Vehicle (HOV) Facilities” for Task ID 3710 (65A0759) has the primary objective of developing a machine learning algorithm which can detect erroneous HOV sensors for the purpose of minimizing erroneous HOV degradation reporting. Under this primary objective are three goals: Firstly, review existing methods in machine learning to achieve a clear understanding of algorithms that are likely to work for the task of identifying HOV misconfigurations. Secondly, test the effectiveness of the methods identified in the literature survey for the purpose of erroneous HOV sensor detection. Lastly, evaluate HOV degradation results for any misconfigured sensors detected using selected machine learning algorithms over an entire Caltrans district.

5.1. PROJECT OUTPUTS

Findings for these three goals have been described within this final report, as well as in three previous technical memorandums titled “Survey of Data-Mining Methods”, “Performance of Methods”, and “Magnitude of HOV Degradation”. An additional byproduct of this project is a functioning computer program which performs three tasks:

1. Uses machine learning algorithms to detect potential erroneous HOV sensors using 5-minute traffic sensor counts.
2. Calculates percent degradation for HOV sensors in conformance with FHWA guidelines using hourly traffic sensor counts.
3. Compares degradation between erroneous HOV sensors and their corrected values to assess magnitude of change.

5.1. SUMMARY

HOV lane sensors in PeMS are sometimes misconfigured as general-purpose lanes. In this situation, HOV lane data is mistakenly aggregated with general-purpose lane data and vice versa. The purpose of this project was to understand how widespread this problem might be and the extent to which it impacts performance reporting on the degradation of HOV lanes.

This project successfully trained machine learning algorithms to flag potentially misconfigured HOV lane sensors. These algorithms were tested over a well-studied section of the I-210 freeway achieving a minimum of 91% and 82% accuracy for supervised and unsupervised methods, respectively.

The detailed study in this report used data from December 6-12, 2020. This corresponded to a week of good data on I-210 for training the models, but relatively low data availability in other parts of district 7. Of the total 866 sensors in the district, 314 sensors had data of sufficient quality to support the analysis. Among the 314, 29 were automatically flagged as suspicious by the algorithms.

Each of the 29 sensors were then subjected to further manual inspection. The goal was to find its partner—another misconfigured sensor in an adjacent general-purpose lane. For nine sensors, it was possible to determine precisely which sensors had been swapped. Another eight sensors were diagnosed as being indeterminate—meaning that they are probably misconfigured, but further analysis is required to determine which lane of data corresponds to the actual HOV lane.

Potential Erroneous Degradation of High Occupancy Vehicle (HOV) Facilities – Final Report

For the nine corrected misconfigurations, most resulted in an improvement in degradation performance (i.e., the degradation of the HOV lane was less serious than reported). Some improved enough that they were no longer considered degraded in one peak hour, and one sensor was no longer considered degraded at all. However, most sensors overall remained at some degraded level of status.

The two machine learning algorithms, supervised and unsupervised, were then applied for all available HOV PeMS sensors located in district 7 for quarter from 2018 to 2021. Based on these results about 5% to 9% of PeMS HOV sensors are misconfigured in district 7, depending on time-specific factors. This means that approximately 28 to 50 miles of HOV lane are erroneously measured, with approximately 11 to 19 miles (38%) of those reporting an erroneously high degradation rating.

5.2. RECOMMENDATIONS

This report provides a list of nine PeMS sensors in Table 0-1, of Appendix A, that are definitively misconfigured. The table provides the correct information necessary for their configurations to be fixed. In addition, this report provides a prioritized list for district 7 of the most suspicious HOV sensors most likely to be misconfigured in Appendix D. The sensors at the top of the list should be checked and fixed.

In Appendix C, visual examples are displayed showing common data patterns in misconfigured sensors. These examples can be used to inform Caltrans personnel who use this data. They may also be used to help train future data quality algorithms, and as a starting point to begin investigations of HOV lane data in other districts.

In the future, the best method to improve data quality would be to run the analysis described in this report continually, ideally keeping a record of sensors that are chronically flagged as erroneous. Whenever misconfigurations are discovered, they could be corrected. New misconfigurations would be expected to appear regularly whenever non-operational sensors are brought online. This ongoing monitoring would help detect misconfigurations before they are used for analysis, providing a level of data validation for HOV degradation, and for performance reporting.

To facilitate this future effort of ongoing data quality monitoring, the authors have provided the detection algorithm on a GitHub repository: <https://github.com/nick-fournier/hov-degradation>. This repository contains a simple executable program file (.exe) to run the detection algorithm for District 7 as well as the opensource Python code for future development. The repository contains all the code architecture documentation and instructions to run the program.

REFERENCES

- Aggarwal, C. C. (2017) *Outlier Analysis*. Second. Springer.
- Borges, D. M. (no date) *Ensemble Learning: 5 Main Approaches*.
- Connected Corridors (2020) *I-210 Pilot | Connected Corridors Program*. Available at: <https://connected-corridors.berkeley.edu/i-210-pilot-landing-page> (Accessed: 17 June 2020).
- Gandhi, R. (2018) *Support Vector Machine Introduction to Machine Learning Algorithms*.
- Hastie, T., Tibshirani, R. and Friedman, J. (2009) *The Elements of Statistical Learning*. Second. Springer. doi: 10.1007/b94608.
- Hawkins, D. M. (1980) *Identification of Outliers, Identification of Outliers*. doi: 10.1007/978-94-015-3994-4.
- James, G. *et al.* (2013) *An Introduction to Statistical Learning with Applications in R*. Springer. doi: 10.1016/j.peva.2007.06.006.
- Kotu, V. and Deshpande, B. (2018) *Data Science Concepts and Practice*. Second. Morgan Kaufmann. doi: 10.1016/B978-0-12-814761-0.00013-7.
- Markus M. Breunig, Hans-Peter Kriegel, Raymond T. Ng, J. S. (2009) 'LOF: Identifying Density-Based Local Outliers Markus', *International Journal of Gynecology & Obstetrics*, 107, pp. S93–S93. doi: 10.1016/s0020-7292(09)60373-8.
- Mehrotra, K. G., Mohan, C. K. and Huang, H. (2017) *Anomaly Detection Principles and Algorithms*. Springer.
- Murphy, K. P. (2012) *Machine Learning A Probabilistic Perspective*. The MIT Press. doi: 10.1007/978-94-011-3532-0_2.
- Navlani, A. (2018) *KNN Classification using Scikit-learn*.
- Wang, H., Bah, M. J. and Hammad, M. (2019) 'Progress in Outlier Detection Techniques : A Survey', 7.
- Wikipedia (no date) *Random Forest*.

APPENDIX A – DETECTION RESULTS TABLE

Table 0-1: Diagnosis of erroneous sensor detections for data on December 9th, 2020

Sensor ID	Freeway	Dir	Abs Post Mile	Location name	Detected by	Diagnosis	Proposed resolution
717822	405	S	66.032	SHERMAN WAY 1	Both	Misconfigured	Swap Lane 1
718270	405	S	40.242	ARTESIA 1	Both	Misconfigured	Swap Lane 2
718313	405	S	58.502	GETTY / SEPULVEDA	Both	Misconfigured	Swap Lane 1
759982	91	W	3.668	ACACIA	Unsupervised only	OK	
761384	210	W	38.208	IRWINDALE 2	Unsupervised only	Corrupted	
762500	10	W	24.792	WALNUT GROVE	Unsupervised only	Misconfigured	Swap Lane 2
762549	405	N	37.582	NORMANDIE1	Both	Misconfigured	Swap Lane 1
762559	405	N	43.902	EL SEGUNDO 1	Both	Indeterminate	
762600	405	S	42.932	ROSECRANS1	Both	Indeterminate	
764615	405	S	66.222	SHERMAN WAY 2	Unsupervised only	OK	
764663	405	S	27.768	REDONDO	Both	Corrupted	
765271	405	S	65.252	VICTORY 2	Both	Indeterminate	
766171	118	E	43.831	COLUMBUS	Unsupervised only	Corrupted	
766518	605	N	5.732	SOUTH 1	Unsupervised only	Indeterminate	
767939	210	W	49.089	LIVE OAK CANYON	Unsupervised only	Corrupted	
767954	210	W	49.889	TOWNE AV	Both	Corrupted	
767985	210	W	50.289	MOUNTAIN AV	Unsupervised only	Corrupted	
767999	210	W	50.749	INDIAN HILL BL	Unsupervised only	OK	
768743	10	E	28.010	VALLEY	Both	Misconfigured	Swap Lane 4
769238	405	S	48.022	LA TIJERA	Both	Misconfigured	Swap Lane 1
769745	210	W	44.189	NB 57 TO WB 210 CONN	Both	Misconfigured	Swap Lane 3
771916	405	S	32.862	WESTWARD	Both	Corrupted	
772533	405	N	52.932	NATIONAL	Unsupervised only	Indeterminate	
773543	60	E	15.121	W/O TURNBULL	Both	Indeterminate	
774013	134	E	10.660	TOWNSEND	Unsupervised only	OK	
774055	134	W	8.403	FM 2 SB TO 134	Both	Misconfigured	Swap Lane 1
774108	405	S	49.602	JEFFERSON	Both	Indeterminate	
776658	60	W	24.491	GRAND AVE	Both	Indeterminate	
776945	91	W	4.128	ALAMEDA	Unsupervised only	OK	

APPENDIX B – DEGRADATION CALCULATION RESULTS TABLE

Table 0-1: AM Degradation change from reassigned misconfigured lanes

Erroneous HOV ID	Correct ID from ML	Correct ML lane #	AM (Existing Erroneous)						AM (Corrected)						Change in % degraded
			VMT	VHT	Avg Speed	Days with data	Days <45mph	% degraded	VMT	VHT	Avg Speed	Days with data	Days <45mph	% degraded	
718313	718312	Lane 1	203,557	8,941	22.8	100	90		236,022	5,306	44.5	100	61		
762549	717742	Lane 1	179,209	7,585	23.6	86	76		139,092	7,008	19.8	86	70		
717822	717821	Lane 1	139,992	8,142	17.2	122	93		116,964	6,717	17.4	122	71		
762500	717121	Lane 2	327,215	8,355	39.2	92	56		158,306	3,339	47.4	103	23		
774055	774053	Lane 1	177,251	4,053	43.7	71	36		17,391	400	43.5	7	4		
769745	769744	Lane 3	174,370	4,134	42.2	105	42		74,622	1,737	43	105	25		
718270	764604	Lane 2	63,883	1,250	51.1	86	22		46,891	689	68.1	86	0		
769238	718287	Lane 1	153,222	2,509	61.1	75	3		76,581	1,062	72.1	67	0		
768743	717152	Lane 4	165,147	2,690	61.4	105	1		43,277	696	62.2	104	0		

Table 0-2: PM Degradation change from reassigned misconfigured lanes

Erroneous HOV ID	Correct ID from ML	Correct ML lane #	PM (Existing Erroneous)						PM (Corrected)						Change in % degraded
			VMT	VHT	Avg Speed	Days with data	Days <45mph	% degraded	VMT	VHT	Avg Speed	Days with data	Days <45mph	% degraded	
718313	718312	Lane 1	154,417	7,557	20.4	104	96		268,933	6,573	40.9120903	103	42		
762549	717742	Lane 1	82,329	4,493	18.3	85	75		97,785	5,282	18.5116741	85	75		
717822	717821	Lane 1	213,498	5,841	36.6	85	74		141,360	2,479	57.0204894	85	0		
762500	717121	Lane 2	176,747	4,237	41.7	73	46		151,376	2,954	51.2522828	66	4		
774055	774053	Lane 1	187,590	3,375	55.6	104	8		71,018	1241.42545	57.2064156	104	8		
769745	769744	Lane 3	125,168	2,250	55.6	72	3		13,727	277	49.547802	7	2		
718270	764604	Lane 2	174,707	2,931	59.6	98	4		148,378	2132.96294	69.5641154	98	2		
769238	718287	Lane 1	216,681	3,597	60.2	127	3		93,427	1,290	72.4386819	127	1		
768743	717152	Lane 4	209,766	3,796	55.3	89	0		55,243	787.163298	70.1800886	102	0		
Legend:			Not Degraded (≤10%)	Slightly Degraded (10 – 49%)	Slightly Degraded (10 – 49%)	(50 – 74%)									

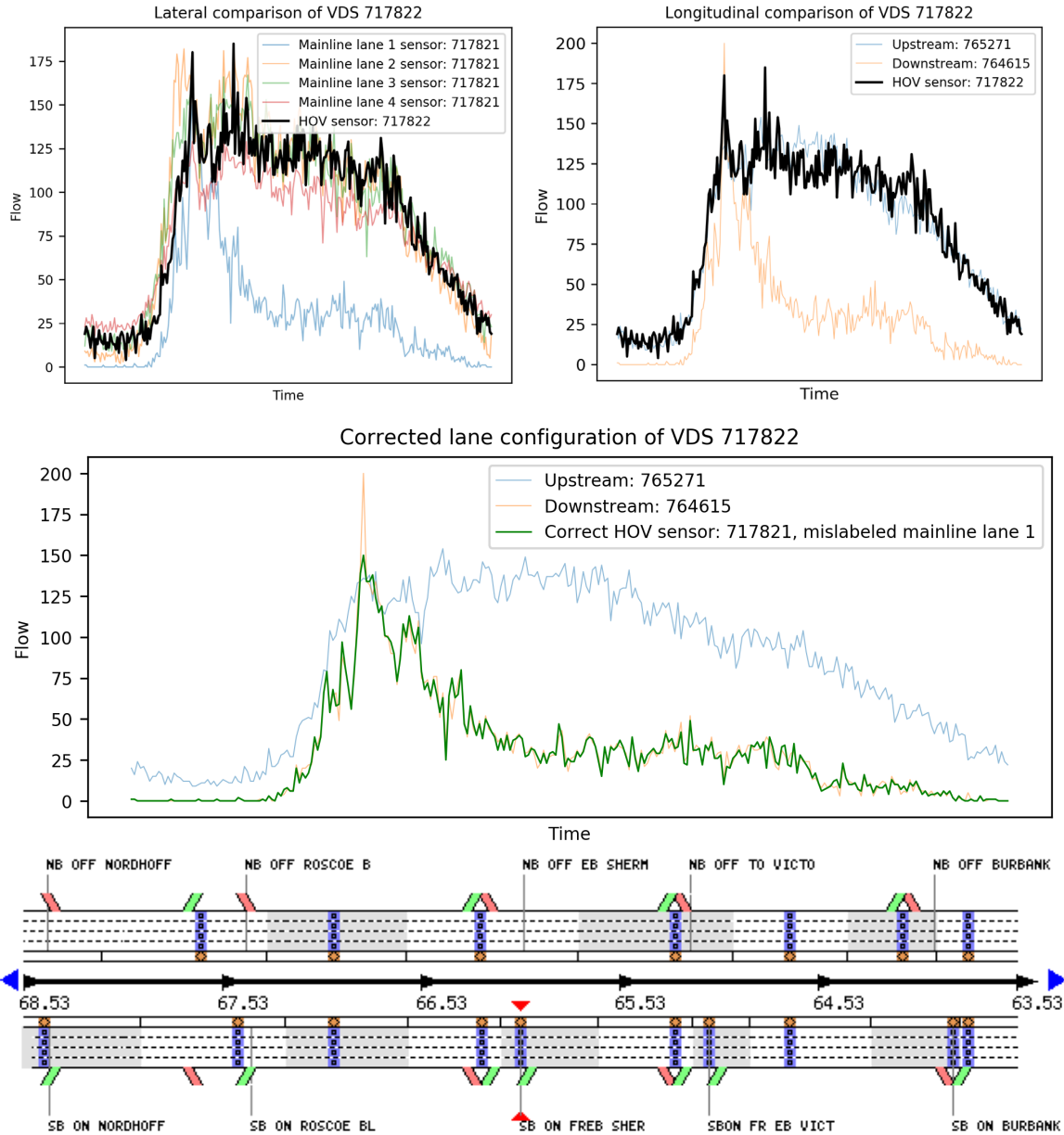
APPENDIX C – COMPARATIVE TRAFFIC FLOW PLOTS

Analysis date	2020-12-06 to 2020-12-12
Total HOVs	866
Analyzed HOVs	314
Identified Misconfigurations (unsupervised)	29
Identified Misconfigurations (supervised)	17

Potential Erroneous Degradation of High Occupancy Vehicle (HOV) Facilities – Final Report

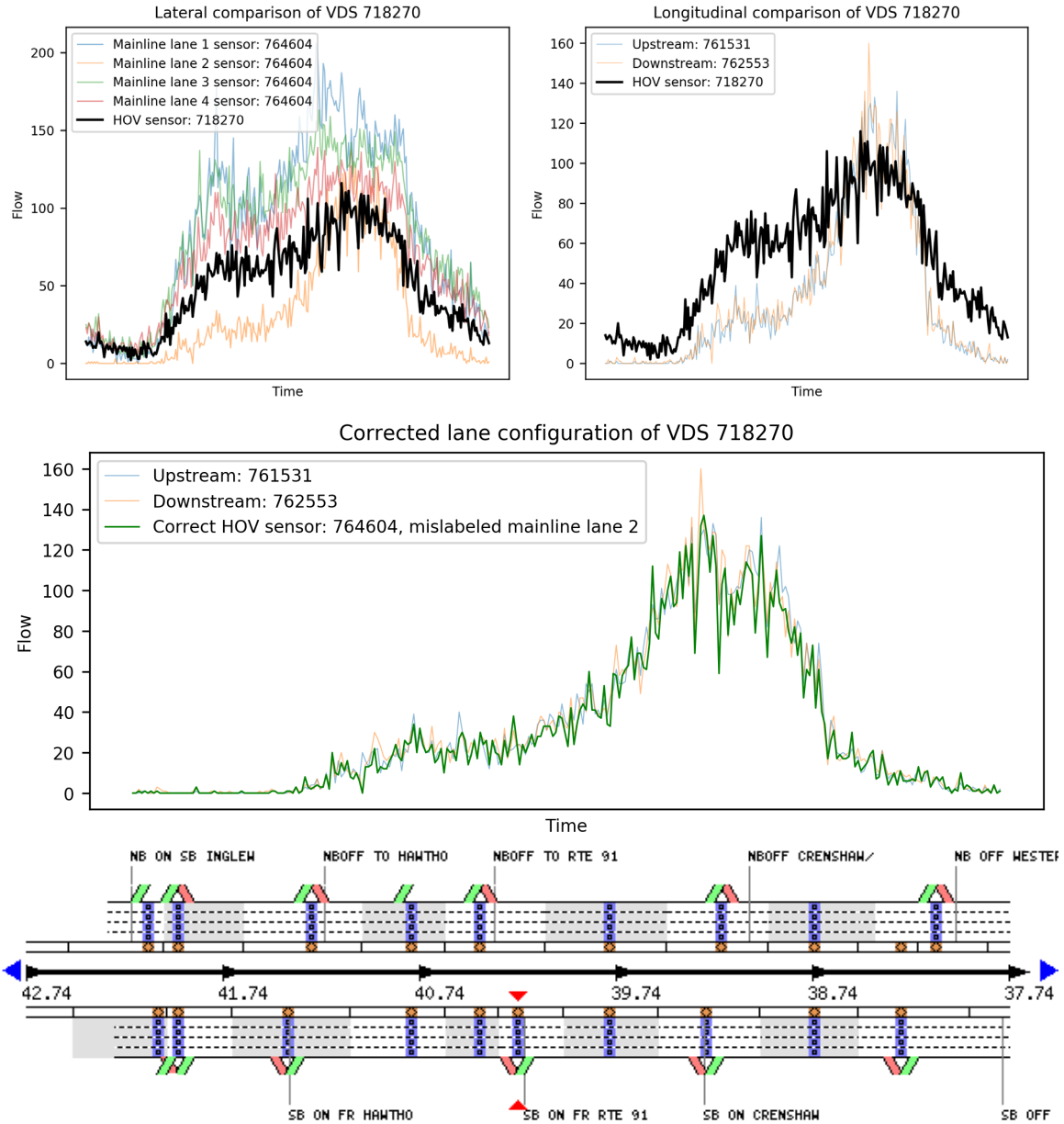
SENSOR: 717822

Misconfiguration detected by both classification and unsupervised methods. Plotted using data for Wednesday, 2020-12-09. Diagnosed as misconfigured with proposed solution to swap Lane 1 with HOV lane.



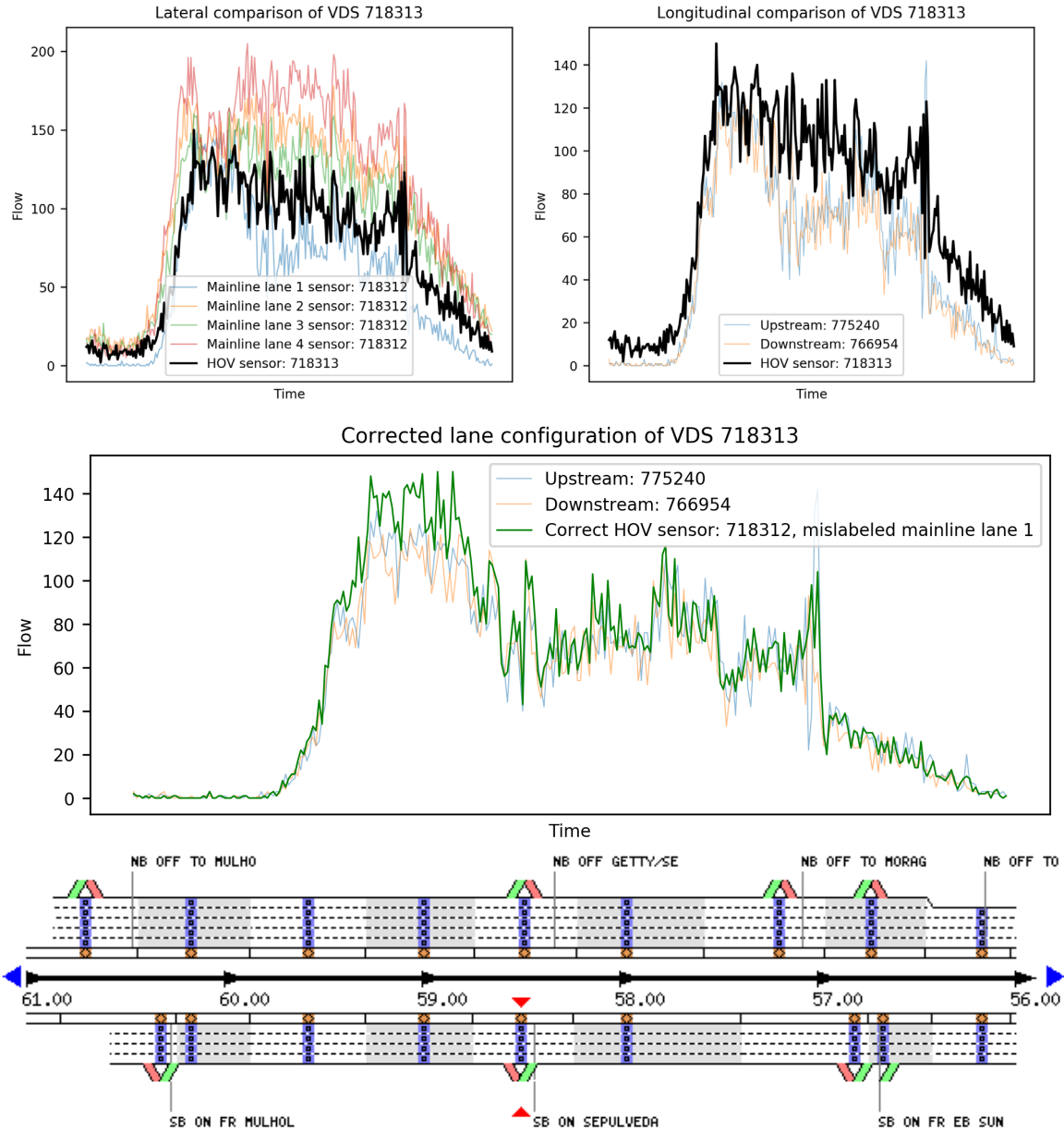
SENSOR: 718270

Misconfiguration detected by both classification and unsupervised methods. Plotted using data for Wednesday 2020-12-09. Diagnosed as misconfigured with proposed solution to swap Lane 2 with HOV lane.



SENSOR: 718313

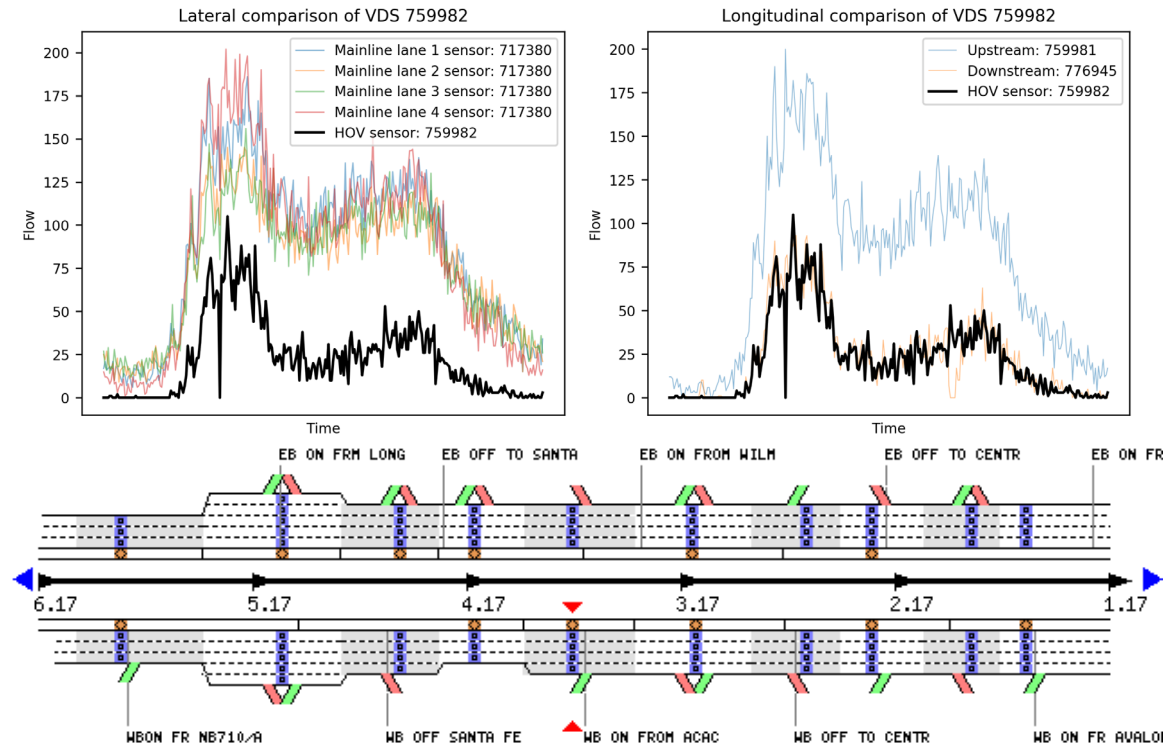
Misconfiguration detected by both classification and unsupervised methods. Plotted using data for Wednesday, 2020-12-09. Diagnosed as misconfigured with proposed solution to swap Lane 1 with HOV lane.



Potential Erroneous Degradation of High Occupancy Vehicle (HOV) Facilities – Final Report

SENSOR: 759982

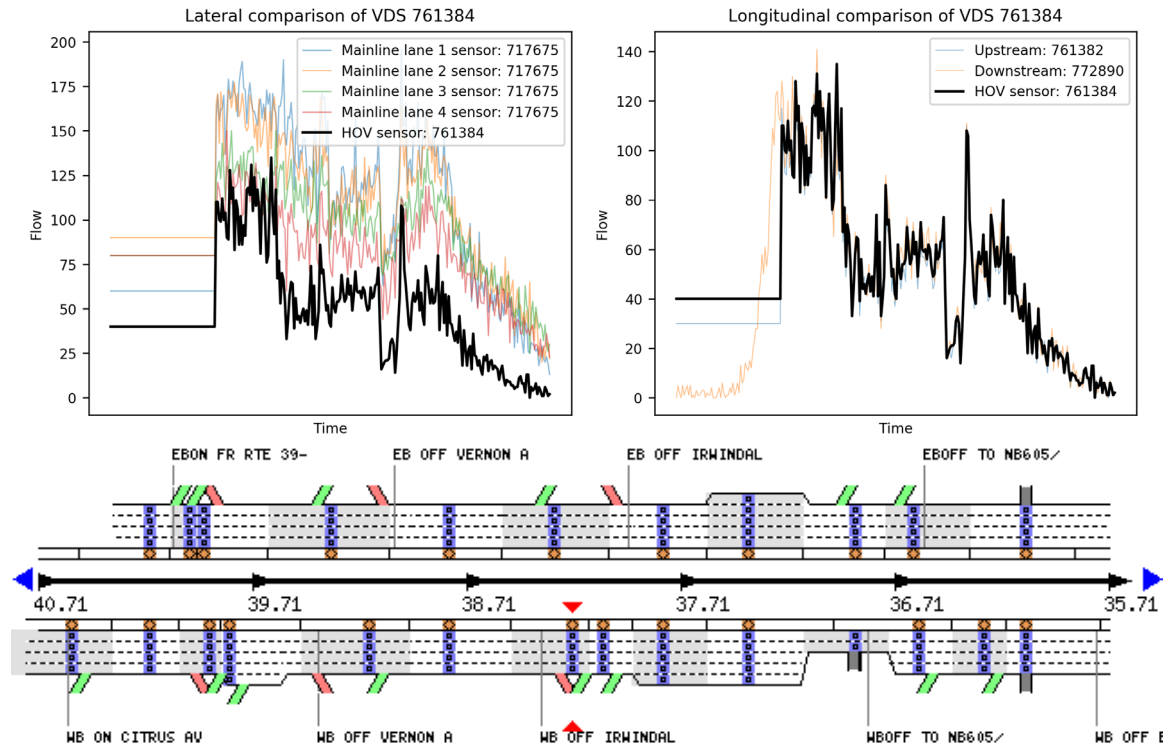
Potential misconfiguration detected by unsupervised method only. Plotted using data for Wednesday, 2020-12-09. Diagnosed as a false positive, data and label are correct. It was likely detected as erroneous because the upstream sensor #759981 is possibly erroneous and thus does not match.



Potential Erroneous Degradation of High Occupancy Vehicle (HOV) Facilities – Final Report

SENSOR: 761384

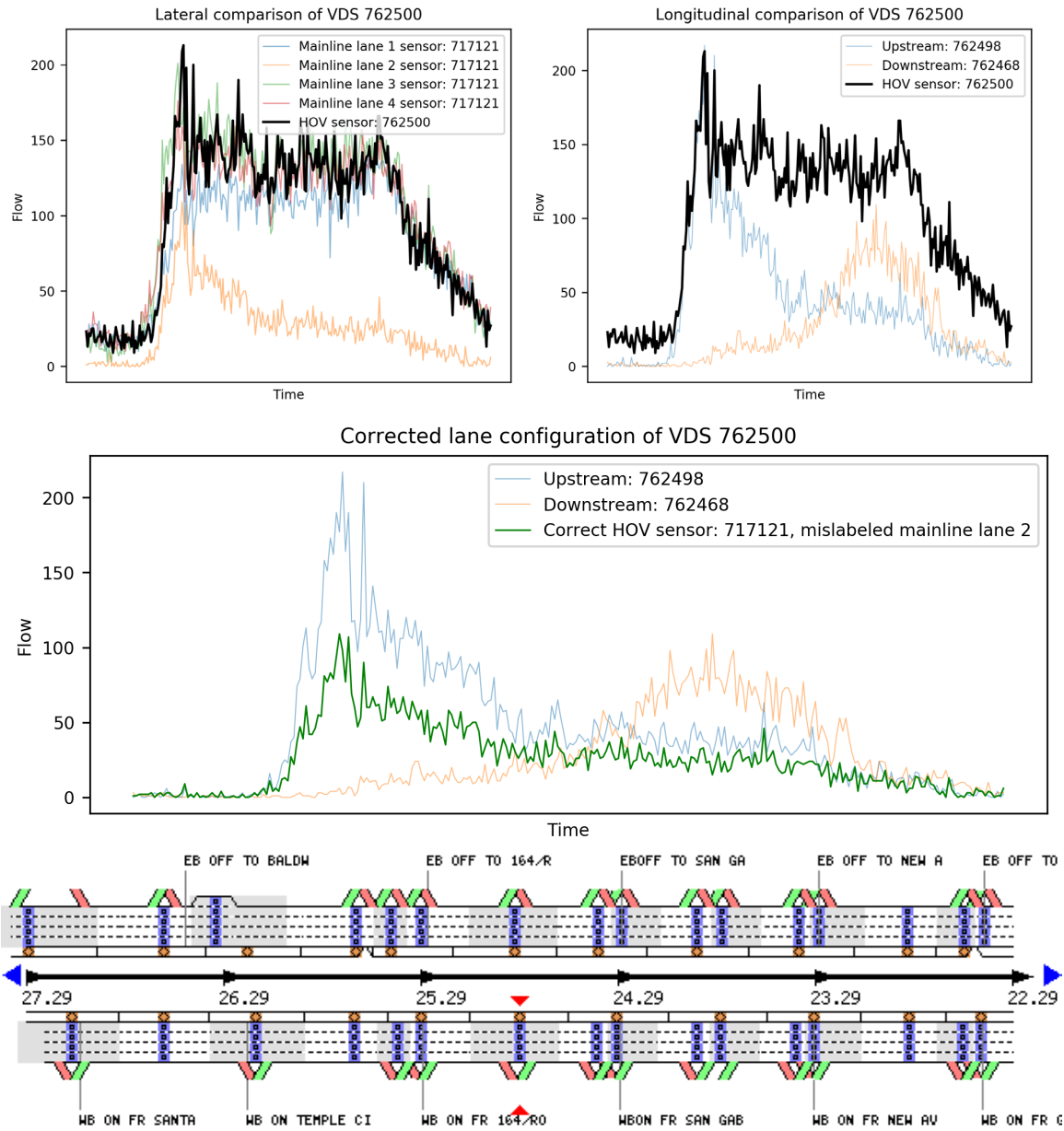
Potential misconfiguration detected by unsupervised method only. Plotted using data for Wednesday, 2020-12-09. Diagnosed as corrupted, which is visually evident in the missing data, represented by the perfectly horizontal/vertical line sections in the plots.



Potential Erroneous Degradation of High Occupancy Vehicle (HOV) Facilities – Final Report

SENSOR: 762500

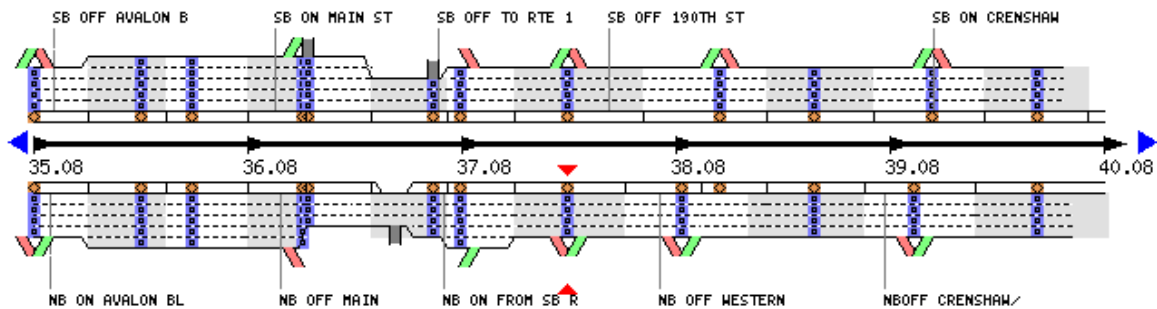
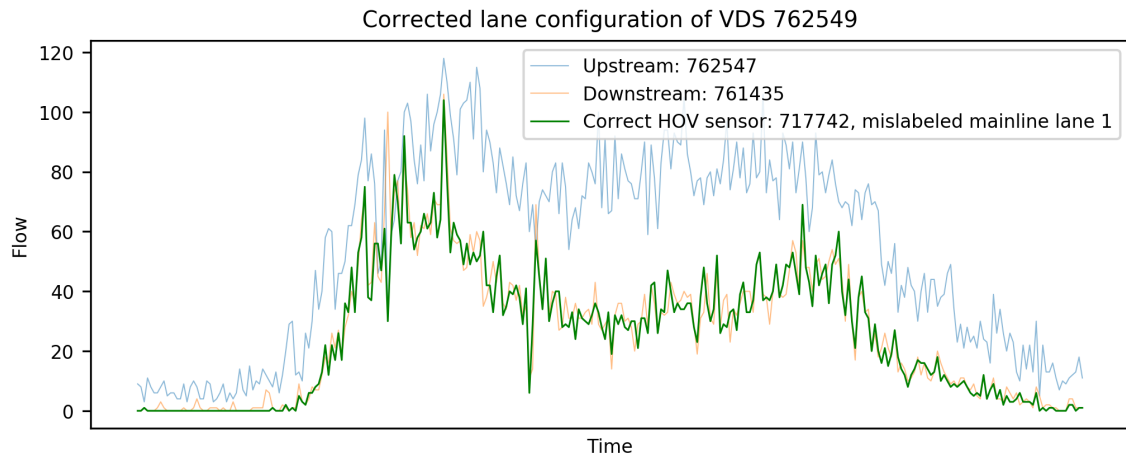
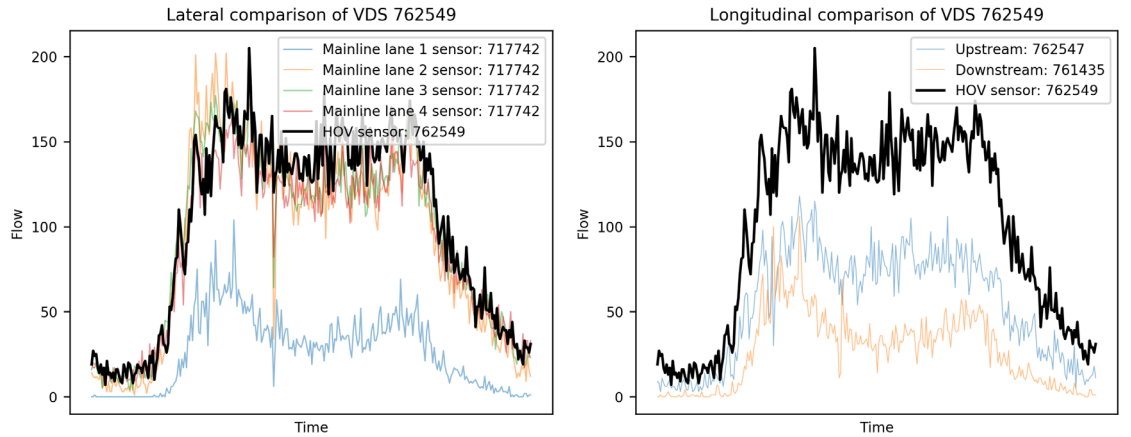
Misconfiguration detected by unsupervised method only. Plotted using data for Wednesday, 2020-12-09. Diagnosed as misconfigured with proposed solution to swap Lane 2 with HOV lane.



Potential Erroneous Degradation of High Occupancy Vehicle (HOV) Facilities – Final Report

SENSOR: 762549

Misconfiguration detected by both classification and unsupervised methods. Plotted using data for Wednesday, 2020-12-09. Diagnosed as misconfigured with proposed solution to swap Lane 1 with HOV lane.

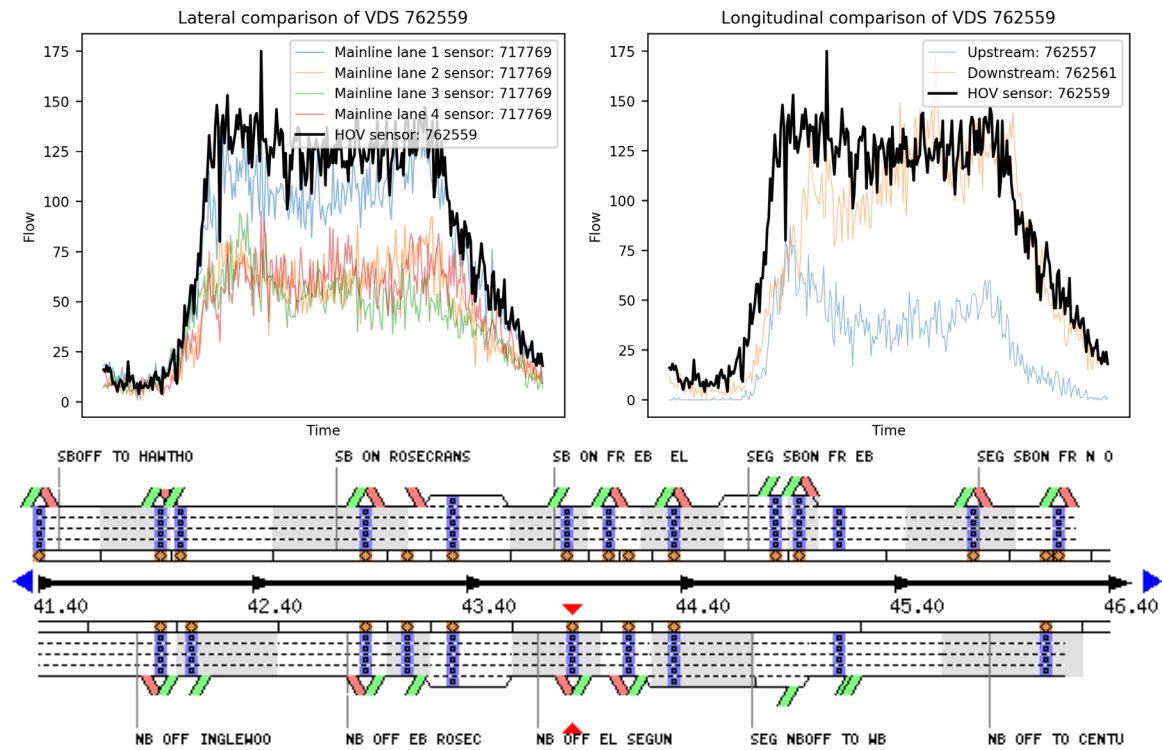


Potential Erroneous Degradation of High Occupancy Vehicle (HOV) Facilities – Final Report

SENSOR: 762559

Potential misconfiguration detected by both classification and unsupervised methods. Plotted using data for Wednesday, 2020-12-09.

This sensor is almost certainly misconfigured, but additional analysis is required. It was diagnosed as indeterminate because the correct HOV lane is unclear. It was detected as erroneous because the HOV lane flow profile is non-zero during nighttime flows and does not match the upstream sensor's flow profile.

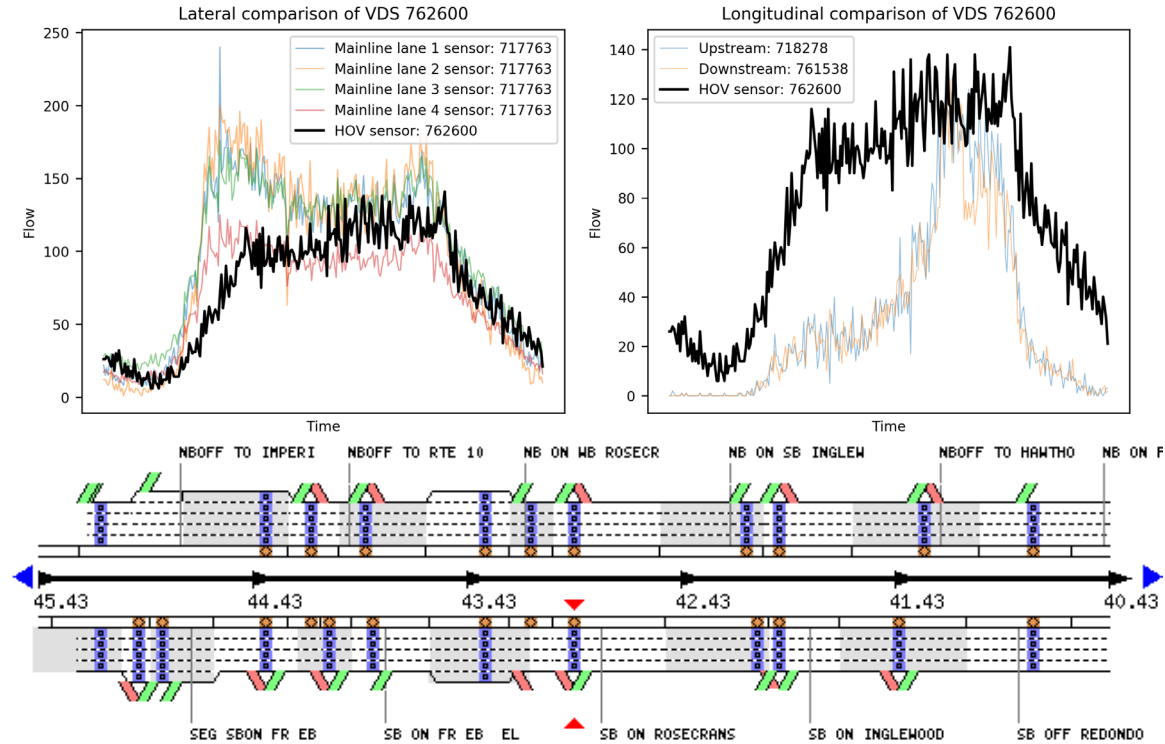


Potential Erroneous Degradation of High Occupancy Vehicle (HOV) Facilities – Final Report

SENSOR: 762600

Potential misconfiguration detected by both classification and unsupervised methods. Plotted using data for Wednesday, 2020-12-09.

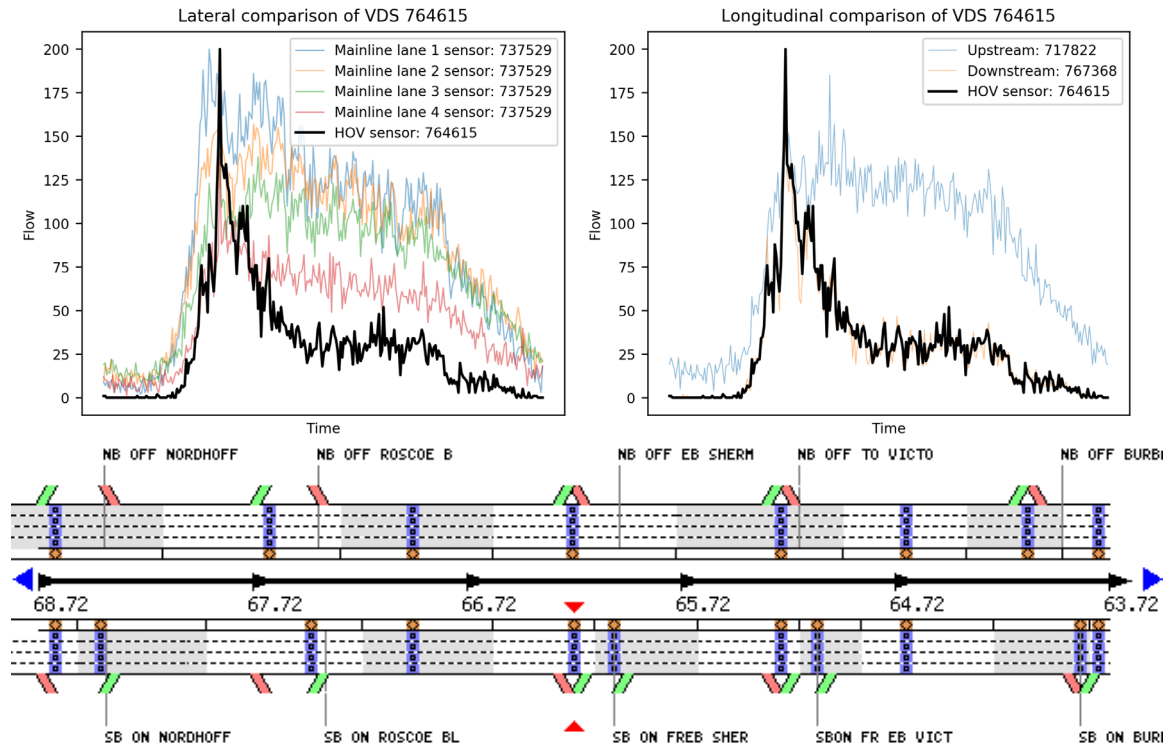
This sensor is likely misconfigured, but additional analysis is required. It was diagnosed as indeterminate because the correct HOV lane is unclear. It was detected as erroneous because the HOV lane flow profile is non-zero during nighttime flows and does not match the upstream sensor's flow profile.



Potential Erroneous Degradation of High Occupancy Vehicle (HOV) Facilities – Final Report

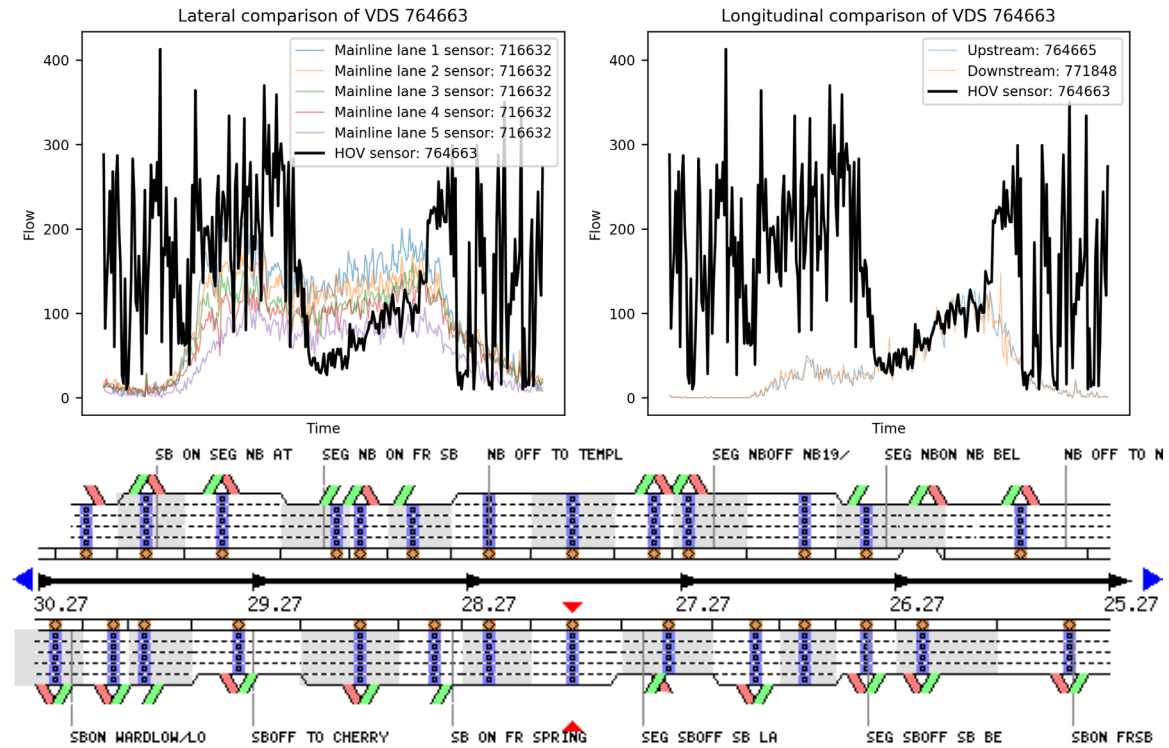
SENSOR: 764615

Potential misconfiguration detected by unsupervised method only. Plotted using data for Wednesday, 2020-12-09. Diagnosed as a false positive, data and label are correct. It was likely detected as erroneous because the upstream sensor #717822 is erroneous and thus does not match.



SENSOR: 764663

Potential misconfiguration detected by both classification and unsupervised methods. Plotted using data for Wednesday, 2020-12-09. Diagnosed as corrupted, which is visually evident with the erratic traffic flow profile.

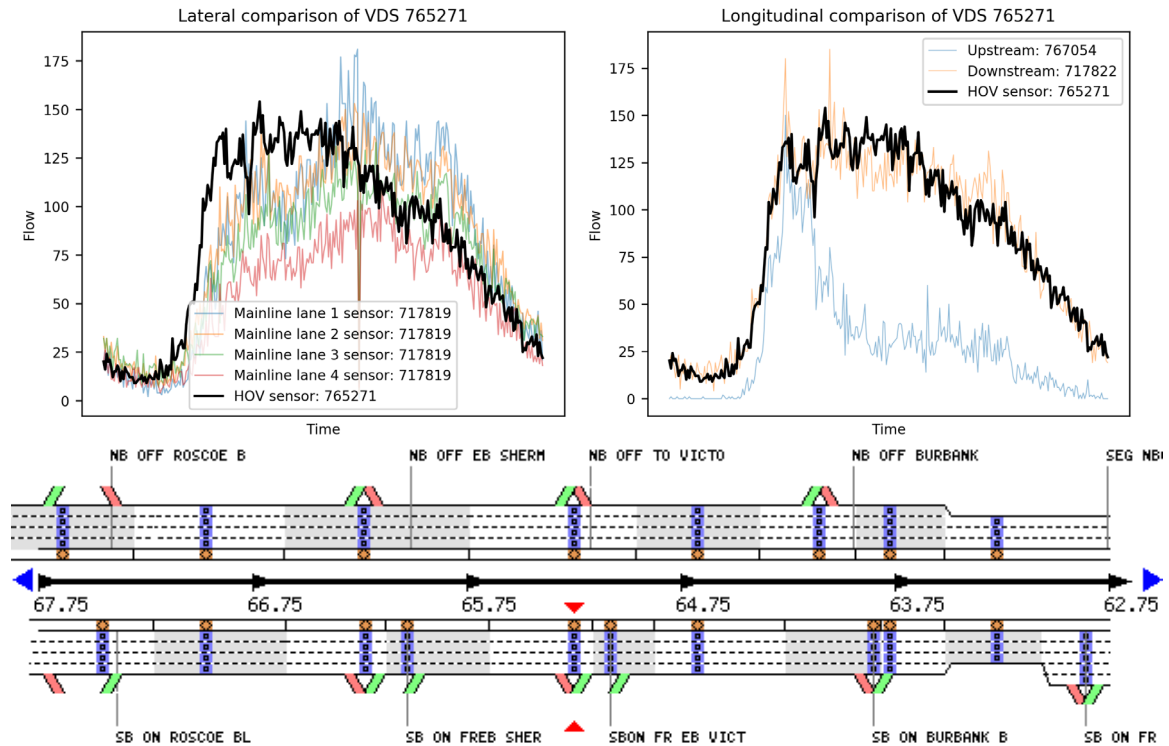


Potential Erroneous Degradation of High Occupancy Vehicle (HOV) Facilities – Final Report

SENSOR: 765271

Potential misconfiguration detected by both classification and unsupervised methods. Plotted using data for Wednesday, 2020-12-09.

This sensor is likely misconfigured, but additional analysis is required. It was diagnosed as indeterminate because the correct HOV lane is unclear. It was detected as erroneous because the HOV lane flow profile is non-zero during nighttime flows and does not match the upstream sensor's flow profile.

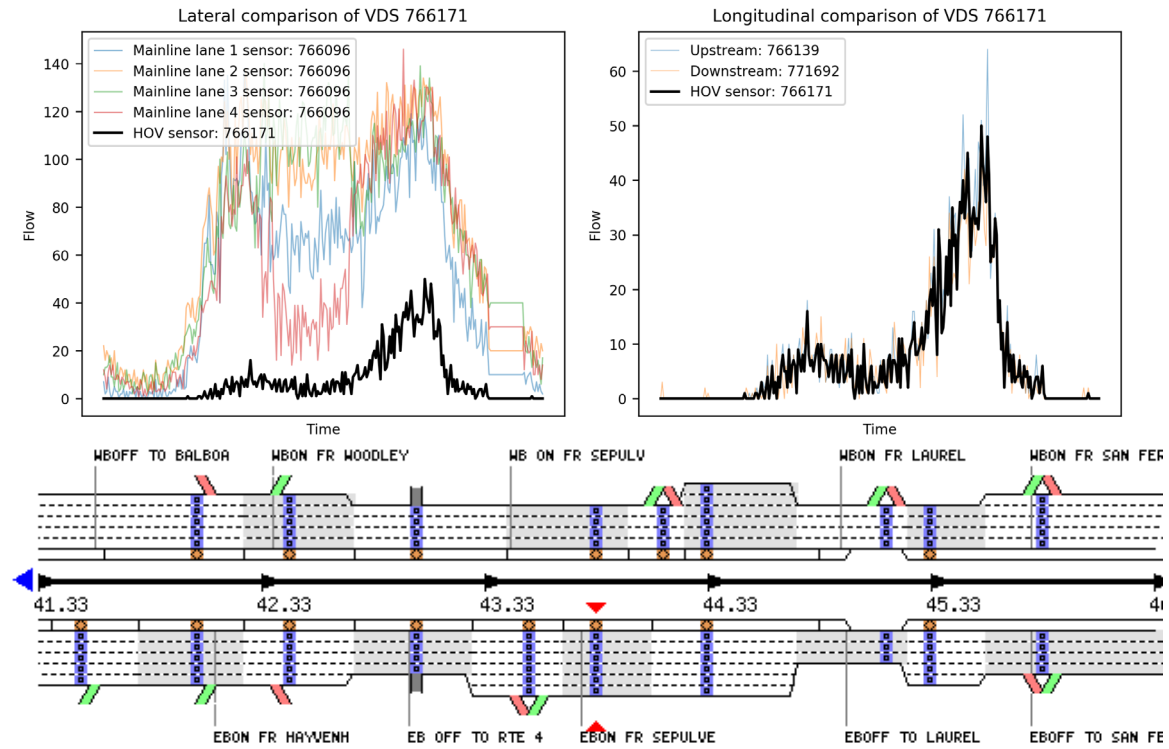


Potential Erroneous Degradation of High Occupancy Vehicle (HOV) Facilities – Final Report

SENSOR: 766171

Potential misconfiguration detected by unsupervised method only. Plotted using data for Wednesday, 2020-12-09.

Judging from the longitudinal comparison, this sensor is likely to be configured correctly. It was diagnosed as corrupted due to the missing data, represented by the perfectly horizontal/vertical line sections in the plots.

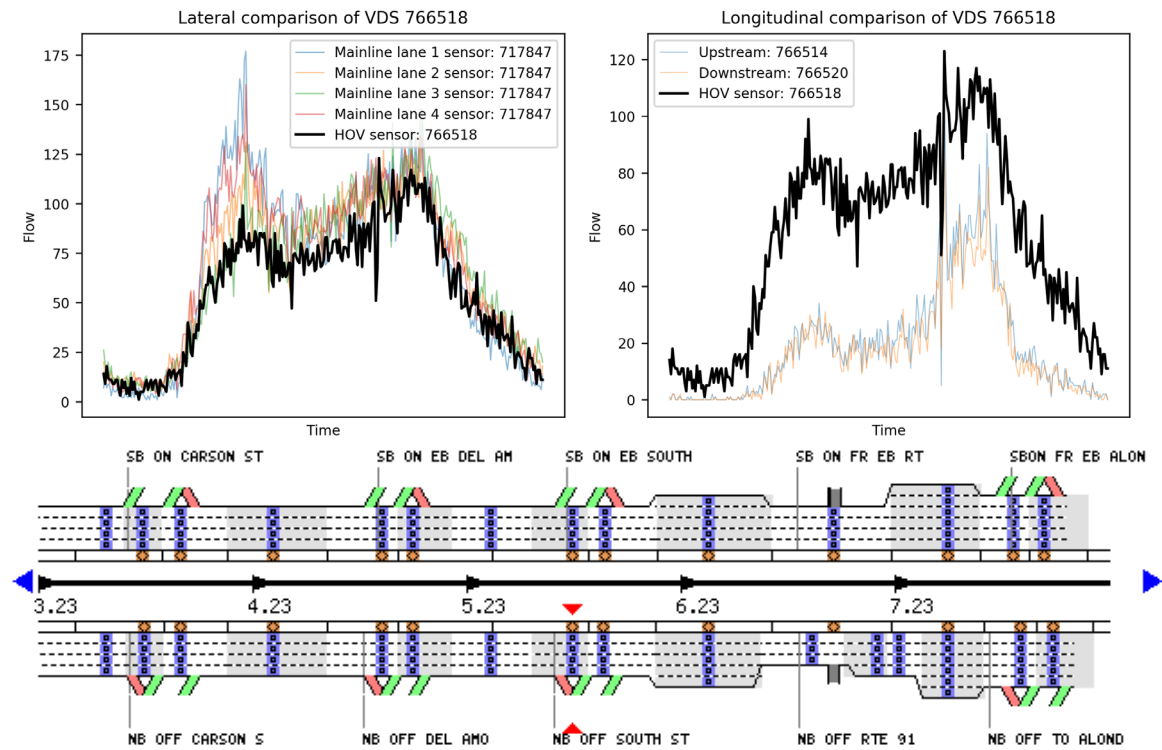


Potential Erroneous Degradation of High Occupancy Vehicle (HOV) Facilities – Final Report

SENSOR: 766518

Potential misconfiguration detected by unsupervised method only. Plotted using data for Wednesday, 2020-12-09.

This sensor could be misconfigured, but additional analysis is required. It was diagnosed as indeterminate because the correct HOV lane is unclear. It was detected as erroneous because the HOV lane flow profile is non-zero during nighttime flows and does not match the upstream sensor's flow profile.

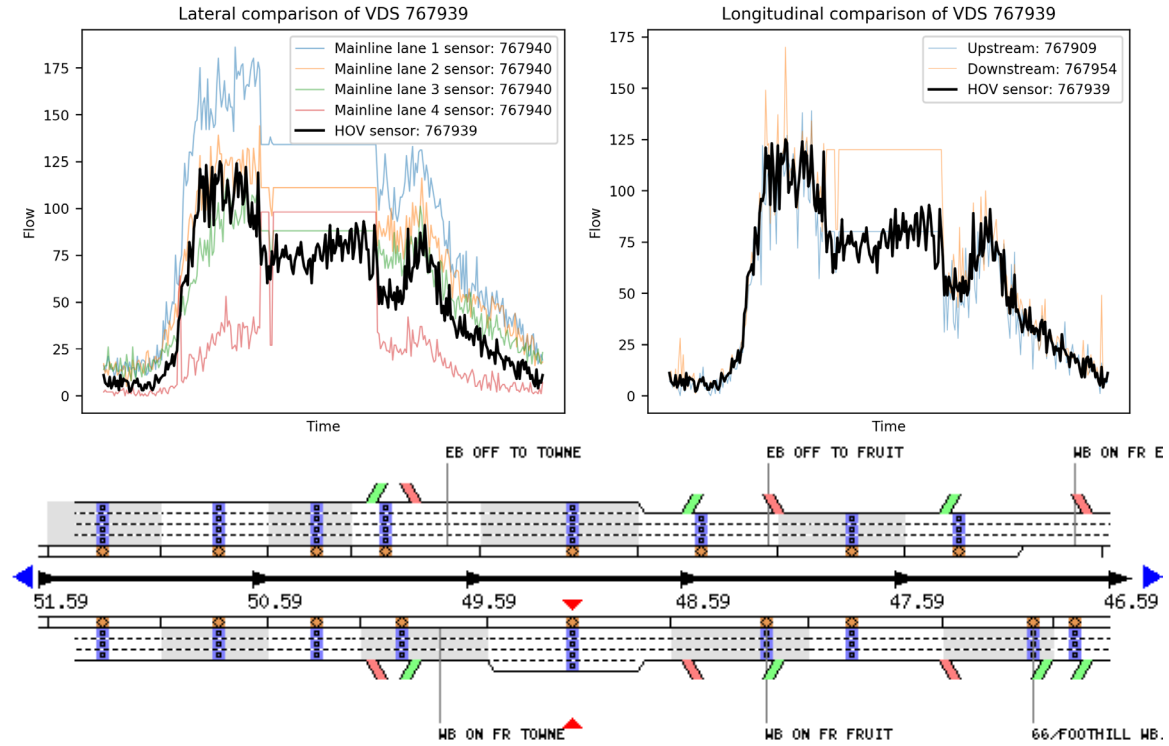


Potential Erroneous Degradation of High Occupancy Vehicle (HOV) Facilities – Final Report

SENSOR: 767939

Potential misconfiguration detected by unsupervised method only. Plotted using data for Wednesday, 2020-12-09.

Judging from the longitudinal comparison, this sensor appears to be correctly configured as an HOV lane. It was diagnosed as corrupted due to the missing data, represented by the perfectly horizontal/vertical line sections in the plots.

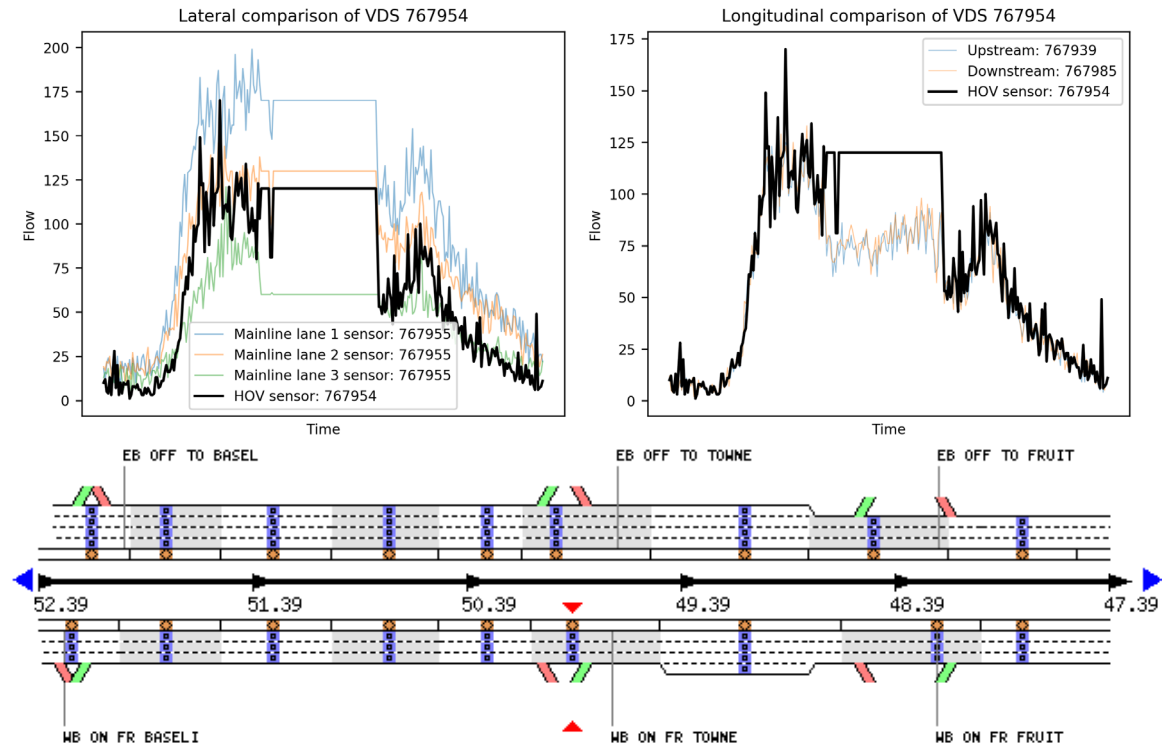


Potential Erroneous Degradation of High Occupancy Vehicle (HOV) Facilities – Final Report

SENSOR: 767954

Potential misconfiguration detected by both classification and unsupervised methods. Plotted using data for Wednesday, 2020-12-09.

Judging from the longitudinal comparison, this sensor appears to be correctly configured as an HOV lane. It was diagnosed as corrupted due to the missing data, represented by the perfectly horizontal/vertical line sections in the plots.

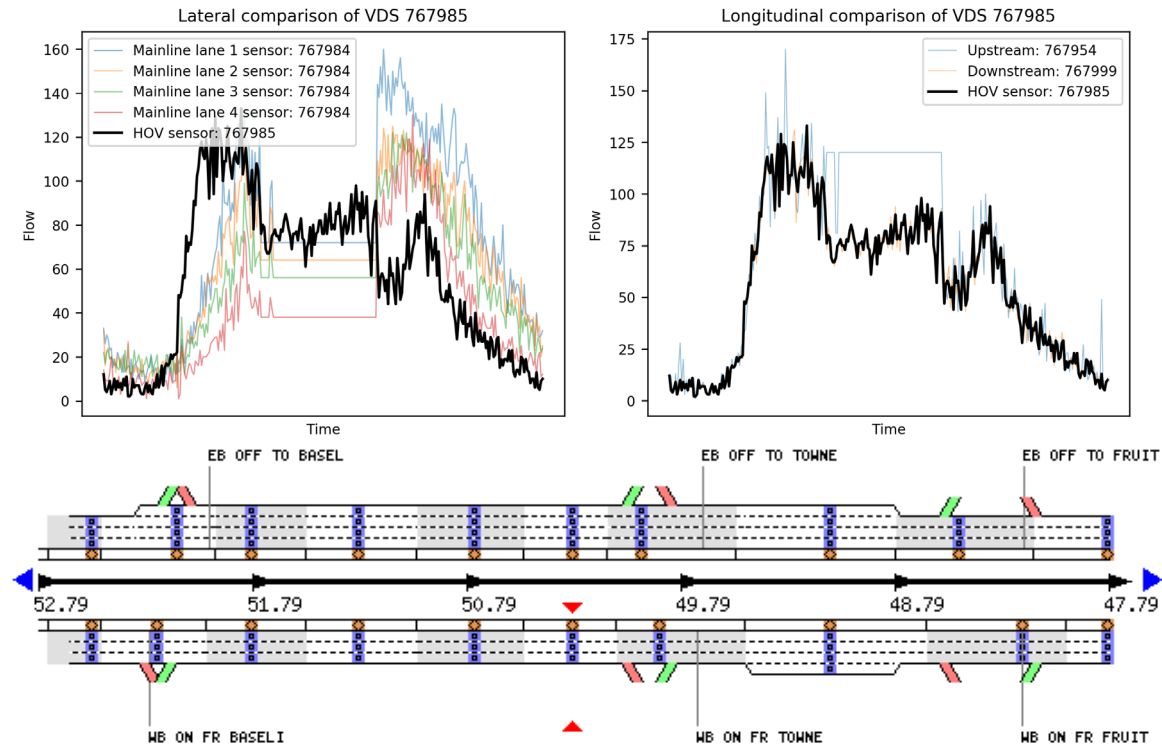


Potential Erroneous Degradation of High Occupancy Vehicle (HOV) Facilities – Final Report

SENSOR: 767985

Potential misconfiguration detected by unsupervised method only. Plotted using data for Wednesday, 2020-12-09.

Judging from the longitudinal comparison, this sensor appears to be correctly configured as an HOV lane. It was diagnosed as corrupted, which is visually evident in the missing data, represented by the perfectly horizontal/vertical line sections in the plots.

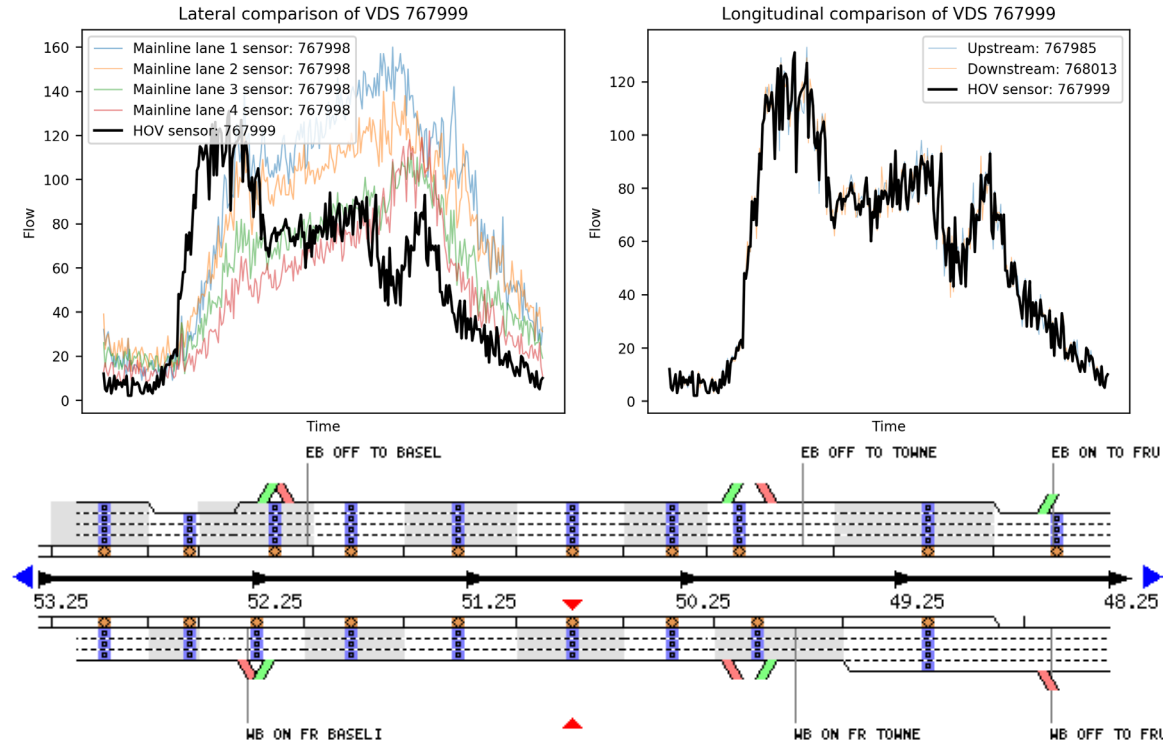


Potential Erroneous Degradation of High Occupancy Vehicle (HOV) Facilities – Final Report

SENSOR: 767999

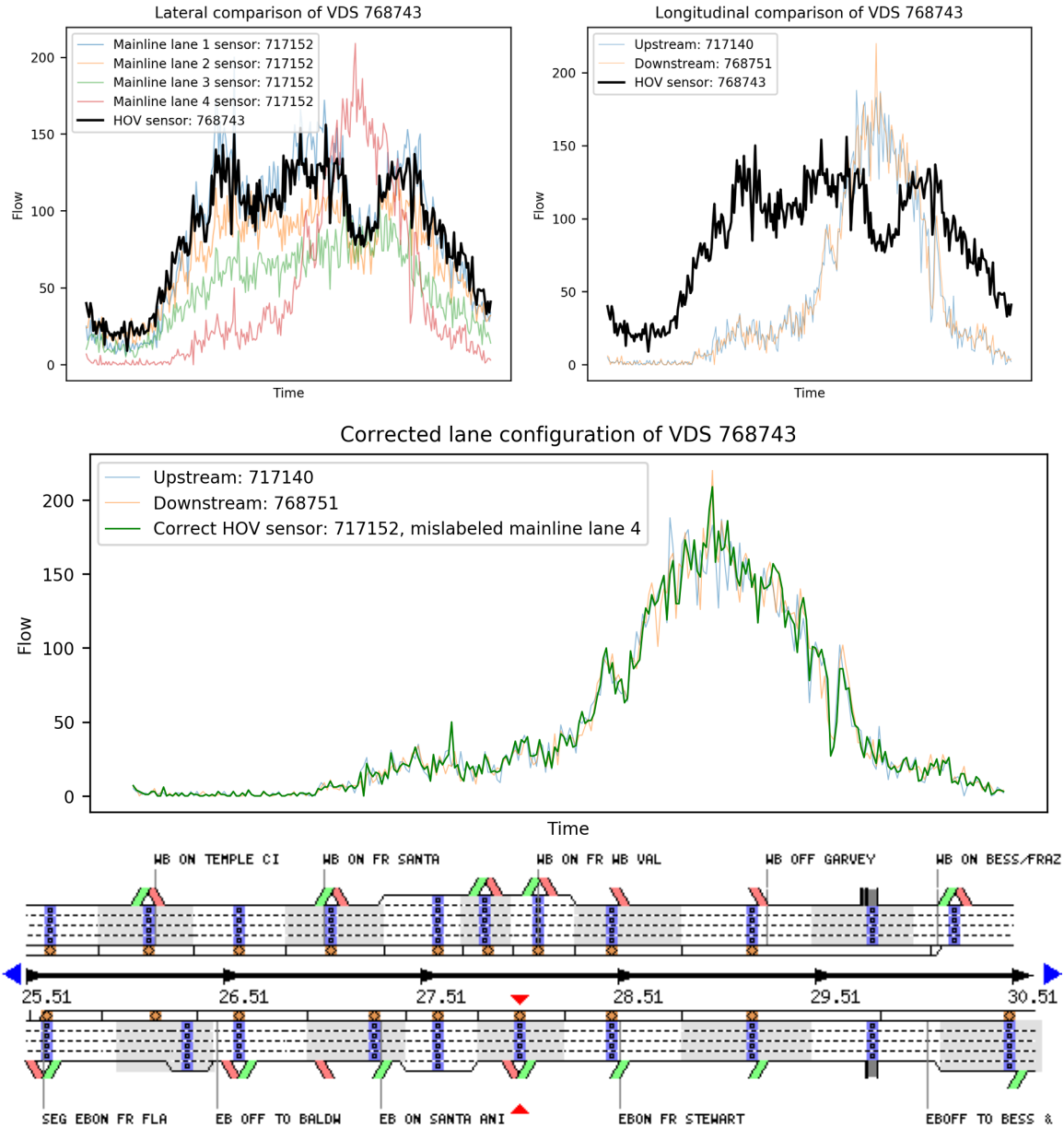
Potential misconfiguration detected by unsupervised method only. Plotted using data for Wednesday, 2020-12-09.

Judging from the longitudinal comparison, this sensor appears to be correctly configured as an HOV lane. Diagnosed as a false positive, data and label are correct. It was likely detected as erroneous because the nighttime flow is non-zero.



SENSOR: 768743

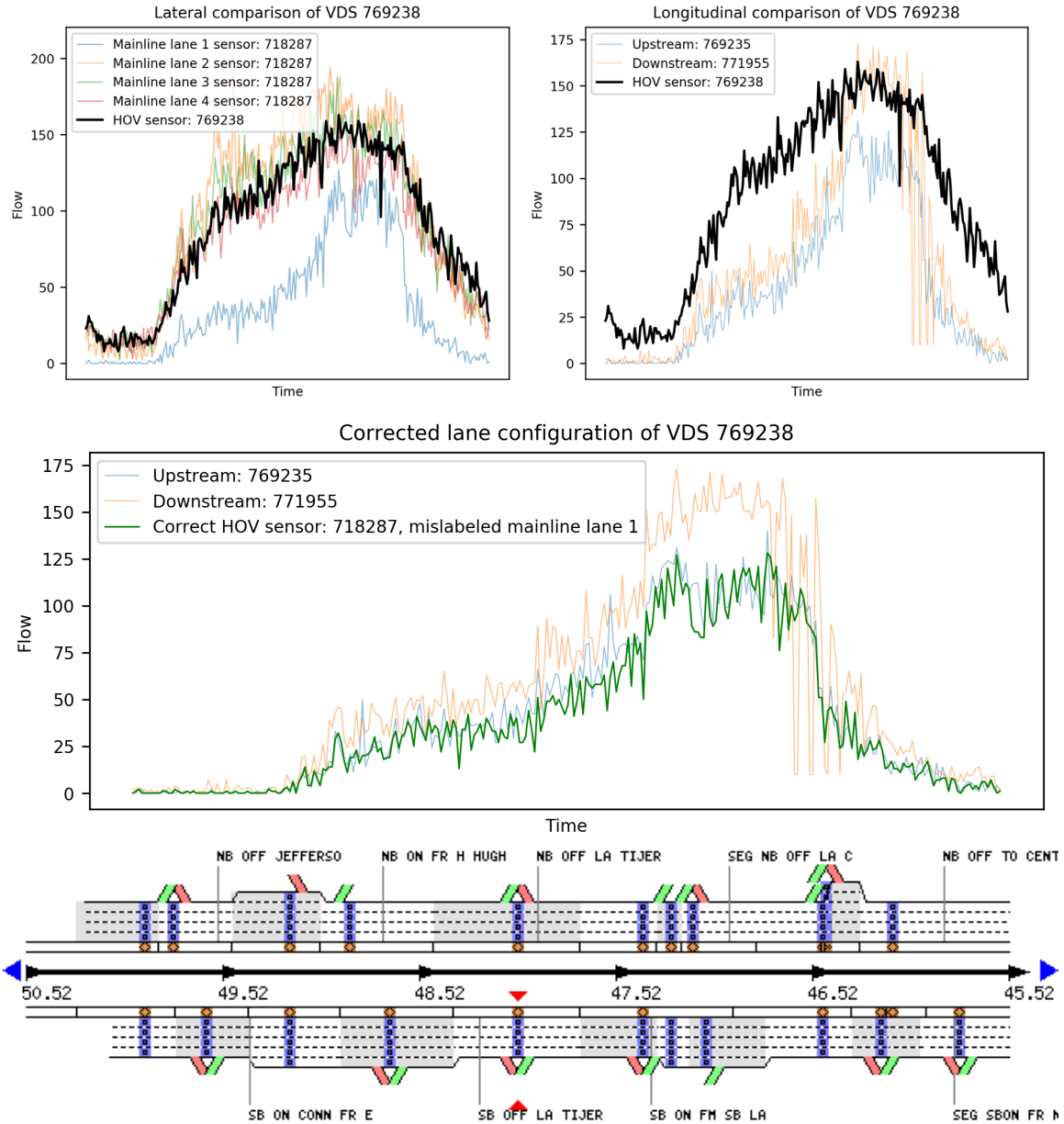
Misconfiguration detected by both classification and unsupervised methods. Plotted using data for Wednesday, 2020-12-09. Diagnosed as misconfigured with proposed solution to swap Lane 4 with HOV lane.



Potential Erroneous Degradation of High Occupancy Vehicle (HOV) Facilities – Final Report

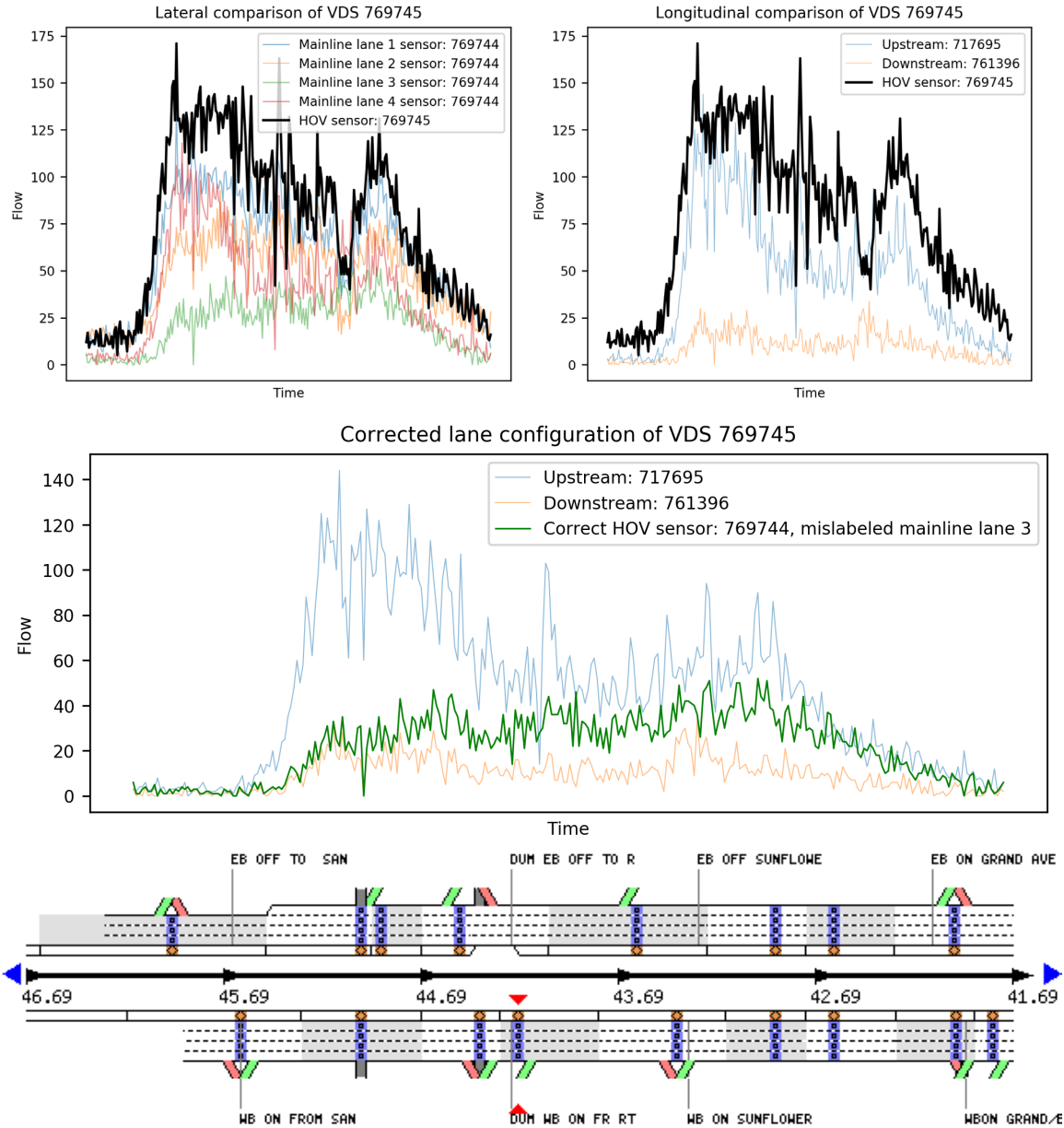
SENSOR: 769238

Misconfiguration detected by both classification and unsupervised methods. Plotted using data for Wednesday, 2020-12-09. Diagnosed as misconfigured with proposed solution to swap Lane 1 with HOV lane.



SENSOR: 769745

Misconfiguration detected by both classification and unsupervised methods. Plotted using data for Wednesday, 2020-12-09. Diagnosed as misconfigured with proposed solution to swap Lane 3 with HOV lane.

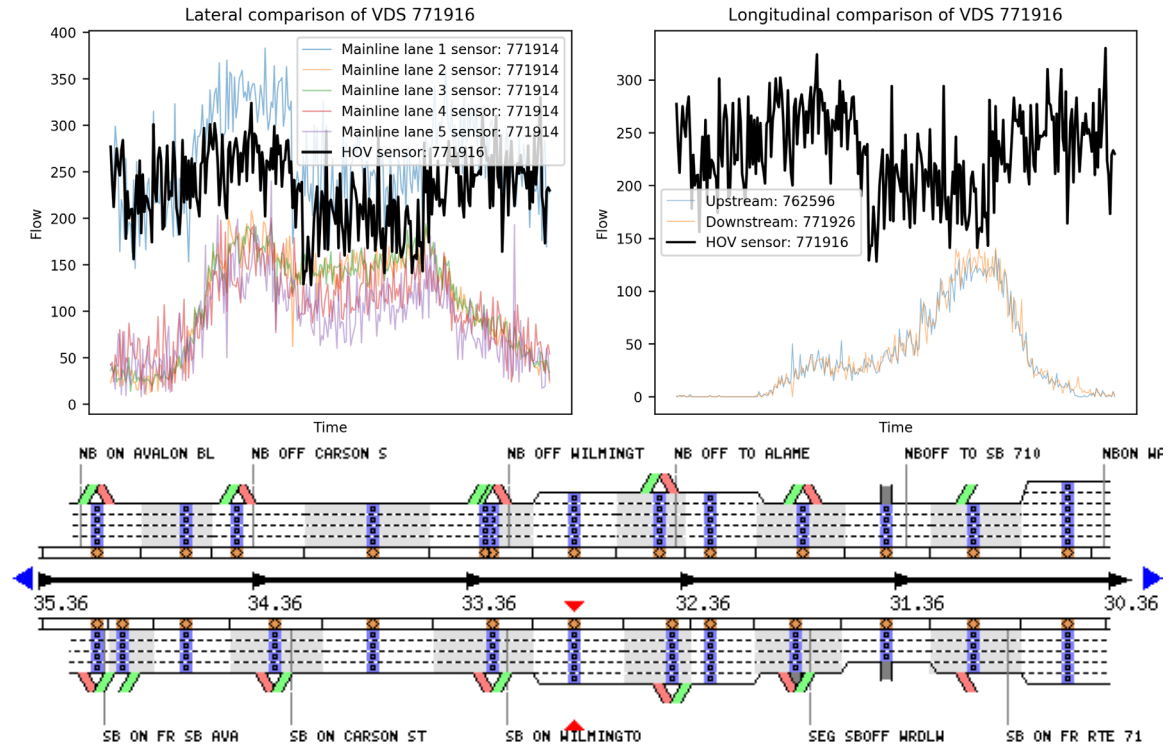


Potential Erroneous Degradation of High Occupancy Vehicle (HOV) Facilities – Final Report

SENSOR: 771916

Potential misconfiguration detected by both classification and unsupervised methods. Plotted using data for Wednesday, 2020-12-09.

Diagnosed as corrupted, which is visually evident with the erratic and unrealistic traffic flow profile.

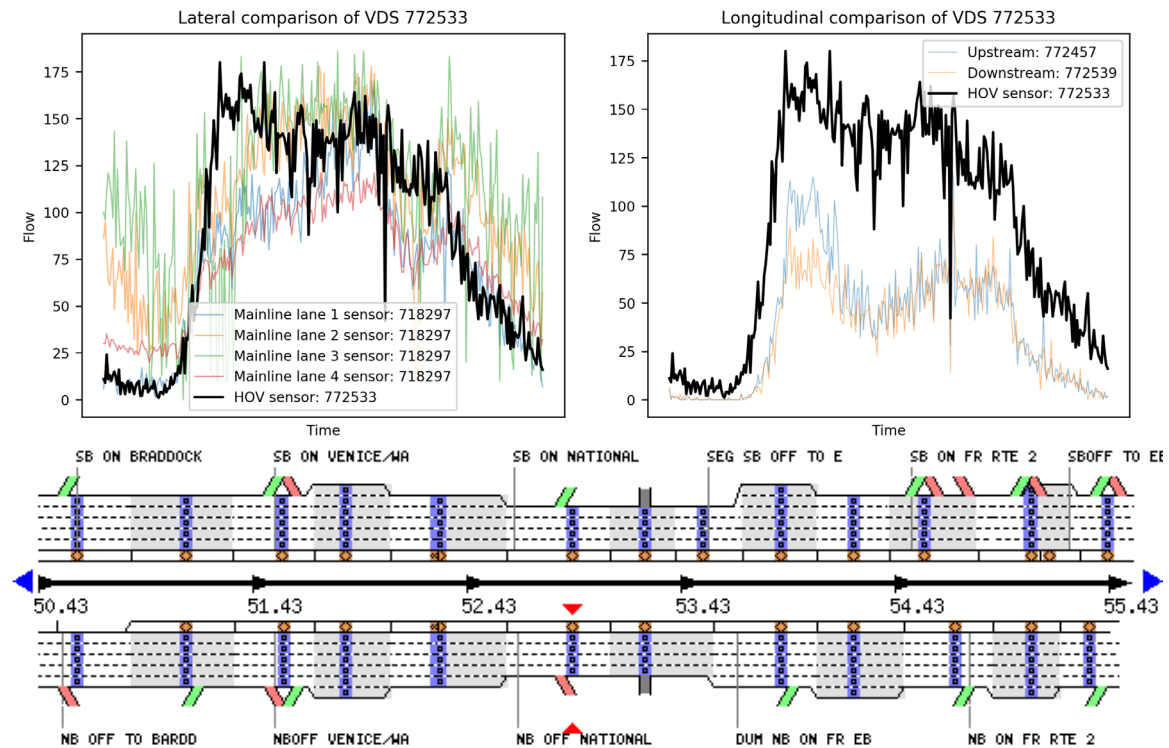


Potential Erroneous Degradation of High Occupancy Vehicle (HOV) Facilities – Final Report

SENSOR: 772533

Potential misconfiguration detected by unsupervised method only. Plotted using data for Wednesday, 2020-12-09.

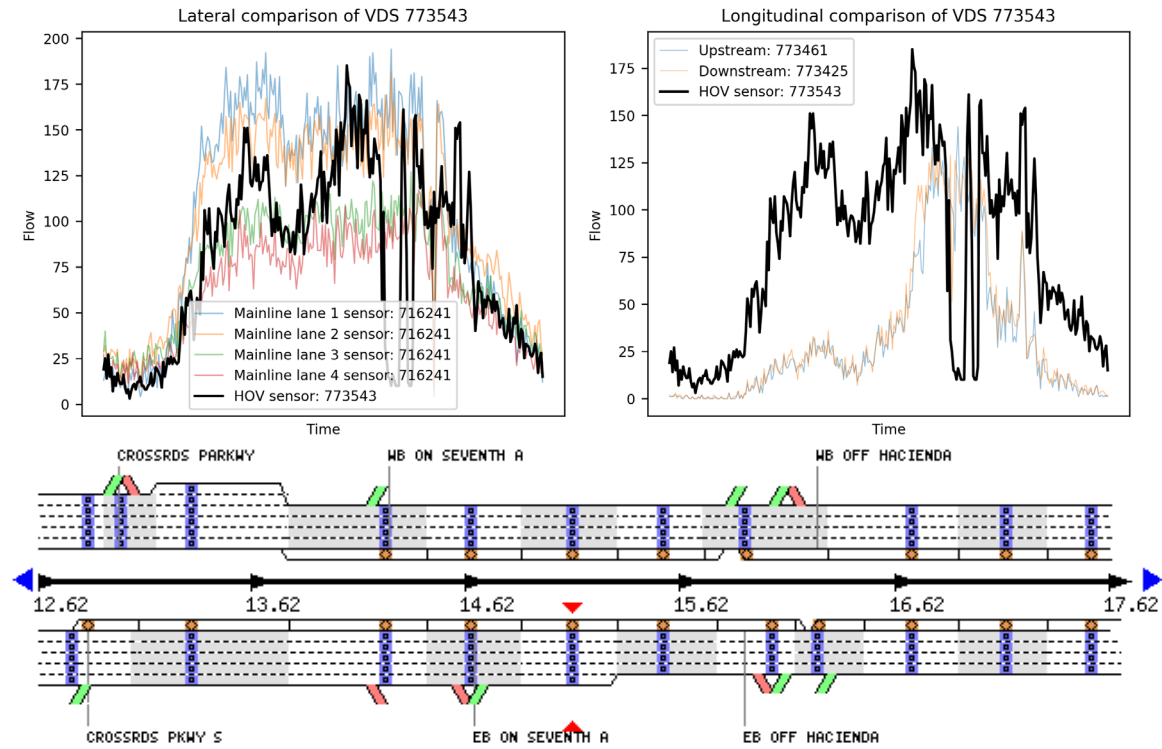
This sensor is probably misconfigured, but additional analysis is required. It was diagnosed as indeterminate because the correct HOV lane is unclear. It was detected as erroneous because the HOV lane flow profile is non-zero during nighttime flows and does not match the flow profile of upstream or downstream sensors.



SENSOR: 773543

Potential misconfiguration detected by both classification and unsupervised methods. Plotted using data for Wednesday, 2020-12-09.

This sensor is probably misconfigured, but additional analysis is required. It was diagnosed as indeterminate because the correct HOV lane is unclear. It was detected as erroneous because the HOV lane flow profile is non-zero during nighttime flows and does not match the flow profile of upstream or downstream sensors.

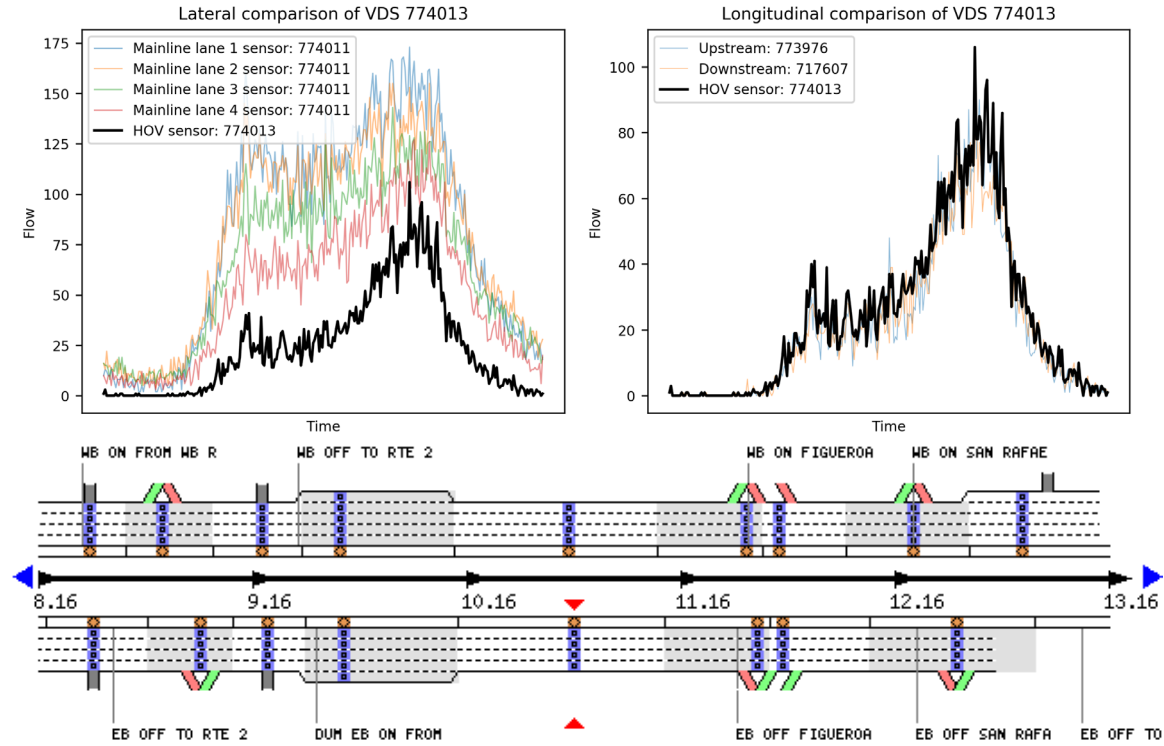


Potential Erroneous Degradation of High Occupancy Vehicle (HOV) Facilities – Final Report

SENSOR: 774013

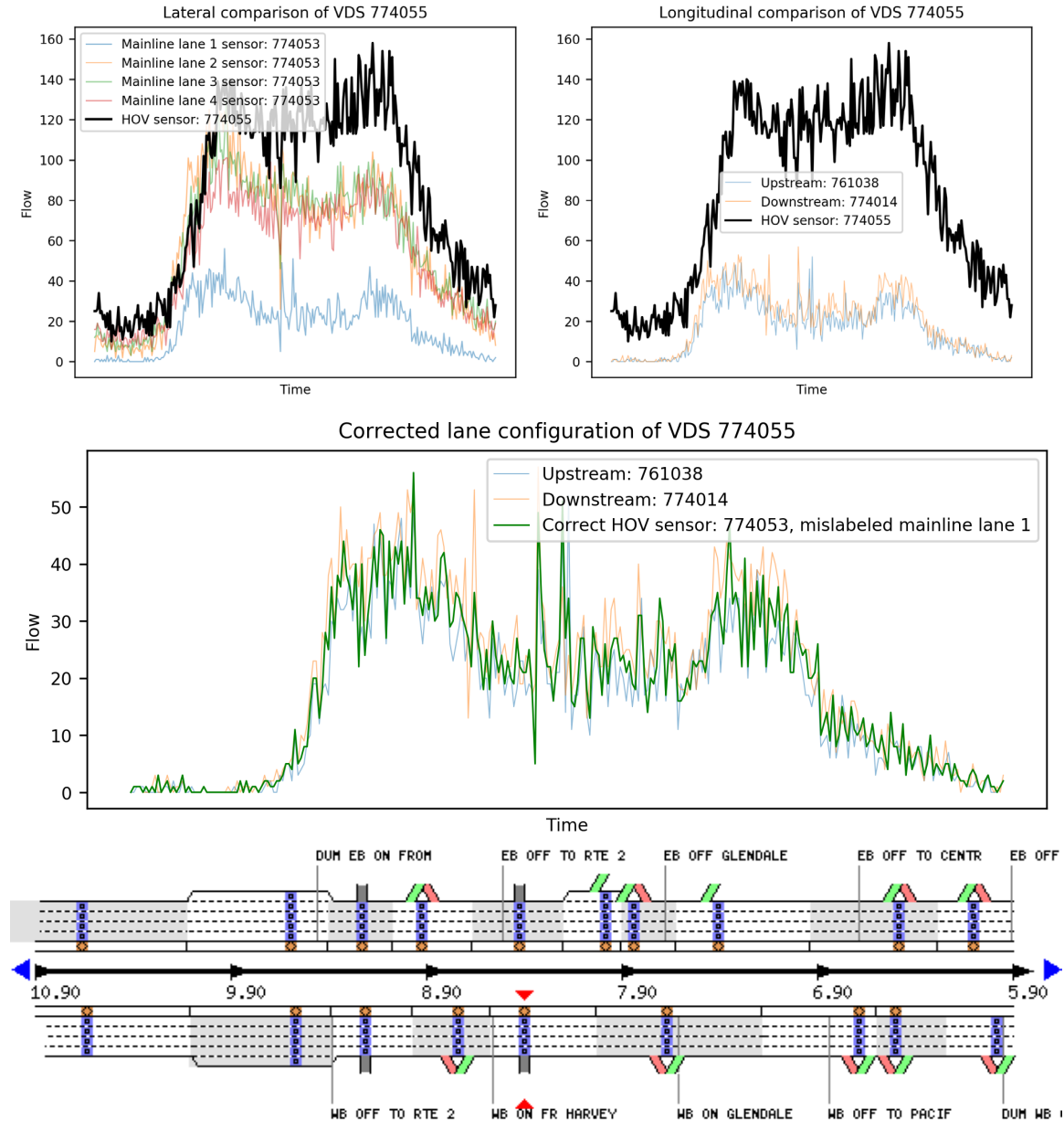
Potential misconfiguration detected by unsupervised method only. Plotted using data for Wednesday, 2020-12-09.

Judging from the longitudinal comparison, this sensor appears to be correctly configured as an HOV lane. Diagnosed as a false positive, data and label are correct. It is unclear exactly why it was detected as erroneous, but possibly because nighttime flow is non-zero.



SENSOR: 774055

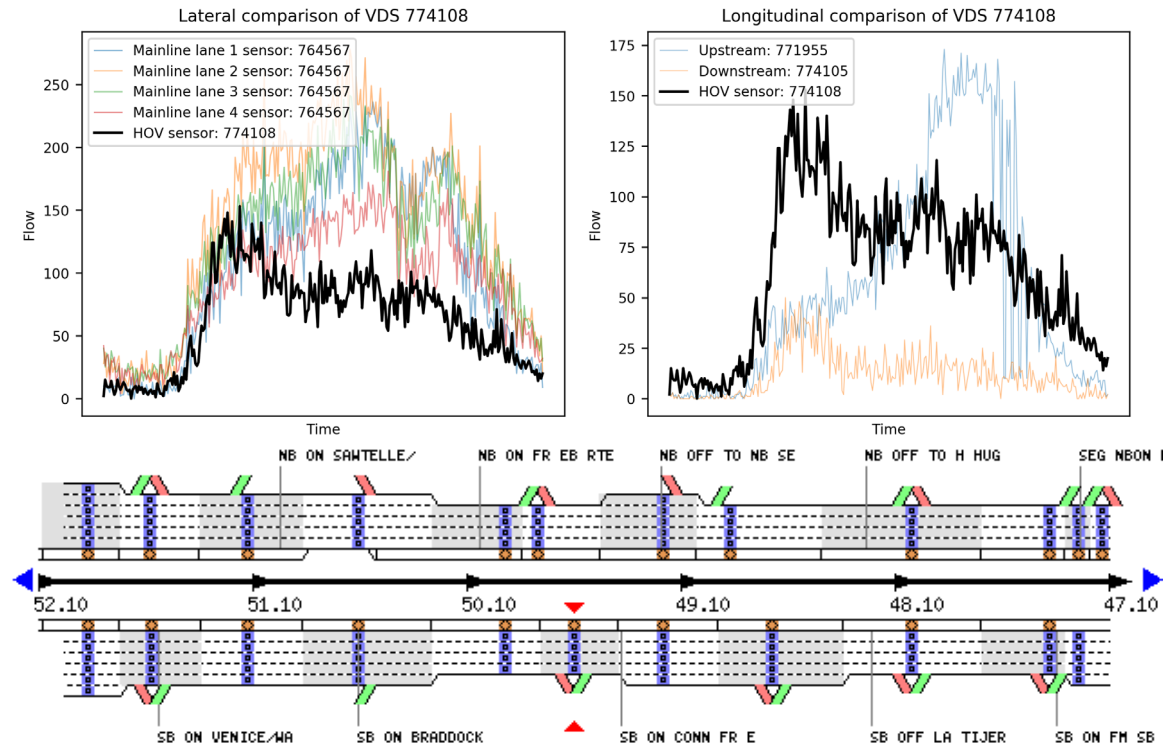
Misconfiguration detected by both classification and unsupervised methods. Plotted using data for Wednesday, 2020-12-09. Diagnosed as misconfigured with proposed solution to swap Lane 1 with HOV lane.



SENSOR: 774108

Potential misconfiguration detected by both classification and unsupervised methods. Plotted using data for Wednesday, 2020-12-09.

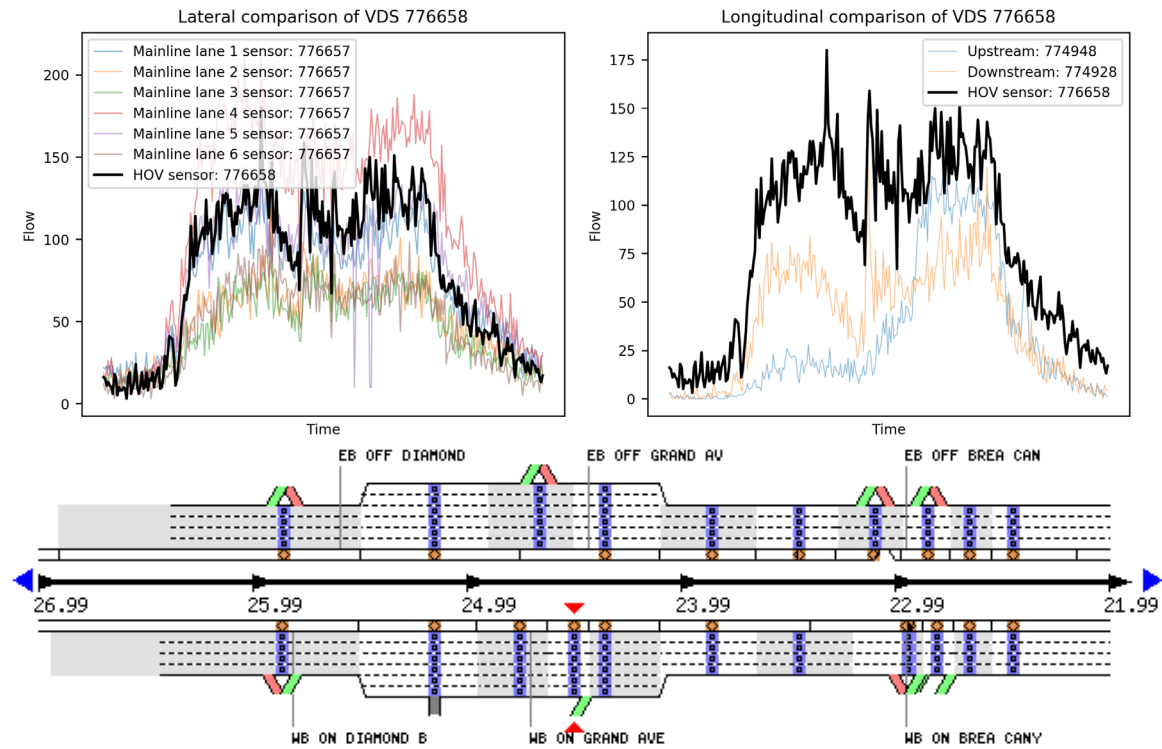
This sensor could be misconfigured, but additional analysis is required. It was diagnosed as indeterminate because the correct HOV lane is unclear. It was detected as erroneous because the HOV lane flow profile is non-zero during nighttime flows and does not match the flow profile of upstream or downstream sensors.



SENSOR: 776658

Potential misconfiguration detected by both classification and unsupervised methods. Plotted using data for Wednesday, 2020-12-09.

This sensor could be misconfigured, but additional analysis is required. It was diagnosed as indeterminate because the correct HOV lane is unclear. It was detected as erroneous because the HOV lane flow profile is non-zero during nighttime flows and does not match the flow profile of upstream or downstream sensors.

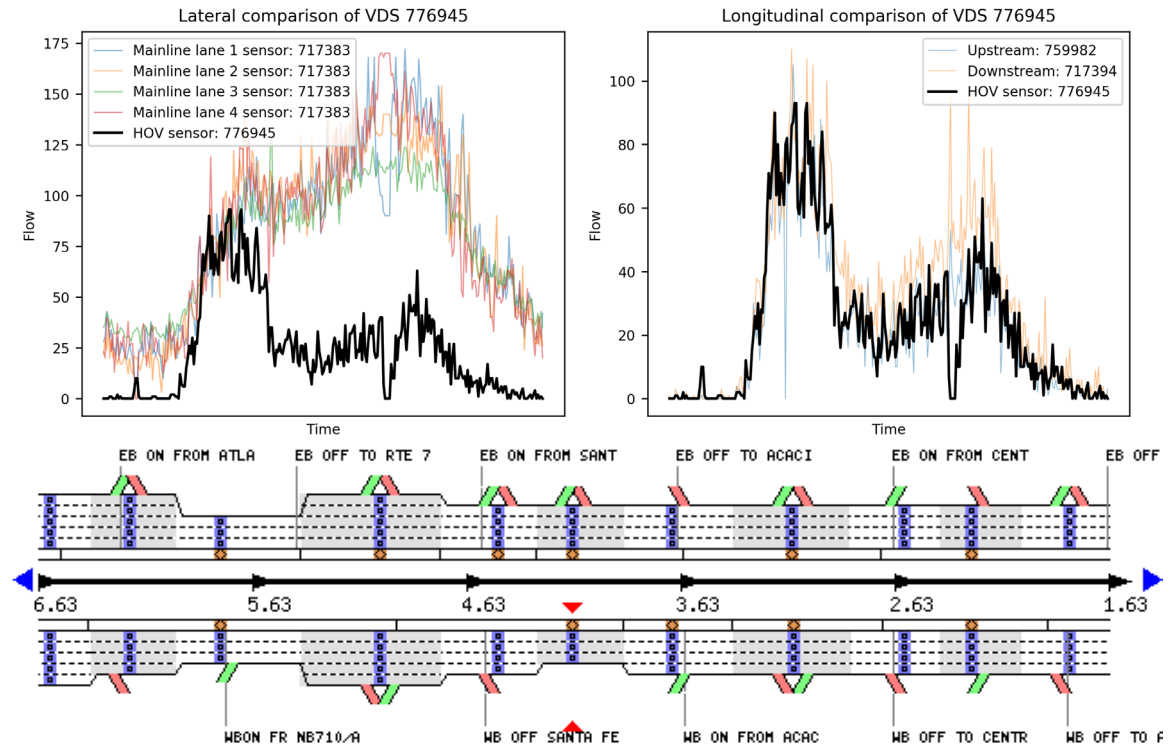


Potential Erroneous Degradation of High Occupancy Vehicle (HOV) Facilities – Final Report

SENSOR: 776945

Potential misconfiguration detected by unsupervised method only. Plotted using data for Wednesday, 2020-12-09.

Judging from the longitudinal comparison, this sensor appears to be correctly configured as an HOV lane. Diagnosed as a false positive, data and label are correct. It was likely detected as erroneous because the the traffic flow is slightly erratic, which causes the flow profiles to be statistically different.



Potential Erroneous Degradation of High Occupancy Vehicle (HOV) Facilities – Final Report

This appendix presents a visualization table of sensor data availability and detection results for the 13 quarterly analyses from 2018 Q1 to 2021 Q1. The results are color-coded based on the following legend.

Legend:

	Not misconfigured
	Data unavailable
	Possible misconfiguration (Supervised)
	Possible misconfiguration (Supervised and Unsupervised)
	Possible misconfiguration (Unsupervised)

VDS ID MS ID	2018 Q1	2018 Q2	2018 Q3	2018 Q4	2019 Q1	2019 Q2	2019 Q3	2019 Q4	2020 Q1	2020 Q2	2020 Q3	2020 Q4	2021 Q1	Total Detections
769745 2430	Red	Red	Red	Red	Grey	Red	Red	Red	Red	Red	Red	Red	Red	12
765271 3395	Red	Red	Red	Red	Red	Red	Red	Red	Red	Red	Red	Red	Red	12
717822 3510	Red	Red	Red	Red	Red	Red	Red	Red	Red	Red	Red	Red	Red	12
762612 3245	Grey	Red	Red	Red	Red	Red	Red	Red	Red	Red	Red	Red	Red	11
766518 3440	Red	Red	Red	Red	Red	Red	Red	Red	Red	Red	Red	Red	Red	11
718313 3424	Red	Red	Red	Red	Red	Red	Red	Red	Red	Red	Red	Red	Red	11
771916 2047	Red	Red	Red	Red	Red	Red	Red	Red	Red	Red	Red	Red	Red	11
762600 3367	Red	Red	Red	Red	Red	Red	Red	Red	Red	Red	Red	Red	Red	10
775205 3208	Red	Red	Red	Red	Red	Red	Red	Red	Red	Red	Red	Red	Red	10
768743 3431	Red	Red	Red	Red	Red	Red	Red	Red	Red	Red	Red	Red	Red	10
767985 2708	Red	Red	Red	Red	Red	Red	Red	Red	Red	Red	Red	Red	Red	10
773872 2704	Red	Red	Red	Red	Red	Red	Red	Red	Red	Red	Red	Red	Red	10
775419 3640	Red	Red	Red	Red	Red	Red	Red	Red	Red	Red	Red	Red	Red	10
763606 4201	Red	Red	Red	Red	Red	Red	Red	Red	Red	Red	Red	Red	Red	9
767999 2709	Green	Red	Red	Red	Red	Red	Red	Red	Red	Red	Red	Red	Red	9
768899 3323	Red	Red	Red	Red	Red	Red	Red	Red	Red	Red	Red	Red	Red	9
774033 4200	Red	Red	Red	Red	Red	Red	Red	Red	Red	Red	Red	Red	Red	9
774108 3195	Red	Red	Red	Red	Red	Red	Red	Red	Red	Red	Red	Red	Red	9
767954 4706	Green	Red	Red	Red	Red	Red	Red	Red	Red	Red	Red	Red	Red	9
772533 3192	Red	Red	Red	Red	Red	Red	Red	Red	Red	Red	Red	Red	Red	9
768027 2711	Red	Red	Red	Red	Red	Red	Red	Red	Red	Red	Red	Red	Red	9
768013 2710	Red	Red	Red	Red	Red	Red	Red	Red	Red	Red	Red	Red	Red	8
776658 4032	Red	Red	Red	Red	Red	Red	Red	Red	Red	Red	Red	Red	Red	8
767939 2715	Green	Red	Red	Red	Red	Red	Red	Red	Red	Red	Red	Red	Red	8
766047 2232	Red	Red	Red	Red	Red	Red	Red	Red	Red	Red	Red	Red	Red	8
762549 3047	Red	Red	Red	Red	Red	Red	Red	Red	Red	Red	Red	Red	Red	7
761592 3524	Red	Red	Red	Red	Red	Red	Red	Red	Red	Red	Red	Red	Red	7
760117 2585	Red	Red	Red	Red	Red	Red	Red	Red	Red	Red	Red	Red	Red	7
769238 3359	Red	Red	Red	Red	Red	Red	Red	Red	Red	Red	Red	Red	Red	7
766952 3385	Red	Red	Red	Red	Red	Red	Red	Red	Red	Red	Red	Red	Red	7
760672 3521	Red	Red	Red	Red	Red	Red	Red	Red	Red	Red	Red	Red	Red	7
759967 3293	Red	Red	Red	Red	Red	Red	Red	Red	Red	Red	Red	Red	Red	7
766061 2730	Red	Red	Red	Red	Red	Red	Red	Red	Red	Red	Red	Red	Red	6
717540 3523	Red	Red	Red	Red	Red	Red	Red	Red	Red	Red	Red	Red	Red	6
767909 4553	Red	Red	Red	Red	Red	Red	Red	Red	Red	Red	Red	Red	Red	6
718270 3371	Red	Red	Red	Red	Red	Red	Red	Red	Red	Red	Red	Red	Red	6
762559 3057	Red	Red	Red	Red	Red	Red	Red	Red	Red	Red	Red	Red	Red	6
717738 3073	Red	Red	Red	Red	Red	Red	Red	Red	Red	Red	Red	Red	Red	6
765959 2230	Red	Red	Red	Red	Red	Red	Red	Red	Red	Red	Red	Red	Red	6
760122 2587	Red	Red	Red	Red	Red	Red	Red	Red	Red	Red	Red	Red	Red	6
774206 3160	Red	Red	Red	Red	Red	Red	Red	Red	Red	Red	Red	Red	Red	6
717645 4306	Red	Red	Red	Red	Red	Red	Red	Red	Red	Red	Red	Red	Red	5
760130 2589	Red	Red	Red	Red	Red	Red	Red	Red	Red	Red	Red	Red	Red	5
773543 2158	Red	Red	Red	Red	Red	Red	Red	Red	Red	Red	Red	Red	Red	5
762449 2533	Red	Red	Red	Red	Red	Red	Red	Red	Red	Red	Red	Red	Red	5
762500 3800	Red	Red	Red	Red	Red	Red	Red	Red	Red	Red	Red	Red	Red	5
760832 3516	Red	Red	Red	Red	Red	Red	Red	Red	Red	Red	Red	Red	Red	5
760199 4836	Red	Red	Red	Red	Red	Red	Red	Red	Red	Red	Red	Red	Red	5
762547 3046	Red	Red	Red	Red	Red	Red	Red	Red	Red	Red	Red	Red	Red	4
762582 3013	Red	Red	Red	Red	Red	Red	Red	Red	Red	Red	Red	Red	Red	4
771621 6009	Red	Red	Red	Red	Red	Red	Red	Red	Red	Red	Red	Red	Red	4

Potential Erroneous Degradation of High Occupancy Vehicle (HOV) Facilities – Final Report

762657 3383		4
774443 2673		4
766097 2131		4
767897 2714		4
766852 3246		4
766619 4037		4
762451 3727		4
768360 3766		4
761532 2042		4
766030 2132		4
765942 2228		4
775443 2086		4
772955 2135		3
761105 4250		3
775166 2051		3
773384 2371		3
760844 3520		3
762455 3731		3
767264 2068		3
760677 3529		3
717531 3527		3
717641 4254		3
765961 2230		3
766532 3445		3
769137 4797		3
769151 4796		3
769259 3355		3
717534 3525		3
764135 2548		3
766063 2730		3
716541 3529		3
767368 2073		2
773997 2397		2
766139 3616		2
774013 2225		2
760835 3518		2
768341 3764		2
774055 2402		2
761388 4289		2
760840 3519		2
761061 3389		2
766643 4039		2
761384 4292		2
761380 4294		2
761014 4194		2
768229 3317		2
773977 2396		2
774112 3200		2
761174 4261		2
766586 2656		2
761025 3496		2
761005 4191		2
762604 3505		2
762410 2487		2
762538 3079		2
772934 2134		2
772440 2448		2
762659 3382		2
762673 3349		2
772969 2408		2
771917 2047		2
762553 3051		2
763608 4202		2
763656 2140		2
762541 3080		2
763658 2141		2
772890 2121		2
773410 2157		2
762520 3008		2
773523 2755		2
769219 3363		2
762453 3729		2
773871 2704		2
762432 2488		2
764615 3508		2

Potential Erroneous Degradation of High Occupancy Vehicle (HOV) Facilities – Final Report

761033 3498		1
766660 4034		1
774634 2161		1
767983 2708		1
717394 3329		1
718257 3074		1
760994 3109		1
776945 4079		1
762675 3348		1
771940 2046		1
717148 3430		1
760387 2597		1
760395 4580		1
760827 3515		1
766961 4687		1
766963 4686		1
760617 4833		1
767882 4586		1
774731 2129		1
766992 4682		1
767847 2918		1
771708 3526		1
760519 4834		1
767234 2373		1
774929 2529		1
774949 2163		1
763602 4080		1
759982 4136		1
717542 3522		1
761102 4249		1
775937 2125		1
766520 3441		1
766525 3447		1
761149 4259		1
761214 4265		1
770407 4266		1
760303 4579		1
768319 3770		1
763612 4211		1
771143 3636		1
761093 4522		1
775401 3611		1
761240 4269		1
771769 4371		0
769263 3357		0
769231 3361		0
771810 2075		0
775425 3610		0
769069 3985		0
771692 2234		0
769062 3986		0
769703 2412		0
771693 2234		0
771809 2075		0
769704 2412		0
769265 3358		0
771723 3517		0
775397 3485		0
769232 3361		0
769759 2431		0
769235 3360		0
771135 2453		0
771153 3633		0
769250 2480		0
771155 3614		0
771157 2283		0
769255 3354		0
769723 2415		0
771223 2195		0
771232 4443		0
769242 2251		0
769236 3360		0
769773 2416		0
775404 3487		0
775407 3486		0

Potential Erroneous Degradation of High Occupancy Vehicle (HOV) Facilities – Final Report

769241 2251		0
775413 3484		0
771147 3635		0
769260 3356		0
771606 6008		0
769249 2480		0
775031 2126		0
768945 4268		0
768937 3325		0
768011 2710		0
776691 4058		0
768025 2711		0
776631 4650		0
768040 4712		0
768054 4713		0
768228 3317		0
776630 4650		0
768304 3763		0
776472 3109		0
768311 3771		0
768314 2107		0
768315 2107		0
768320 3770		0
768329 3769		0
776711 4043		0
776741 3001		0
767997 2709		0
767870 2906		0
767352 2071		0
767353 2071		0
777168 3725		0
767369 2073		0
767839 2907		0
767859 2905		0
767895 2714		0
776825 4834		0
777068 2423		0
767924 4563		0
777067 2423		0
767941 2715		0
776846 2057		0
767969 4707		0
768330 3769		0
768340 3764		0
775806 4444		0
768751 3432		0
768724 3810		0
768738 3796		0
768741 3795		0
775476 3609		0
775463 3232		0
768746 3794		0
768752 3432		0
768426 3797		0
775461 3232		0
775442 2086		0
768909 3298		0
768914 2384		0
768934 4505		0
775426 3610		0
768625 3504		0
768370 2106		0
768351 3765		0
775538 2699		0
768352 3765		0
775692 2149		0
768354 3768		0
768357 2109		0
775691 2149		0
775553 3434		0
775537 2699		0
768369 2106		0
768358 2109		0
768362 3767		0
775477 3609		0

Potential Erroneous Degradation of High Occupancy Vehicle (HOV) Facilities – Final Report

771828 2418		0
768363 3762		0
768365 3772		0
771827 2418		0
772528 2059		0
771847 2123		0
774345 3634		0
775200 3201		0
774093 2285		0
775199 3201		0
774095 3197		0
774097 4555		0
774099 3193		0
774105 2420		0
774106 2420		0
775193 2066		0
775191 3205		0
774126 4057		0
774166 2360		0
774167 2360		0
775186 2065		0
774182 2362		0
774183 2362		0
775185 2065		0
775214 2068		0
774085 2424		0
774056 2402		0
773955 2004		0
773668 4152		0
775263 3426		0
775251 2062		0
773881 2700		0
773891 2701		0
773907 2523		0
773908 2523		0
775250 2062		0
775217 2069		0
773956 2004		0
773976 2396		0
775240 3191		0
773998 2397		0
775230 3206		0
774014 2225		0
774034 4200		0
774329 3209		0
774442 2673		0
771848 2123		0
775170 2060		0
775138 2064		0
775123 2067		0
775122 2067		0
775032 2126		0
774648 4030		0
774650 4031		0
774705 2584		0
774730 2129		0
774745 2128		0
774746 2128		0
774828 2187		0
774829 2187		0
774856 2512		0
774857 2512		0
774928 2529		0
774948 2163		0
774959 4044		0
774646 4029		0
774644 4028		0
775139 2064		0
774623 2159		0
774476 4036		0
774492 4040		0
774562 2489		0
774615 4816		0
774619 4020		0
774620 4020		0

Potential Erroneous Degradation of High Occupancy Vehicle (HOV) Facilities – Final Report

762486 2095		0
762488 3808		0
762492 2096		0
762494 3806		0
762496 3804		0
762498 3802		0
762502 3799		0
762413 2487		0
762408 2485		0
761329 4303		0
761435 3048		0
761339 4299		0
761353 4298		0
761363 4297		0
761371 4296		0
761382 4293		0
761396 4283		0
761428 4569		0
761431 4304		0
761439 2043		0
762405 2092		0
761440 2043		0
761441 3049		0
761444 3050		0
761452 3058		0
761523 3374		0
761531 2042		0
761538 3366		0
762404 2092		0
760476 4570		0
760460 2586		0
762508 3185		0
717910 3337		0
717722 3030		0
717725 3031		0
717756 3052		0
717759 3053		0
717761 3054		0
717876 3249		0
717892 3350		0
717899 3335		0
717920 3345		0
717665 4302		0
717935 3342		0
717938 3342		0
718233 3018		0
718236 3019		0
718254 3075		0
718260 3073		0
718278 3368		0
718331 3433		0
717707 3016		0
717643 4307		0
718448 4451		0
717422 3297		0
717056 3816		0
717140 3741		0
717158 3433		0
717385 4079		0
717400 3328		0
717412 3326		0
717417 3324		0
717419 3296		0
717429 3322		0
717632 4311		0
717526 3528		0
717545 3521		0
717586 4195		0
717588 4196		0
717593 4197		0
717604 4209		0
717607 4203		0
717609 3390		0
718441 3017		0
718480 3369		0

Potential Erroneous Degradation of High Occupancy Vehicle (HOV) Facilities – Final Report

764295 4677		0
764316 4681		0
764609 3372		0
764427 3189		0
764556 3031		0
764559 3046		0
764561 3056		0
764563 3058		0
764565 3083		0
764588 3364		0
764596 3365		0
765994 2229		0
766111 2235		0
763716 2643		0
766965 4689		0
766789 4042		0
766829 4038		0
766844 4814		0
766873 4585		0
766930 4436		0
766936 4437		0
766954 2066		0
766956 3425		0
766967 4685		0
766621 4037		0
766969 4683		0
766971 3391		0
766994 4684		0
766996 4688		0
766998 4681		0
767054 3396		0
767258 3513		0
767260 3514		0
766641 4039		0
766601 2655		0
766113 2235		0
766522 2137		0
766210 3299		0
766494 2045		0
766506 2044		0
766508 3436		0
766510 3437		0
766512 2138		0
766514 3438		0
766516 3439		0
766528 3446		0
766599 2655		0
766530 2138		0
766534 3444		0
766536 3443		0
766538 3442		0
766554 3304		0
766568 2167		0
766570 2167		0
766584 2656		0
763968 3974		0
763710 2612		0
762526 3014		0
762631 2146		0
762598 3076		0
762608 3502		0
762616 3248		0
762619 2144		0
762622 3334		0
762624 3336		0
762627 3338		0
762629 2146		0
762634 3339		0
762594 3078		0
762637 3340		0
762640 2449		0
762641 2449		0
762643 4424		0
762645 4423		0
762648 2139		0

Potential Erroneous Degradation of High Occupancy Vehicle (HOV) Facilities – Final Report

762649 2139		0
762652 2440		0
762596 3077		0
762590 3028		0
762655 3384		0
762565 3512		0
762528 3021		0
762531 3023		0
762533 3025		0
762535 3027		0
762543 3081		0
762545 3082		0
762552 3051		0
762555 3055		0
762567 3511		0
762588 3026		0
762569 3509		0
762571 3506		0
762573 3504		0
762576 3007		0
762578 3009		0
762580 3011		0
762584 3022		0
762586 3024		0
762653 2440		0
762661 3381		0
763693 2454		0
763551 3976		0
763416 3184		0
763444 3189		0
763464 3247		0
763466 3297		0
763473 3329		0
763475 3339		0
763537 3974		0
763544 3975		0
763588 3985		0
763405 3183		0
763595 3986		0
763604 4138		0
763610 4210		0
763614 4311		0
763634 4585		0
763654 2140		0
763679 2373		0
763687 2447		0
763413 3183		0
763397 3182		0
762663 3379		0
762686 3343		0
762665 3378		0
762667 3377		0
762669 2454		0
762671 3351		0
762678 2145		0
762679 2145		0
762681 3346		0
762685 3343		0
762688 3341		0
763389 3181		0
763243 3059		0
763256 3062		0
763264 3063		0
763272 3064		0
763280 3064		0
763283 3065		0
763291 3066		0
763323 3110		0
777169 3725		0